



Australia's National
Science Agency

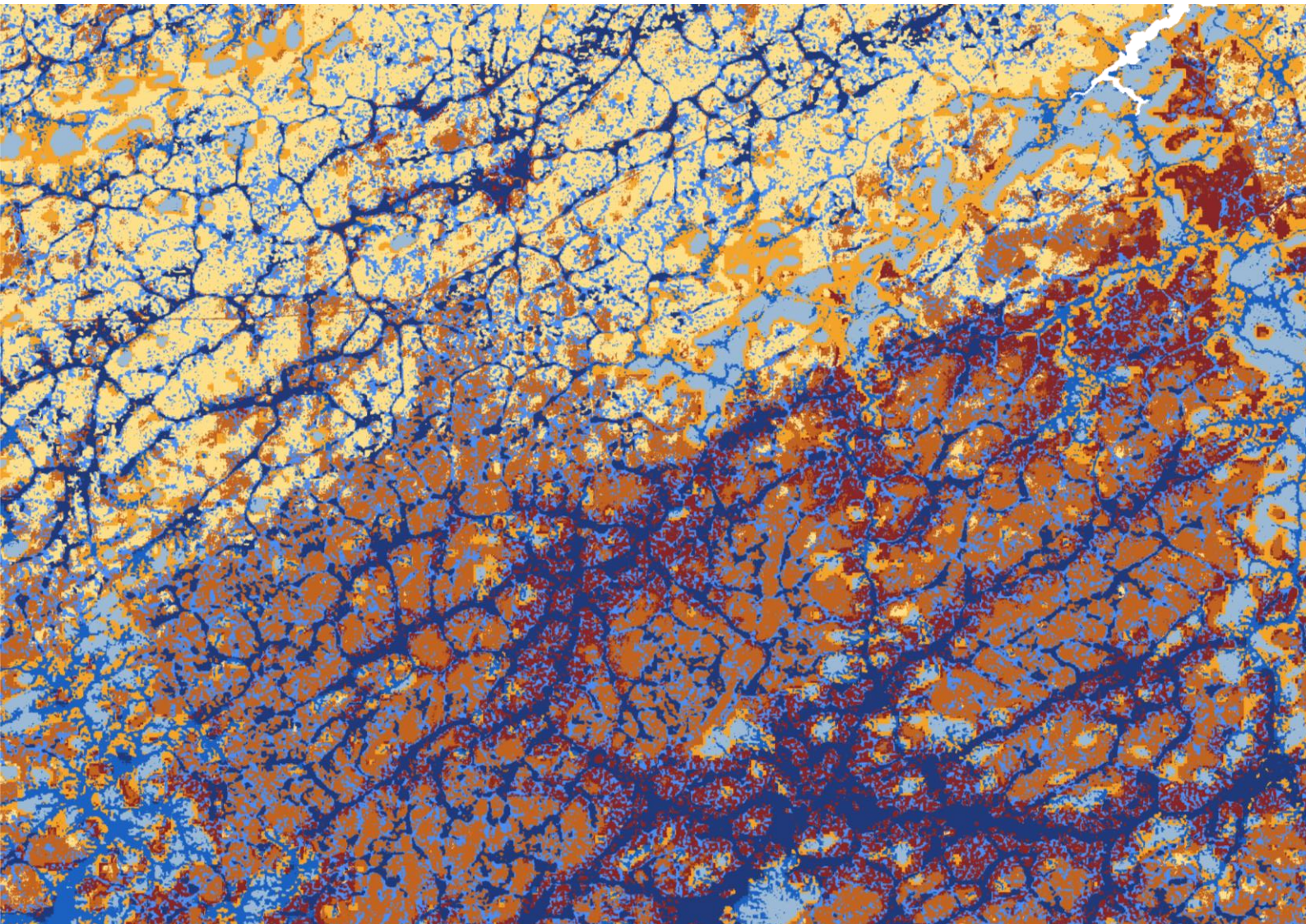
UltraFine+[®] Next Gen Analytics

Geological Survey of New South Wales – Cobar Projects

Anicia Henne, Ryan RRP Noble, Fang Huang, Dave Cole, Morgan Williams, Tania Ibrahimi, Ian C
Lau, Bobby Pejic

EP2022-3306

17 August 2022 (updated October 2023)



Citation

Henne A, Noble RRP, Huang F, Cole D, Williams M, Ibrahimi T, Lau I, Pejcic B (2022). UltraFine+® Next Gen Analytics. Geological Survey of New South Wales – Cobar Projects. CSIRO Report EP2022-3306, CSIRO, Australia.

Copyright

© Commonwealth Scientific and Industrial Research Organisation 2022. To the extent permitted by law, all rights are reserved and no part of this publication covered by copyright may be reproduced or copied in any form or by any means except with the written permission of CSIRO.

Important disclaimer

CSIRO advises that the information contained in this publication comprises general statements based on scientific research. The reader is advised and needs to be aware that such information may be incomplete or unable to be used in any specific situation. No reliance or actions must therefore be made on that information without seeking prior expert professional, scientific and technical advice. To the extent permitted by law, CSIRO (including its employees and consultants) excludes all liability to any person for any consequences, including but not limited to all losses, damages, costs, expenses and any other compensation, arising directly or indirectly from using this publication (in part or in whole) and any information or material contained in it.

CSIRO is committed to providing web accessible content wherever possible. If you are having difficulties with accessing this document, please contact csiroenquiries@csiro.au.

Addendum:

During the project closure and review (Aug-Sep 2023), the authors recognised an error on p.44 relating to Principal Component Analysis interpretation applied to the Federation site. The text incorrectly associated a positive PC1 loading with Ag, Au, Bi, Cd, Cu, Mo, Pb, S, W and Zn. PC1 is associated with elevated As, Au, Ba, Ta, and Tl. We have since replaced the text in this version on p. 44 to accurately reflect the data presented.

UltraFine⁺® Next Gen Analytics Sponsors



UltraFine+® Next Gen Analytics for Discovery

The Geological Survey of New South Wales used the Federation and Wagga Tank project sites as part of the UltraFine+® Next Gen Analytics research project conducted by the CSIRO in collaboration with LabWest and over 20 industry sponsors and state geological surveys. The aim of this research project is to facilitate a paradigm shift for precious, base, and critical metals exploration in Australia by combining UltraFine+® soil analytical methods with intelligent data integration tools, adding value to routine soil sampling in frontline exploration and shaping mineral exploration approaches for decades.

It has been common practice to use soil geochemistry in mineral exploration with little regard for physicochemical soil parameters or landform settings and how these relate to buried mineralisation. The UltraFine+® Next Gen Analytics research addresses this challenge by delivering an analytical refinement of the UltraFine+® soil analysis method and by adding relevant mineral proxies via spectral mineralogy and soil properties pH, EC and particle size distribution to the workflow and interpretation. UltraFine+® Next Gen Analytics utilises machine learning approaches to integrate these soil parameters with spatial data and regolith landscape models. This improves our ability to identify targets and false positives as well as understand the spatial variance and influence of regolith types. With the development of a robust set of measurable parameters and new data products to fully assess underappreciated soil properties, UltraFine+® Next Gen Analytics provides the next generation analytical tools for mineral explorers to make qualified decisions on when and where to explore further.

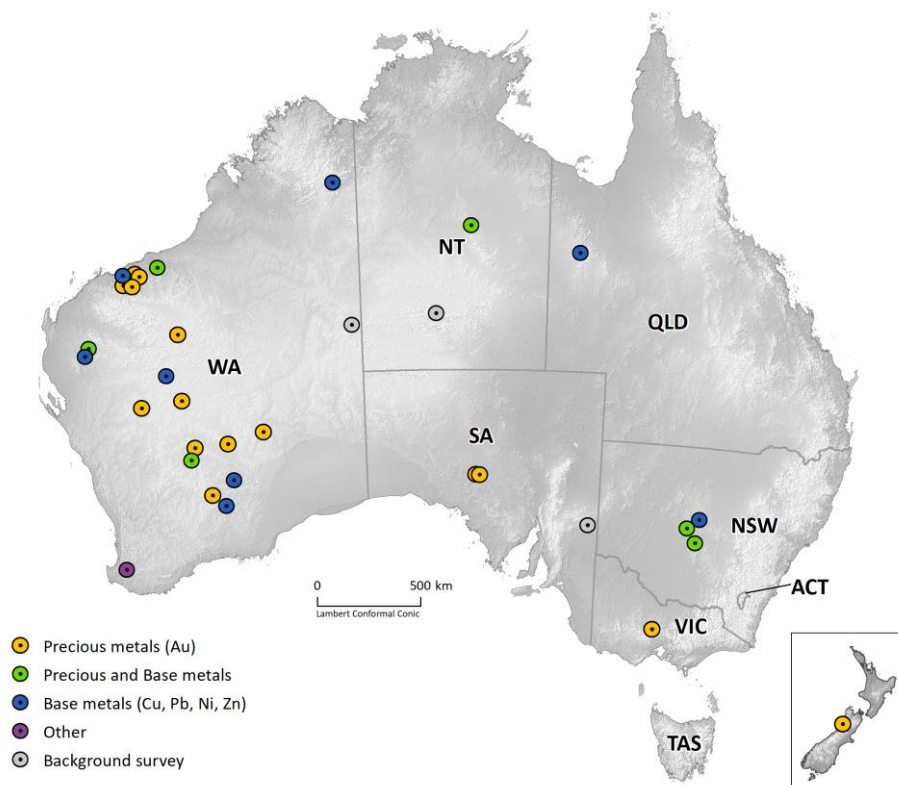


Figure 1: UltraFine+® Next Gen Analytics for Discovery project sponsor’s site locations (as of 18 May 2022).

Contents

UltraFine+® Next Gen Analytics Sponsors	iii
UltraFine+® Next Gen Analytics for Discovery	i
Acknowledgments.....	x
Executive summary	xi
1 The UltraFine+® Next Generation Analytics for Discovery Research Project.....	1
1.1 Geological Survey of New South Wales – Cobar projects.....	1
2 The UltraFine+® Next Gen Analytics Workflow	5
2.1 Sample collection	5
2.2 UltraFine+® laboratory soil analyses	5
2.3 Automated QA/QC	7
2.4 Machine Learning - Spatial data integration and clustering	9
3 The UltraFine+® Next Gen Analytics Outputs.....	13
3.1 Landscape clusters.....	13
3.2 UltraFine+® geochemistry results	26
3.3 Outliers by landscape type	30
3.4 Exploration Indices	44
3.5 Other Soil Properties	49
3.6 Dispersion and Source Direction	59
4 Summary.....	62
References	64
Appendix A - UltraFine+® Sampling Workflow	66
Appendix B - UltraFine+® Standard – UFF320	67
Appendix C - UltraFine+® Next Gen Analytics data package – Federation.....	68
Appendix D - UltraFine+® Next Gen Analytics data package – Wagga Tank	69

Figures

Figure 1: UltraFine+® Next Gen Analytics for Discovery project sponsor’s site locations (as of 18 May 2022).	i
Figure 2: GSNSW’s Cobar project areas (main tile) near Gilgunnia in central western NSW. (A) Wagga Tank project area with Peel Mining’s Wagga Tank and Southern Nights prospects indicated. (B) Federation project area with Aurelia Metal’s Federation and Dominion prospects indicated.....	2
Figure 3: Surface and regolith geology in the Wagga Tank and Federation project areas. Dashed boxes indicate the extend of the modelled areas.	4
Figure 4: (A) Scatter diagram of pixel values for GSNSW’s Federation project site embedded in a 3-dimensional latent space using the dimensionality reduction algorithm UMAP. Points are coloured using an RGB of the axes (u0, u1, u2) values. (B) Pixel values projected into 2-dimensional space for spatial context over the Federation project area.	10
Figure 5: Clustered data points of the GSNSW’s Federation Project site in the 3-dimensional latent space grouped by cluster colour to visualise data separation. (A) Data points clustered into 4 clusters using the k-means algorithm (kmeans4). (B) Data points clustered into 8 clusters by an agglomerative clustering algorithm (agg8). Refer to Appendix B for an interactive plot. .	11
Figure 6: Proxy regolith clustering input layers (A-D) and comparison of traditional geological maps (E, F) to machine learning derived outputs (G, H) over the Federation project area. (A) 1-second DEM SRTM (Gallant et al. 2011). (B) Continuous MrVBF (Gallant et al. 2012). (C) RGB image of radiometric grid of Australia (Poudjom Djomani and Minty 2019). (D) RGB image of sentinel-2 regolith ratios. (E) Surface Geology (Raymond et al. 2012) (F) Regolith Geology (Gibson 1998). (G) Proxy regolith types derived via k-means with four clusters plotted in spatial context. (H) Proxy regolith types derived via agglomerative clustering with eight clusters plotted in spatial context.....	15
Figure 7: Comparison of 3-dimensional projection plots of data points for the Federation project area derived via UMAP and how these data points are clustered when different cluster numbers are applied. Colours are applied to each landscape cluster to visualise data separation. (A) Pixel values coloured using an RGB of the axes (u0, u1, u2) derived via the dimensionality reduction algorithm UMAP. (A) Data points clustered into 4 clusters using the k-means algorithm (kmeans4). (B) Data points clustered into 8 clusters using the agglomerative algorithm (agg8). (D) Data points clustered into 12 clusters using the agglomerative algorithm (agg12).	15
Figure 8: Comparison of dimensionality reduction and clustering algorithm outputs plotted in spatial context over the Federation project area. (A) Spatial representation of cluster similarities in RGB colours derived via the dimensionality reduction algorithm UMAP; the more similar the colour, the more similar the spatial characteristics of the data points. Subsequent landscape cluster outputs are derived from this output and in general, the closer they match the UMAP distribution the more representative these clusters are. (B) Landscape clusters derived via k-means clustering with four clusters. (C) Landscape clusters derived via agglomerative clustering	

with eight clusters. (D) Landscape clusters derived via agglomerative clustering with 12 clusters. 16

Figure 9: Proxy regolith clustering input layers (A-D) and comparison of traditional geological maps (E, F) to machine learning derived outputs (G, H) over the Wagga Tank project area. (A) 1-second DEM SRTM. (B) Continuous MrVBF. (C) RGB image of radiometric grid of Australia. (D) RGB image of sentinel-2 regolith ratios. (E) Surface Geology. (F) Regolith Geology. (G) Proxy regolith types derived via k-means with four clusters plotted in spatial context. (H) Proxy regolith types derived via agglomerative clustering with eight clusters plotted in spatial context. 16

Figure 10: Correlation of proxy regolith types with landscape clusters for the Federation project area generated by (A) an agglomerative clustering algorithm with eight clusters and (B) a k-means clustering algorithm with four clusters. Please refer to the text for more detail on these proxy regolith types. 19

Figure 11 (next page): Spatial layers used for the assessment of landscape clusters produced by machine learning over the Federation project area. (A) Landscape clusters derived via agg8. (B) Landscape clusters derived via kmeans4. (C) 2-dimensional representation of cluster similarities derived via UMAP. (D) MrVBF as proxy for depth of cover. (E) Radiometric data as indication for differences in parent materials. (F) Satellite imagery. (G) DEM. (H) Regolith ratio. (I) Weathering intensity. Grey diamonds in the figure indicate the approximate location of the Federation and Dominion prospects. 20

Figure 12: Correlation of proxy regolith types with landscape clusters for the Wagga Tank project area generated by (A) an agglomerative clustering algorithm with eight clusters and (B) a k-means clustering algorithm with four clusters. Please refer to the text for more detail on these proxy regolith types. 22

Figure 13 (next page): Spatial layers used for the assessment of landscape clusters produced by machine learning over the Wagga Tank project area. (A) Landscape clusters derived via agg8. (B) Landscape clusters derived via kmeans4. (C) 2-dimensional representation of cluster similarities derived via UMAP. (D) MrVBF as proxy for depth of cover. (E) Radiometric data as indication for differences in parent materials (F) Satellite imagery. (G) DEM. (H) Regolith ratio. (I) Weathering intensity. Grey diamonds in the figure indicate the approximate location of the Wagga Tank and Southern Nights prospects. 24

Figure 14: Boxplots of UltraFine+® analyses for Au, Cu, Zn and Pb on logarithmic scales. The Federation soil analyses results are displayed in green and the Wagga Tank results are displayed in red. 28

Figure 15: Spatial distribution of Pb (A), Zn (B), Cu (C), and Au (D) concentrations over the Federation project area. 29

Figure 16: Spatial distribution of Pb (A), Zn (B), Cu (C), and Au (D) concentrations over the Wagga Tank project area. 29

Figure 17: Example of machine learning derived outputs for outliers by landscape type over the Wagga Tank project area. (A) Boxplots for all Bi data (white box) and by landscape type (coloured boxes). Dashed line indicates the upper 25% boundary for the whole sample

population. Easily observed soil anomalies are samples above the dashed horizontal line. Those shown below the dashed mauve line would not be easily observed without the landscape context. (B) Spatial distribution of Bi outliers (triangles) by proxy regolith type. Outliers in dashed boxes correlate to outliers below the dashed horizontal line in (A) in depositional landscape settings..... 31

Figure 18: Comparison of Au outliers in the whole sample population to Au outliers by landscape clusters over the Federation project area. Outliers are plotted as triangles; background value samples are plotted in grey. (A) Spatial distribution of Au outliers for all data. (B) Spatial distribution of Au outliers by landscape population with four clusters. (C) Spatial distribution of Au outliers by landscape population with eight clusters. (D) Boxplots for all data (white box) and by landscape type (coloured boxes) when calculated based on four landscape clusters. (E) Boxplots for all data (white box) and by landscape type (coloured boxes) when calculated based on eight landscape clusters. Easily observed soil anomalies are samples above the dashed horizontal line (white triangles in (A)). Those shown below the dashed mauve line would not be easily observed without the landscape context (coloured triangles in (B) and (C). *Note that outliers in clusters with <10 samples will not display on maps as these are statistically not meaningful..... 33

Figure 19: Comparison of Ag outliers in the whole sample population to Ag outliers by landscape clusters over the Federation project area. Outliers are plotted as triangles; background value samples are plotted in grey. (A) Spatial distribution of Ag outliers for all data. (B) Spatial distribution of Ag outliers by landscape population with four clusters. (C) Spatial distribution of Ag outliers by landscape population with eight clusters. (D) Boxplots for all data (white box) and by landscape type (coloured boxes) when calculated based on four landscape clusters. (E) Boxplots for all data (white box) and by landscape type (coloured boxes) when calculated based on eight landscape clusters. Easily observed soil anomalies are samples above the dashed horizontal line (white triangles in (A)). Those shown below the dashed mauve line would not be easily observed without the landscape context (coloured triangles in (B) and (C). *Note that outliers in clusters with <10 samples will not display on maps as these are statistically not meaningful..... 34

Figure 20: Comparison of Zn outliers in the whole sample population to Zn outliers by landscape clusters over the Federation project area. Outliers are plotted as triangles; background value samples are plotted in grey. (A) Spatial distribution of Zn outliers for all data. (B) Spatial distribution of Zn outliers by landscape population with four clusters. (C) Spatial distribution of Zn outliers by landscape population with eight clusters. (D) Boxplots for all data (white box) and by landscape type (coloured boxes) when calculated based on four landscape clusters. (E) Boxplots for all data (white box) and by landscape type (coloured boxes) when calculated based on eight landscape clusters. Easily observed soil anomalies are samples above the dashed horizontal line (white triangles in (A)). Those shown below the dashed mauve line would not be easily observed without the landscape context (coloured triangles in (B) and (C). *Note that outliers in clusters with <10 samples will not display on maps as these are statistically not meaningful. 35

Figure 21: Comparison of Pb outliers in the whole sample population to Pb outliers by landscape clusters over the Federation project area. Outliers are plotted as triangles;

background value samples are plotted in grey. (A) Spatial distribution of Pb outliers for all data. (B) Spatial distribution of Pb outliers by landscape population with four clusters. (C) Spatial distribution of Pb outliers by landscape population with eight clusters. (D) Boxplots for all data (white box) and by landscape type (coloured boxes) when calculated based on four landscape clusters. (E) Boxplots for all data (white box) and by landscape type (coloured boxes) when calculated based on eight landscape clusters. Easily observed soil anomalies are samples above the dashed horizontal line (white triangles in (A)). Those shown below the dashed mauve line would not be easily observed without the landscape context (coloured triangles in (B) and (C)). *Note that outliers in clusters with <10 samples will not display on maps as these are statistically not meaningful..... 36

Figure 22: Comparison of Cu outliers in the whole sample population to Cu outliers by landscape clusters over the Federation project area. Outliers are plotted as triangles; background value samples are plotted in grey. (A) Spatial distribution of Cu outliers for all data. (B) Spatial distribution of Cu outliers by landscape population with four clusters. (C) Spatial distribution of Cu outliers by landscape population with eight clusters. (D) Boxplots for all data (white box) and by landscape type (coloured boxes) when calculated based on four landscape clusters. (E) Boxplots for all data (white box) and by landscape type (coloured boxes) when calculated based on eight landscape clusters. Easily observed soil anomalies are samples above the dashed horizontal line (white triangles in (A)). Those shown below the dashed mauve line would not be easily observed without the landscape context (coloured triangles in (B) and (C)). *Note that outliers in clusters with <10 samples will not display on maps as these are statistically not meaningful..... 37

Figure 23: Comparison of Cu outliers in the whole sample population to Cu outliers by landscape clusters over the Wagga Tank project area. Outliers are plotted as triangles; background value samples are plotted in grey. (A) Spatial distribution of Cu outliers for all data. (B) Spatial distribution of Cu outliers by landscape population with four clusters. (C) Spatial distribution of Cu outliers by landscape population with eight clusters. (D) Boxplots for all data (white box) and by landscape type (coloured boxes) when calculated based on four landscape clusters. (E) Boxplots for all data (white box) and by landscape type (coloured boxes) when calculated based on eight landscape clusters. Easily observed soil anomalies are samples above the dashed horizontal line (white triangles in (A)). Those shown below the dashed mauve line would not be easily observed without the landscape context (coloured triangles in (B) and (C)). *Note that outliers in clusters with <10 samples will not display on maps as these are statistically not meaningful..... 38

Figure 24: Comparison of Pb outliers in the whole sample population to Pb outliers by landscape clusters over the Wagga Tank project area. Outliers are plotted as triangles; background value samples are plotted in grey. (A) Spatial distribution of Pb outliers for all data. (B) Spatial distribution of Pb outliers by landscape population with four clusters. (C) Spatial distribution of Pb outliers by landscape population with eight clusters. (D) Boxplots for all data (white box) and by landscape type (coloured boxes) when calculated based on four landscape clusters. (E) Boxplots for all data (white box) and by landscape type (coloured boxes) when calculated based on eight landscape clusters. Easily observed soil anomalies are samples above the dashed horizontal line (white triangles in (A)). Those shown below the dashed mauve line would not be easily observed without the landscape context (coloured triangles in (B) and (C)).

*Note that outliers in clusters with <10 samples will not display on maps as these are statistically not meaningful..... 40

Figure 25: Comparison of Zn outliers in the whole sample population to Zn outliers by landscape clusters over the Wagga Tank project area. Outliers are plotted as triangles; background value samples are plotted in grey. (A) Spatial distribution of Zn outliers for all data. (B) Spatial distribution of Zn outliers by landscape population with four clusters. (C) Spatial distribution of Zn outliers by landscape population with eight clusters. (D) Boxplots for all data (white box) and by landscape type (coloured boxes) when calculated based on four landscape clusters. (E) Boxplots for all data (white box) and by landscape type (coloured boxes) when calculated based on eight landscape clusters. Easily observed soil anomalies are samples above the dashed horizontal line (white triangles in (A)). Those shown below the dashed mauve line would not be easily observed without the landscape context (coloured triangles in (B) and (C)). *Note that outliers in clusters with <10 samples will not display on maps as these are statistically not meaningful. 41

Figure 26: Comparison of Au outliers in the whole sample population to Au outliers by landscape clusters over the Wagga Tank project area. Outliers are plotted as triangles; background value samples are plotted in grey. (A) Spatial distribution of Au outliers for all data. (B) Spatial distribution of Au outliers by landscape population with four clusters. (C) Spatial distribution of Au outliers by landscape population with eight clusters. (D) Boxplots for all data (white box) and by landscape type (coloured boxes) when calculated based on four landscape clusters. (E) Boxplots for all data (white box) and by landscape type (coloured boxes) when calculated based on eight landscape clusters. Easily observed soil anomalies are samples above the dashed horizontal line (white triangles in (A)). Those shown below the dashed mauve line would not be easily observed without the landscape context (coloured triangles in (B) and (C)). *Note that outliers in clusters with <10 samples will not display on maps as these are statistically not meaningful..... 42

Figure 27: Comparison of Ag outliers in the whole sample population to Ag outliers by landscape clusters over the Wagga Tank project area. Outliers are plotted as triangles; background value samples are plotted in grey. (A) Spatial distribution of Ag outliers for all data. (B) Spatial distribution of Ag outliers by landscape population with four clusters. (C) Spatial distribution of Ag outliers by landscape population with eight clusters. (D) Boxplots for all data (white box) and by landscape type (coloured boxes) when calculated based on four landscape clusters. (E) Boxplots for all data (white box) and by landscape type (coloured boxes) when calculated based on eight landscape clusters. Easily observed soil anomalies are samples above the dashed horizontal line (white triangles in (A)). Those shown below the dashed mauve line would not be easily observed without the landscape context (coloured triangles in (B) and (C)). *Note that outliers in clusters with <10 samples will not display on maps as these are statistically not meaningful..... 43

Figure 28: Automated PCA outputs from the UltraFine+® Next Gen Analytics workflow over the Federation project area. (A) Elemental loadings for each of the first five principal components. The further away an element plots from the 0 line, the greater the loading for (influence on) the specific principal component. (B) Automated output of the spatial distribution of principal components weighted by both colour and symbol size (absolute magnitude). The top five

elemental loadings (greatest influence) for each principal component are indicated as headings. The colour red indicates a positive component weight (association); the colour blue indicates a negative component weight (association). The larger the symbols the stronger the association. From left to right boxes display spatial distribution of principal component 0, 1, 2, 3 and 4 weightings. 45

Figure 29: Spatial distribution of principal component 1 (A) and principal component 2 (B) over the Federation project area. 46

Figure 30: Automated PCA outputs from the UltraFine+® Next Gen Analytics workflow over the Wagga Tank project area. (A) Elemental loadings for each of the first five principal components. The further away an element plots from the 0 line, the greater the loading for (influence on) the specific principal component. (B) Automated output of the spatial distribution of principal components weighted by both colour and symbol size (absolute magnitude). The top five elemental loadings (highest influence) for each principal component are indicated as headings. The colour red indicates a positive component weight (association); the colour blue indicates a negative component weight (association). The larger the symbols the stronger the association. From left to right boxes display Spatial distribution of principal component 0, 1, 2, 3 and 4 weightings. The larger the symbols the stronger the association. 47

Figure 31: Spatial distribution of principal component 1 (A) and principal component 2 (B) over the Wagga Tank project area. 48

Figure 32: Spatial distribution of soil pH and EC over the Wagga Tank and Federation project areas. (A) pH over Wagga Tank. (B) EC over Wagga Tank. (C) pH over Federation. (D) EC over Federation. 50

Figure 33: Spatial distribution of spectrally active mineral groups over the Federation project area. (A) Mineral group 1. (B) Mineral group 2. 52

Figure 34: Example VNIR parameters in ultrafine soil samples over the Federation project area. (A) Relative iron oxide abundance. (B) Iron oxide species. Lower values (blue) indicate more hematitic materials, whereas higher values (red) mean the material is more goethitic. Note that where Fe-oxide abundance is very low, the iron oxide species is not defined and data is not plotted. (D) Relative kaolinite abundance. (E) Relative kaolinite crystallinity. (C) Munsell colour. (F) Saturation which indicates how washed out or pure the hue of a colour is. 54

Figure 35: Spatial distribution of spectrally active mineral groups over the Wagga Tank project area. (A) Mineral group 1. (B) Mineral group 2. 55

Figure 36: Example VNIR parameters in ultrafine soil samples over the Wagga Tank project area. (A) Relative iron oxide abundance. (B) Iron oxide species. Lower values (blue) indicate more hematitic materials, whereas higher values (red) mean the material is more goethitic. (C) Munsell colour. (D) Relative kaolinite abundance. (E) Relative kaolinite crystallinity. (F) Saturation which indicates how washed out or pure the hue of a colour is. 56

Figure 37: Spatial distribution of clay abundance (A), quartz abundance (B), total organic carbon (C), and gibbsite index (D), analysed via FTIR over the Wagga Tank project area. 57

Figure 38: Spatial distribution of example metal concentrations normalised by clay abundance over the Wagga Tank project area. (A) Au concentrations in ppb. (B) Au concentrations

normalised by clay abundance. (C) Cu concentrations in ppm (D) Cu concentrations normalised by clay abundance..... 58

Figure 39: Soil texture triangle and spatial distribution over the Federation (A and C) and Wagga Tank (B and D) project areas..... 59

Figure 40: Source and dispersion direction over the Federation and Wagga Tank project areas. (A) Source direction of individual soil sample points and Au outliers by landscape type (kmeans4) within the Federation project area. Source direction is calculated from the DEM (background) but is dependent on accurate GPS readings. (B) Dispersion direction grid and Cu outliers by landscape type (agg8) within the Wagga Tank project area. Dispersion directions indicate broad scale trends..... 60

Tables

Table 1: Number of samples analysed with the UltraFine+® workflow for GSNSW’s Federation and Wagga Tank project areas. *Added to the workflow after project data acquisition. **Added to the workflow after data acquisition for the Federation project but before data acquisition for the Wagga Tank project. †Analyses via ICP-OES..... 6

Table 2: Geospatial covariates used for landscape clustering for the Federation and Wagga Tank project areas. 9

Table 3 (next page): Comparison of detection limits, minimum, maximum, average and median values for available elements in the Wagga Tank (WT) and Federation (Fed) project areas. Values below the detection limit were replaced by half the detection limit prior to calculations, and values rounded to significant numbers according to the detection limit. Refer to the data packages in Appendix C and D for raw data. Differences in detection limits due to improvements in the methodology highlighted in bold. Detection limits in blue font are current as of July 2022. *Analyses added after acquisition of Federation project data. **Analyses added after acquisition of both the Federation and Wagga Tank project data. 26

Acknowledgments

This project received financial support from many government and industry bodies. Financial support include the Minerals Research Institute of Western Australia, Geological Survey of Queensland, Geological Survey of South Australia, Geological Survey of New South Wales, Northern Territory Geological Survey, Geological Survey of Western Australia, Kalamazoo Resources, MCA Nominees, Icen Gold, Siren Gold, Dreadnought Resources, De Grey Mining, Carnavale Resources, Fortescue Metals Group, Newmont, Northern Star Resources, Kairos Minerals, Emmerson Resources, Independence Group, Western Gold Resources, Capricorn Metals, Hexagon Energy Materials, Monger Gold, Strategic Energy Resources, Barton Gold, Ozz Resources, Anax Metals and Lodestar Minerals. In-kind support for the project was provided by CSIRO and LabWest.

Most critically, we thank the in-kind support of the above contributors who provided UltraFine+® analytical results of many, many soils across Australia. This support totalled several millions of dollars and without the large number of results the outcomes of this project would have been severely limited.

In addition to the above industry sponsors, Aurelia Metals (Federation and Dominion prospects) and Peel Mining (Southern Nights and Wagga Tank prospects) provided the Geological Survey of New South Wales and Joe Schifano with access to tenements for sampling soils for this project. Part of the sample collection and analyses for the Federation project area were funded by the MinEX CRC, and Aurelia Metals kindly provided the surface projection of their planned mine shell at Federation.

Executive summary

Assessing geochemical data in mineral exploration often focuses on understanding outliers, such as elevated Au, Cu or Zn. Commonly the largest concentrations are followed up, but landscape types and soil types can significantly influence concentrations. For example, high metal concentrations may be readily identifiable as outliers in a geochemical dataset where samples were collected over mineralisation in areas of shallow residual soils, while the same mineralisation would have a much weaker elemental signal in samples collected over thicker depositional landscapes. With the ability to approximate landscape types from spatial data via machine learning, the UltraFine+® Next Gen Analytics workflow was developed to improve outlier identification within landscape types. As part of a broad research project, the Federation and Wagga Tank project sites were part of early developments with a focus on refining the UltraFine+® method, principal functionality of the machine learning workflow, and first-pass testing of the outputs over areas with tangible exploration targets. For this purpose, the Geological Survey of New South Wales provided 433 soil samples collected over four prospects in Peel Mining and Aurelia Resource's tenements, and we present some example outputs of the workflow here.

These outputs include proxy regolith landscape clusters to provide context for geochemical samples, maps and boxplots of elemental outliers by landscape type, exploration indices for a rapid, first-pass identification of element associations and potential exploration indices, dispersion and source directions, and soil texture diagrams. The data package also contains geochemistry, VNIR (visible to near-infrared spectral mineralogy), FTIR (Fourier transform infrared spectroscopy), particle size distribution and pH and EC (electrical conductivity) as shapefiles. This provides a basic, first-pass interpretation of geochemical samples by proxy regolith type and the identification of otherwise "overlooked or subtle" potential anomalies of interest to mineral exploration.

The data presented herein was analysed in November and December 2020. Since then, the components of the workflow have undergone continuous improvements, especially with regards to the consistency of pH, VNIR measurements, as well as the addition of soil particle size analysis, FTIR and Pd analyses. Both the Wagga Tank and Federation data were essential in developing these improvements. The data has been used in many iterations of the machine learning workflow and the final output for these project sites was run in April 2022 where data availability permitted.

A variety of clustering methods were trialled to generate appropriate proxies for regolith types, and all outputs presented in this report provide a more detailed landscape context than publicly available regolith products. The recommended outputs for the Wagga Tank project area are those produced via an agglomerative algorithm with eight landscape clusters (agg8). Due to the complexity of the landscape, an even larger number of clusters would result in a more detailed approximation of these regolith types. This is also the case for the Federation project area. However, the number of landscape clusters is the result of a balanced approach to represent the major landscape types of the area while also enabling meaningful interpretation of geochemical data. Hence, the recommended outputs for the Federation project area are those produced via a k-means algorithm with four landscape clusters (kmeans4). Larger numbers of clusters (12) were trialled over both sites and have triggered improvements to the future workflow. Future outputs

will contain all outputs for four, eight and twelve landscape clusters. Some of these preliminary outputs are contained in the data packages attached to this report.

The data presented in this report provides useful background concentrations in soil samples as well as those over mineralisation in different landscape settings (shallow to deeper cover) for future exploration activities in the region and surrounding areas. Maximum concentrations for Ag, Cu and Zn were measured within the Wagga Tank project area with 1020 ppb Ag, 146 ppm Cu and 598 ppm Zn and maximum concentrations for Au and Pb were measured within the Federation project area with 51 ppb Au and 585 ppm Pb.

The data also shows some interesting trends in other soil properties with a link to known mineralisation, which provides case study sites for future work within the overall research project with the potential to incorporate these sites with broader background areas and combine landscape types from other areas to “train” data sets for future supervised machine learning to identify similar patterns in other areas.

The UltraFine+® Next Gen Analytics workflow clearly identified the Federation and Wagga Tank mineralisation. The two other prospects, Dominion and Southern Nights were less evident. Some pathfinder element anomalies were located down slope from the prospects when outliers were calculated by individual landscape cluster, highlighting the value of the dispersion direction and slope analysis in landscape context. Southern Nights was approximately 200 m away from a very strong multielement geochemical anomaly, although this appears more influenced by outcropping rock with a radiometric (K-rich, Th-poor) signature. It is not evident whether the geochemical signature identifies the prospect as an offset anomaly. The resulting geochemical signature would clearly identify this region as interesting, but more detailed work would have been required for discovery. Overall, the UltraFine+® Next Gen Analytics approach was robust and effective, providing explorers with much more information to improve exploration using soil samples.

1 The UltraFine+® Next Generation Analytics for Discovery Research Project

Much of Australia's remaining potential mineral wealth is masked by regolith cover that poses a challenge for future mineral exploration, especially in transported cover. The mobile element signature of interest for exploration in these materials is commonly contained in the < 2 µm "ultrafine" particle size fraction (Noble et al. 2020). This is likely due to the presence of "scavenging phases" such as clays, organic compounds and various oxides/oxyhydroxides that dominate this fine fraction (Hall 1998). The CSIRO in collaboration with LabWest developed the novel UltraFine+® method which is optimised for multielement analysis of this ultrafine soil fraction. This improved soil geochemistry workflow generates results with more contrast and increased concentrations of Au, Cu and Zn, and removes the nugget effect, thereby enhancing the reproducibility and reliability of results (Noble et al. 2020).

The UltraFine+® Next Gen Analytics research project leverages and expands on this workflow by adding relevant soil parameters including spectral mineral proxies, pH, EC and particle size distribution to the UltraFine+® method as standard analyses. This provides a wealth of additional data to the standard soil sample exploration package, which enables exploration geologists to investigate the relationships between soil geochemistry and other physicochemical soil parameters and how these relate to buried mineralisation. In addition, the UltraFine+® Next Gen Analytics workflow utilises machine learning approaches to produce landscape context for, and first-pass data interpretation of, these soil sample analyses.

The components of the workflow are undergoing continuous improvements over the course of the research project (conducted from April 2020 to April 2023) which is reflected in improved detection limits and refined outputs. The data for the Wagga Tank and Federation projects presented herein were analysed in October 2020 and November 2020, respectively. However, for this report, the VNIR and FTIR spectra were reprocessed with the latest TSG™-processing template update from November 2021 (for VNIR) and February 2022 (for FTIR) and the UltraFine+® Next Gen Analytics outputs presented in this report were re-processed in June 2022.

1.1 Geological Survey of New South Wales – Cobar projects

The Geological Survey of New South Wales (GSNSW) submitted 433 soil samples from two project sites located within the Cobar Basin near Gilgunnia, approximately 110 km south of Cobar, NSW, as part of the UltraFine+® Next Gen Analytics project (Figure 2). These project sites are herein termed the Wagga Tank and Federation projects.

The Federation project area is located approximately 15 km south of the township of Nymagee and 10 km south of the Hera Mine, Aurelia's operating polymetallic underground mine (Figure 2B). The Federation project covers an area of about 11 km² within Aurelia Metal's tenement package, with two known prospects for copper, lead, zinc, silver and gold, Federation and Dominion. Since the sampling campaign in 2020, Aurelia's Federation Project is being evaluated as a proposed

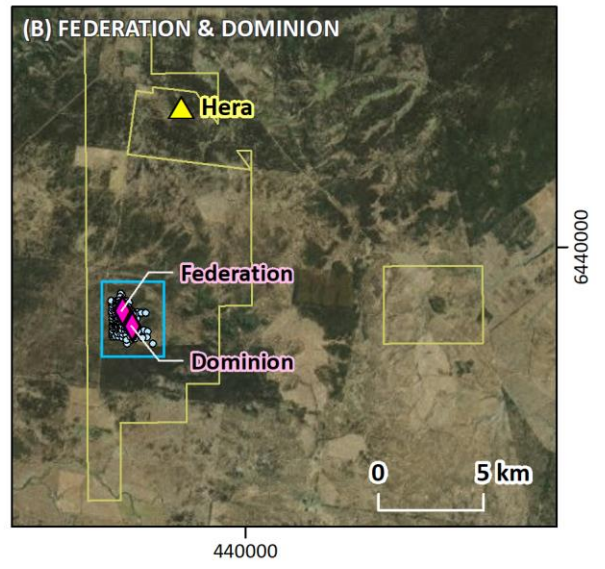
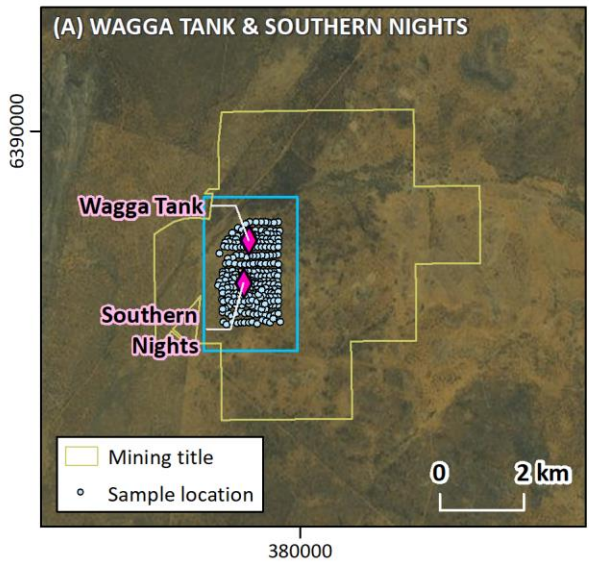
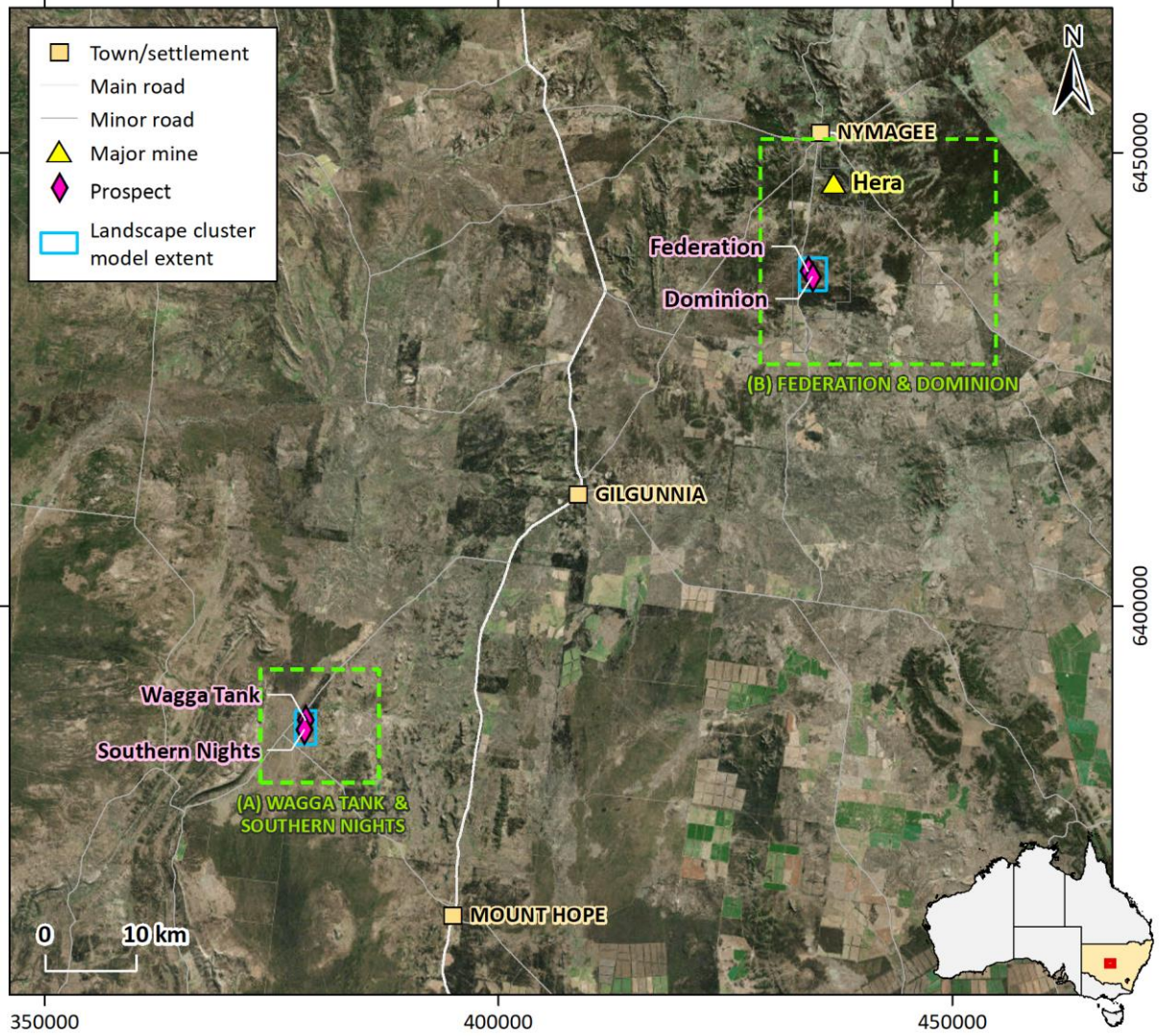


Figure 2: GSNSW’s Cobar project areas (main tile) near Gilgunnia in central western NSW. (A) Wagga Tank project area with Peel Mining’s Wagga Tank and Southern Nights prospects indicated. (B) Federation project area with Aurelia Metal’s Federation and Dominion prospects indicated.

underground mine. The structurally controlled sulphide mineralisation at both prospects is associated with steeply dipping zones of veins and breccia. Dominion is prospective for supergene and sulphide base metal and gold mineralisation, while Federation is prospective for zinc-lead sulphide mineralisation. Gossanous outcrop is present at Dominion while little outcrop has been observed near Federation which is dominated by relatively flat country. Soil anomalies near Dominion show elevated Pb-Zn-Au-As-Sb-Sn and Au-Pb near Federation (McKinnon and Munro 2019).

The Wagga Tank project area is located approximately 30 km northwest of Mount Hope in central NSW (Figure 2A). Wagga Tank covers an area of approximately 8 km² with two known, laminated to massive stratiform zinc-lead sulphide prospects within Peel Mining's tenement package, Wagga Tank and Southern Nights. Both are part of a steeply dipping mineralised zone between the Lower and Upper Amphitheatre Group. The Wagga Tank lead-zinc-copper-gold-silver prospect is a shallow oxide target with some outcrop in the area, while the Southern Nights polymetallic zinc-lead prospect is situated in an area of thicker transported cover (up to 50 m) over *in situ* laterite profiles (up to 100 m; Edgecombe and Soininen 2019).

The UltraFine+® Next Gen Analytics workflow was designed primarily for greenfield exploration over areas with 100s to 1000s of samples, and to generate interpretation of these soil samples prior to significant ground disturbance caused by major roads, built-up areas, and mining and agricultural infrastructure as these can influence the spatial data input layers. However, despite the small number of samples, especially in the immediate vicinity of the Federation and Dominion prospects, and some ground disturbance, both the Wagga Tank (270 samples) and Federation (163 samples) project areas provide valuable example sites to develop and test the workflow over known mineralisation for a suite of elements. While the UltraFine+® Next Gen Analytics for Discovery research project will continue until April 2023, we present here two first-generation, small-scale trial sites with a focus on principal functionality and application of the workflow in a known exploration setting.

The Cobar project areas are dominated by grassland with hot, dry summers and cold winters, an average annual rainfall of 391 mm and an average annual evapotranspiration rate between 200 to 400 mm/year. The mean minimum and maximum temperatures are 12.9 and 25.4°C, respectively (Cobar MO station; Bureau of Meteorology 2022). The groundwater ranges from mainly fresh and marginal salinity (<1600 µS/cm electrical conductivity), with a neutral to slightly alkaline pH usually ranging from 6.8 to 8.2 (Gray et al. 2019).

The two study areas are located within the Cobar region with extensive regolith developed during weathering and erosion which has been extensively studied (Gibson 1999; Chan et al. 2001, 2002, 2004; McQueen 2008). Weathering, erosion and deposition of transported sediments produced a wide variety of *in situ* and transported regolith with weathering profiles ranging from 0 m to >100 m in depth (e.g., outcrop to deep buried palaeovalleys; McQueen 2008). The transported regolith within the Wagga Tank project area is dominated by alluvial sand, silt and minor gravel and clays, and colluvial and aeolian sediments. Slightly weathered, *in situ* bedrock of the Mount Kennan Volcanics outcrops or is covered by a veneer of colluvium/alluvium in the eastern centre of the project area (Figure 3A, B). The Federation project area is dominated by colluvial, residual and aeolian sediments with one prominent feature of slightly weathered bedrock of the Amphitheatre Group (Figure 3C, D) at higher elevation.

The major soil types in both the Federation and Wagga Tank project areas are dominated by kandosols, with smaller areas of calcarosols and rudosols based on the Australian Soil Classification System (Isbell, 2021). These soils are very common for the Cobar region of Australia. Rudosol soils commonly show very weak (B) horizon formation, while kandosols lack significant clay changes with depth and commonly have a sandy to loamy-surface soil, grading to porous sandy-clay subsoils. The soils of the area have low fertility and poor water-holding capacity. Calcarosols include some clay formation and evident pedogenesis, with the abundance of calcium due to the calcareous aeolian sediment parent material.

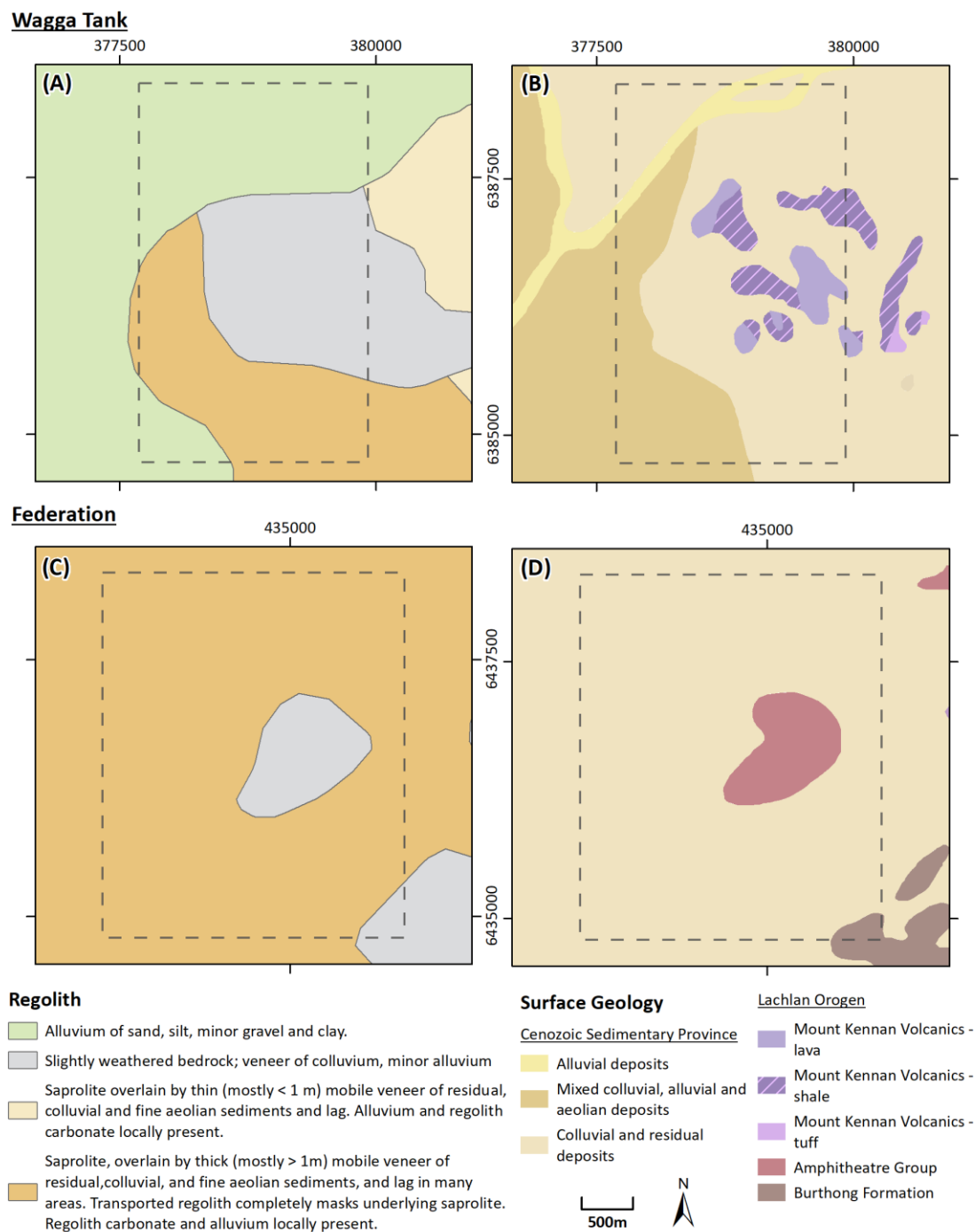


Figure 3: Surface and regolith geology in the Wagga Tank and Federation project areas. Dashed boxes indicate the extend of the modelled areas.

2 The UltraFine+[®] Next Gen Analytics Workflow

The UltraFine+[®] Next Gen Analytics workflow is based on the UltraFine+[®] soil sampling method previously developed by the CSIRO in collaboration with LabWest (Noble et al. 2020). In addition to further improving the UltraFine+[®] method by lowering detection limits and adding valuable soil properties, such as spectral mineralogy, to the standard analyses, the focus of the UltraFine+[®] Next Gen Analytics project is to provide landscape context for the geochemical data acquired and a basic, first-pass data interpretation by incorporating semi-automated machine learning into the workflow.

2.1 Sample collection

Soil samples for the Federation and Wagga Tank project areas were collected by the Geological Survey of New South Wales as part of a collaboration between industry partners, GSNSW and Joe Shifano's PhD study (using soil pXRF analysis and biogeochemistry). Samples were collected in August 2020 and followed the sampling guidelines for UltraFine+[®] (Appendix A). Analyses for 443 samples, including 167 for the Federation project site (Laboratory Job ALW005652) and 276 for the Wagga Tank project site (Laboratory Job ALW005606), were received by CSIRO. Of these, 10 samples were geochemical standards (QC_UFF_320).

2.2 UltraFine+[®] laboratory soil analyses

All soil samples were analysed using the UltraFine+[®] method (Noble et al. 2020) at LabWest Pty Ltd, Perth, Australia. The complete workflow requires <40 g of soil and includes particle size distribution analysis, pH and EC measurements, separation of the ultrafine (<2 µm) size fraction, elemental analyses, and spectral reflectance mineralogy. The components of the UltraFine+[®] workflow are undergoing continuous improvements over the course of the UltraFine+[®] Next Gen Analytics research project, which is reflected in improved detection limits and refined outputs over time. The data presented herein was analysed in November 2020 (Federation) and December 2020 (Wagga Tank). However, VNIR spectra were reprocessed with TSG™ 3.1 (version 3.1 of the VNIR The Spectral Geologist-processing template) and the FTIR spectra were reprocessed with TSG™ 3.3 (version 3.3 of the FTIR The Spectral Geologist-processing template), which were the latest workflow updates at the time of writing this report.

2.2.1 Bulk soil properties

Electrical conductivity (EC) and pH were measured on bulk sample slurries using a TPS AQUA-CP/A meter. Slurries were prepared using de-ionised water with a 1:5 w/w soil-to-water ratio.

2.2.2 Soil sizing

Particle size analyses were conducted on the bulk sample and measured using a Malvern Mastersizer 2000 in suspension. At the time of analysing the Federation and Wagga Tank samples, specific surface area (SSA) was not yet included in the analyses. Hence, SSA will not be reported.

2.2.3 UltraFine+® fine fraction separation

The ultrafine fraction (<2 µm; clay fraction) was extracted from each bulk sample via suspension in de-ionised water, addition of a dispersant and subsequent centrifugation and drying (Noble et al. 2020).

2.2.4 UltraFine+® extraction

The ultrafine fraction (< 2 µm) of all soil samples was processed using a microwave-assisted aqua regia digestion (LabWest MAR-04) at LabWest Pty Ltd, Perth, Australia. The extractions were analysed for a suite of elements (Table 1) using ICP-OES (Perkin Elmer Optima 7300DV) and ICP-MS (Perkin Elmer Nexion 300Q). The microwave-assisted aqua regia digestion uses 0.2 - 0.4 g of soil with a 100 % mixture of 3:1 concentrated HCl:HNO₃. Unlike conventional extraction methods, the material is heated in a closed Teflon tube in an Anton Paar Multiwave PRO Microwave Reaction System for increased metal recovery (Noble et al. 2020).

Table 1: Number of samples analysed with the UltraFine+® workflow for GSNSW’s Federation and Wagga Tank project areas. *Added to the workflow after project data acquisition. **Added to the workflow after data acquisition for the Federation project but before data acquisition for the Wagga Tank project. †Analyses via ICP-OES.

ANALYSES	NUMBER OF SAMPLES	OUTPUTS
Microwave-assisted aqua regia on ultrafine fraction (LabWest MAR-04)	433	Ag, Al [†] , As, Au, Ba [†] , Be, Bi, Br ^{**} , Ca [†] , Cd, Ce, Co, Cr [†] , Cs, Cu, Fe [†] , Ga, Ge, Hf, Hg, I ^{**} , In, K [†] , La, Li [†] , Mg [†] , Mn [†] , Mo, Nb, Ni, Pb, Pd [*] , Pt, Rb, Re, S [†] , Sb, Sc [†] , Se, Sn, Sr [†] , Ta, Te, Th, Ti [†] , Tl, U, V [†] , W, Y, Zn, Zr
Other bulk soil properties	433	EC, pH
Particle size distribution on bulk sample (LabWest SIZE-01)	433	Size fractions <2 µm, <50 µm, <125 µm, <250 µm, <1000 µm, <2000 µm, >2000 µm; d(0.1); d(0.5); d(0.9); specific surface area*
Visible-near-infrared (VNIR) on ultrafine fraction (LabWest NIR/SWIR)	433	Main minerals; kaolinite crystallinity; iron oxide species; relative abundance of iron oxide, kaolinite, white mica and aluminium smectite, iron substitution in kaolinite, chlorite and dark mica, iron and magnesium smectite, mafic minerals with OH; white mica and aluminium smectite composition; Munsell colour; hue; saturation; intensity
Fourier transform infrared spectroscopy (FTIR) on ultrafine fraction (LabWest FTIR)	433	Clay, quartz, and carbonate abundances; total organic carbon; gibbsite index

2.2.5 Visible near-infrared reflectance and short-wave infrared reflectance (VNIR-SWIR)

Visible near-infrared and short-wave infrared reflectance measurements were acquired on the ultrafine fraction (< 2 µm) using a Spectral Evolution RS-3500 spectrometer (Serial Number 18980N3). The spectrometer measures electromagnetic radiation reflected off materials relative to that of a known reference material. The instrument collects spectra in the 350–2500 nm wavelength region, with a resolution of 2.8 nm at 700 nm, 8 nm at 1500 nm and 6 nm at 2100 nm. The spectral bandwidths of the RS-3500 are 1.3 nm at 700 nm, 3.5 nm at 1500 nm and 2.3 nm at 2100 nm, which are resampled to 1 nm to provide 2151 bands. A calibrated piece of sintered Polytetrafluoroethylene (PTFE, also known commercially as Spectralon or Fluorilon) was used as the reflectance standard and measured before each set of soil measurements. The samples were measured with a bifurcated probe with a halogen light source. Each sample measurement consisted of 10 scans, averaged into a single measurement. Spectra were processed using The Spectral Geologist (TSG™) software to extract the main features reported as part of the UltraFine+® output (Table 1).

Final data for GSNSW was reprocessed with version 3.1 of the VNIR TSG™ -processing template and may differ from previously reported, unrefined outputs.

2.2.6 Fourier transform infrared spectroscopy (FTIR)

Mid-infrared spectroscopy measurements were performed using a Bruker Alpha Fourier transform infrared (FTIR) spectrometer (Bruker). All FTIR spectra were collected between 4000 to 360 cm⁻¹ using 16 scans at a resolution of 4 cm⁻¹ and a deuterated lanthanum triglycine sulfate (DLaTGS) detector. Attenuated total reflectance (ATR) measurements were conducted on the ultrafine samples by pressing approximately 10 mg of powder onto the single reflection diamond ATR module using the attached press. The surface of the diamond ATR was cleaned with ethanol and wiped dry with a laboratory cleaning tissue (Kimwipe). Background spectra were obtained in the air with no sample present on the diamond surface prior to the sample measurement. All FTIR measurements were undertaken at room temperature (20 ± 3 °C). Prior to measurements, the interferogram signal (ADC counts) was monitored and only when it passed the QA/QC test were spectra recorded. The processing of spectra was performed using OPUS version 7.2 (Bruker) and TSG™ software. The FTIR spectra are displayed as raw absorbance data and the intensity was not corrected for changes in penetration depth/pathlength.

Final data for GSNSW was reprocessed with version 3.3 of the FTIR TSG™-processing template and may differ to previously reported, unrefined outputs.

2.3 Automated QA/QC

The UltraFine+® Next Gen Analytics workflow is developing automated QA/QC on standards and duplicates for all available analyses, whereby analysis batch quality and internal reproducibility as recorded by standard and duplicate measurements can be assessed via a “traffic light system” which indicates the level of accuracy (standards) and precision (standards and duplicates) of the analyses. The QA/QC automation requires consistent formatting of input data which was not

available at the time the Federation and Wagga Tank data was submitted. Therefore, QA/QC was carried out manually for this project.

2.3.1 Standards

The incorporation of the CSIRO UltraFine+[®] reference material QC_UFF_320 (Appendix B) is routinely recommended every 50 samples for all UltraFine+[®] Next Gen analysis batches (MAR-04, NIR/SWIR and FTIR) excepting SIZE-01, to assess accuracy. The Federation project analyses included 4 QC_UFF_320 for 163 analysed samples and the Wagga Tank project included 6 QC_UFF_320 for 270 analysed samples.

Geochemistry

The analyses for QC_UFF_320 for the Wagga Tank and Federation project area in batches ALW005606 and ALW005652 show that all elements are within acceptable variation (refer to ALW005652_QAQC_Federation.xlsx in Appendix C and ALW005606_QAQC_WaggaTank.xlsx in Appendix D for detailed QA/QC).

Visible near-infrared reflectance

The analyses for QC_UFF_320 for the Wagga Tank and Federation project area in batches ALW005606 and ALW005652 show that all parameters are within acceptable variation (refer to ALW005652_QAQC_Federation.xlsx in Appendix C and ALW005606_QAQC_WaggaTank.xlsx in Appendix D for detailed QA/QC).

Fourier transform infrared spectroscopy

The analyses for QC_UFF_320 for the Wagga Tank project area in batch ALW005606 show that all parameters are within acceptable variation (Refer to ALW005606_QAQC_WaggaTank.xlsx in Appendix D for detailed QA/QC). The analyses for QC_UFF_320 for the Federation project area in batch ALW005652 show that more than 50% of all parameters were not within acceptable variation limits (refer to ALW005652_QAQC_Federation.xlsx in Appendix C for detailed QA/QC).

The Federation and Wagga Tank soil samples were a crucial part of the developmental phase of the FTIR method for the UltraFine+[®] Next Gen Analytics project. Unfortunately, for the Federation project, subsequently developed QA/QC failed 90 of the 163 samples for FTIR. While it was possible to re-process spectra with the latest TSG™ version, material was not retained to collect new measurements. As such, only 73 analyses were reported for the Federation project area. However, the Federation samples were crucial in developing the final method and QA/QC procedure for the FTIR analyses and future analyses have been improved accordingly.

2.3.2 Duplicates

The incorporation of field duplicates is routinely recommended for all UltraFine+[®] Next Gen analyses (MAR-04, NIR/SWIR, FTIR, SIZE-01) to assess precision. We recommend duplicates every 50 samples or a minimum of 10 to 20 duplicate pairs per survey.

No duplicates were supplied for the Federation and Wagga Tank projects.

2.4 Machine Learning - Spatial data integration and clustering

The UltraFine+® Next Gen Analytics workflow applies unsupervised dimensional reduction and clustering methods to spatial data to derive proxy landscapes. These and a range of other spatial outputs are designed to aid a first-pass interpretation of soil analysis results in a broader landscape context.

2.4.1 Spatial data clustering

The UltraFine+® Next Gen Analytics workflow uses semi-automated, unsupervised machine learning (ML) methods to cluster publicly available spatial data to produce proxy regolith types. The spatial data layers used in this workflow were specifically selected for their relationship to regolith landforms and can provide information on landscape position, depth of transported cover, and parent material while minimising the introduction of human interpretation, such as would be the case by including surface geology or regolith landscape type maps. Spatial data layers included in the workflow are Digital Elevation Model Shuttle Radar Topography Mission (DEM SRTM), Multi-resolution Valley Bottom Flatness (MrVBF), Radiometric K (ppm) %, Th (ppm) %, U (ppm) % and barest earth Sentinel-2 satellite data (Table 2). Sentinel-2 satellites, launched via European Union Copernicus Program’s Earth observation mission, collect high-resolution multispectral imagery data of the Earth with a revisit period of 3-5 days (see [Digital Earth Australia data product documentation](#)). The Sentinel-2 data used in this workflow is cropped from the Sentinel 2A Barest Earth Analysis Ready Data based on the soil sample locations. Ten out of thirteen spectral bands are collected: B02, B03, B04, B05, B06, B07, B08, B8A, B11, and B12. A three-component band ratio image is generated from the Sentinel-2 imagery (approximating the equivalent Landsat-7 ETM+ arrangement of Wollrych and Batty, 2007; see [USGS comparison of band equivalence here](#)), with respective RGB bands calculated using $R = B11/B12$, $G = B08/B12$ and $B = B08/B03$.

Table 2: Geospatial covariates used for landscape clustering for the Federation and Wagga Tank project areas.

GEOSPATIAL COVARIATE	LANDSCAPE INFORMATION	RESOLUTION [M]	DATA SOURCE
DEM SRTM	Landscape Position	29	Gallant, J., Wilson, N., Dowling, T., Read, A., Inskeep, C., 2011. SRTM-derived 1 Second Digital Elevation Models Version 1.0. Record 1. Geoscience Australia, Canberra. http://pid.geoscience.gov.au/dataset/ga/72759
MrVBF	Depth of transported cover	86	Gallant, J., Dowling, T., Austin, J., 2012. Multi-resolution Valley Bottom Flatness (MrVBF). v3. CSIRO. Data Collection. https://doi.org/10.4225/08/5701C885AB4FE
Radiometrics K pct	Parent material	104	Poudjom Djomani, Y., Minty, B.R.S., 2019a. Radiometric Grid of Australia (Radmap) v4 2019 filtered pct potassium grid. Geoscience Australia, Canberra. http://dx.doi.org/10.26186/5dd48d628f4f6
Radiometrics Th ppm	Parent material	104	Poudjom Djomani, Y., Minty, B.R.S., 2019b. Radiometric Grid of Australia (Radmap) v4 2019 filtered ppm thorium. Geoscience Australia, Canberra. http://dx.doi.org/10.26186/5dd48e3eb6367
Radiometrics U ppm	Parent material	104	Poudjom Djomani, Y., Minty, B.R.S. 2019c. Radiometric Grid of Australia (Radmap) v4 2019 filtered ppm uranium. Geoscience Australia, Canberra. http://dx.doi.org/10.26186/5dd48ee78c980
Sentinel-2	Surface material and dispersion	20	Digital Earth Australia https://explorer.sandbox.dea.ga.gov.au/products/s2_barest_earth

The total area modelled for the Federation and Wagga Tank project sites were 11 km² and 8 km², respectively, and all spatial data layers were re-gridded to the highest input layer resolution (20 m). The dimensionality reduction algorithm UMAP (Uniform Manifold Projection and Approximation; McInnes et al. 2018) was applied to transform the data to a three-dimensional latent space (a representation of data compressed to 3 dimensions, in which similar data points are closer together in space; Figure 4) to aid more efficient clustering and provide a framework for visualisation. The UMAP algorithm was used as it captures non-linearities within the data and preserves local structures. The method does not explicitly include any location information, spatial relationships, or spatial features (e.g., textures) as only the per-pixel values of each input layer were considered.

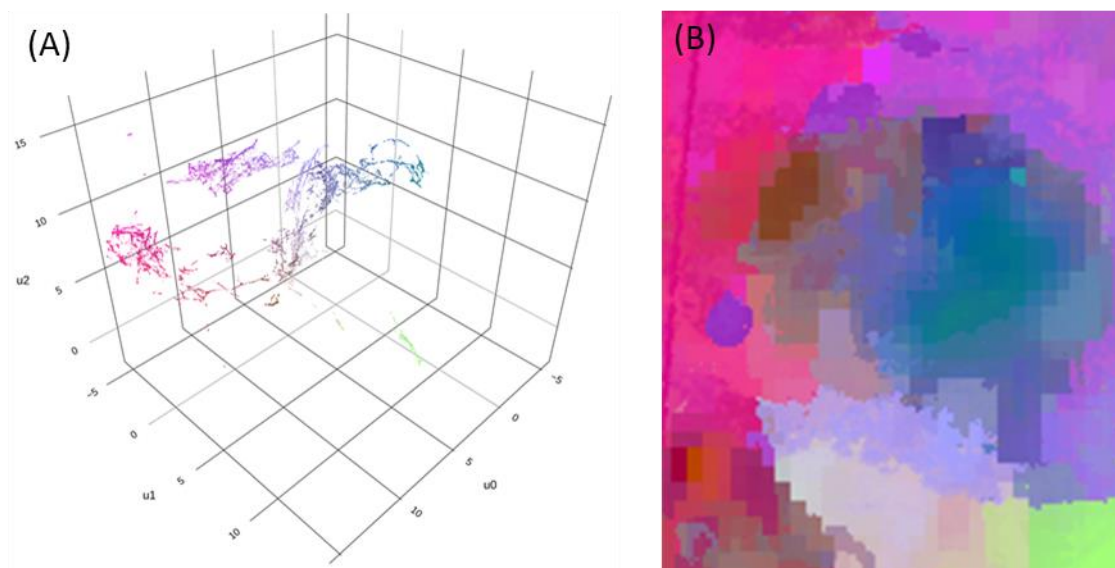


Figure 4: (A) Scatter diagram of pixel values for GSNSW's Federation project site embedded in a 3-dimensional latent space using the dimensionality reduction algorithm UMAP. Points are coloured using an RGB of the axes (u0, u1, u2) values. (B) Pixel values projected into 2-dimensional space for spatial context over the Federation project area.

Two clustering algorithms are used in the UltraFine+[®] Next Gen Analytics workflow to cluster locations with similar spatial data signatures after reduction with UMAP: k-means and agglomerative (hierarchical) clustering. Both algorithms force all sample points into a given number of clusters. Due to the intended application of the clustered proxy landscape types to geochemical sample interpretation and the added complication that these landscape models are intended to be used over a variety of area sizes (1 km² to 50,000 km²) the number of clusters has been predetermined for the workflow. Four clusters are routinely used for k-means (for project areas <20 km²) and eight clusters are routinely used for agglomerative clustering (for project areas >20 km²). Herein, we term these 'kmeans4' and 'agg8'.

K-means is an iterative clustering algorithm that randomly selects a cluster centre from a dataset to compute distances of all data points from this selected centre from which it calculates a new centre point. This is repeated until four centroids (geometric centres) with maximum distance from each other have been sampled. During each iteration, all data points are subsequently assigned to the closest cluster centre based on their Euclidean distance. The algorithm then calculates the average of all points in each cluster and moves the centre point to this location.

Agglomerative clustering is a hierarchical clustering algorithm that successively merges individual data points. The UltraFine+® Next Gen Analytics workflow agglomerative clustering model uses a Ward linkage criterion (scikit-learn default) to determine the distances between clusters for merging. Due to the nature of the hierarchical clustering algorithm, training an agglomerative clustering model uses large computational resources and the trained model could not be used for predicting new samples. Therefore, we used 1) a subset of the samples to train an agglomerative clustering model and predict the labels; 2) these samples and their predicted cluster labels were used to train a Random Forest model; and 3) we used the Random Forest model to put the remaining samples into corresponding clusters. At step one, about 70% of samples were randomly selected and the remaining samples were predicted in step three. The out-of-bag (OOB) score of the Random Forest model is above 0.99, indicating a good representation of the agglomerative clustering model.

Once all data points are clustered, a colour is assigned to each cluster with similar projected spatial features (Figure 5; colours are assigned based on mean cluster MrVBF values). These clusters can be plotted by cluster colour according to their corresponding spatial reference (Figure 6G, H) to generate maps which are used to evaluate the proxy regolith type each cluster corresponds to. These maps are output as GeoTIFF files (see Appendix C and D) as well as PNG files (see section 3.1).

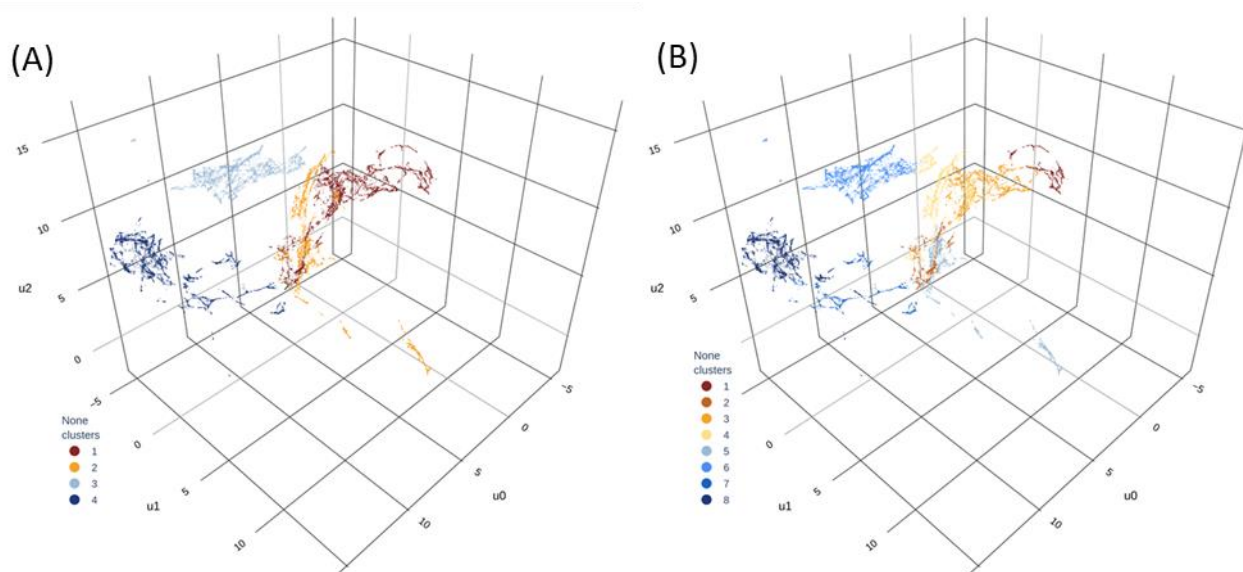


Figure 5: Clustered data points of the GSNW’s Federation Project site in the 3-dimensional latent space grouped by cluster colour to visualise data separation. (A) Data points clustered into 4 clusters using the k-means algorithm (kmeans4). (B) Data points clustered into 8 clusters by an agglomerative clustering algorithm (agg8). Refer to Appendix B for an interactive plot.

2.4.2 Geochemical outliers by landscape type

Prior to identifying outliers within the geochemical dataset, all values below the detection limit were replaced with half the detection limit value for each respective element. Outliers were calculated on log-transformed data and are defined as values that are greater than 1.5 times the interquartile range outside the first and third quartiles. Geochemical data were also grouped by

their corresponding landscape cluster and outliers were calculated for each of these clusters. The workflow automatically produces boxplots by element and landscape type as well as in spatial context plotted over a landscape cluster map for each element (see section 3.3). In addition, shapefiles with outliers grouped by element and landscape type are produced (see Appendix C and D).

2.4.3 Principal Component Analysis

Principal Component Analysis (PCA) is performed on centred-log-ratio and quantile-normalised transformed geochemical data for each soil sample. All values below the detection limit were replaced with half the detection limit value for the respective element. The workflow reduces each data point (soil sample) from n dimensions (number of analysed elements) into five principal components (PC0 to PC4) while preserving the maximum of information. The explained variance (importance) of the principal components decreases from PC0 to PC4. For each principal component, the loading (influence) of each element is plotted on a spider diagram to illustrate the general geochemical affinity (see Section 3.4). The spatial distribution of samples coloured by the weight of the principal component is another automatic output (see Section 3.4). A threshold of 10 % is applied for missing data points (due to non-analysis) to determine if an element is included in the PCA analysis. If less than 10 % of data points of a given element are missing, the element is included in the PCA analysis, but no principal components are calculated for the affected sample.

2.4.4 Soil sizing

Particle size analysis is conducted on the field sample (<2 mm) dried soil with the results reported with % of sand, silt and clay. These values are plotted in a ternary plot commonly used in soil science to provide a general textural class (Soil Science Division Staff, 2017). These are plotted using pyrolite (<https://doi.org/10.21105/joss.02314>) with colours depicted as the broad soil textural classes (e.g., sandy loam, silty clay). These classes are presented on the soil textural triangle and in spatial context allowing users to see key changes in the landscape soil morphology.

2.4.5 Dispersion and source direction

Dispersion/source direction and slope are extracted at each point from Australia-wide slope (Gallant and Austin 2012a) and aspect (Gallant and Austin 2012b) datasets which were derived from a smoothed version of the SRTM DEM processed to reduce noise. Dispersion direction indicates the direction in which the land surface slope faces (i.e., the aspect) and is generated on a grid over a given project area. Source direction is the opposite of this (i.e., uphill) and is generated for each sample point. Outputs are available as shape files with associated layer files that display both source and dispersion direction as scaled arrows. The size of the arrow is proportional to the slope degree. At the time of writing this report, the source direction outputs were still under development to produce automated and uniformly spaced grids that are applicable over a wide range of project area sizes. However, we present here an initial output for the Wagga Tank and Federation project areas.

3 The UltraFine+® Next Gen Analytics Outputs

The UltraFine+® Next Gen Analytics workflow uses machine learning to integrate spatial data and soil properties in several derived outputs. For each project area, these outputs include proxy regolith landscape clusters for a given project area, maps and boxplots of elemental outliers by landscape type, exploration indices, soil texture diagrams, source and dispersion directions, regolith geochemical indices and catchment analysis. At the time of writing this report, regolith geochemical indices and catchment analysis were still under development. As a result, these parameters will not be reported for the GSNSW data. Most outputs are available in GeoTIFF, PNG, shapefile and CSV formats. Please refer to Appendix C and D for available outputs contained in the Federation and Wagga Tank project data packages, respectively.

3.1 Landscape clusters

As part of the UltraFine+® Next Gen Analytics workflow, spatial data clustering is used to derive proxy regolith types to provide landscape context for geochemical samples. These proxies are derived from spatial data only, and are not based on physical soil sampling. A variety of clustering methods with varying numbers of clusters (proxy landscape types) have been trialled in several locations across the Australian continent, with the aim to apply landform mapping over a wide range of settings and project sizes. At the time of writing this report the output of the UltraFine+® Next Gen Analytics includes “kmeans4” (a four-cluster k-means clustering) for small areas (< 20 km²) and “agg8” (an eight-cluster agglomerative hierarchical clustering) for larger areas (> 20 km²). All outputs of the workflow are automatically generated for both algorithms and can be found in Appendix C for the Federation and Appendix D for the Wagga Tank projects. Optimising and ground-truthing the UltraFine+® Next Gen Analytics workflow for application on all scales and for a variety of landscapes across the Australian continent as well as a trial site in New Zealand (Figure 1) is part of ongoing research.

3.1.1 Comparison of unsupervised clustering methods

Since the UltraFine+® Next Gen Analytics workflow is designed primarily for greenfield exploration for interpretation of soil samples prior to significant ground disturbance, anthropogenic infrastructure such as major roads, built-up areas, as well as mining and agriculture related infrastructure are usually masked to be excluded from the landscape models, as these can influence the spatial input layers, such as the regolith ratios derived from Barest Earth Sentinel-2 data. However, given that the main areas of interest within the Federation and Wagga Tank project areas are those with the most apparent ground disturbance, masking was not applied to either project area. The potential influence of surface disturbance on the machine learning derived landscape cluster outputs should be considered when interpreting geochemical data by landscape type.

Federation project area

For the Federation project area, the agglomerative clustering algorithm (with 8 clusters; Figure 6H), captured the main features (maximum variation) of the input layers (Figure 6A-D) in more detail than k-means (with 4 clusters; Figure 6G). In both cases however, the resulting outputs provide a more detailed landscape context than publicly available interpreted regolith and surface geology products (Figure 6E, F). The appropriate number of clusters for a given project area depends on area size, the resolution of the input layers, the complexity of the respective landscape, and the needs of the data user.

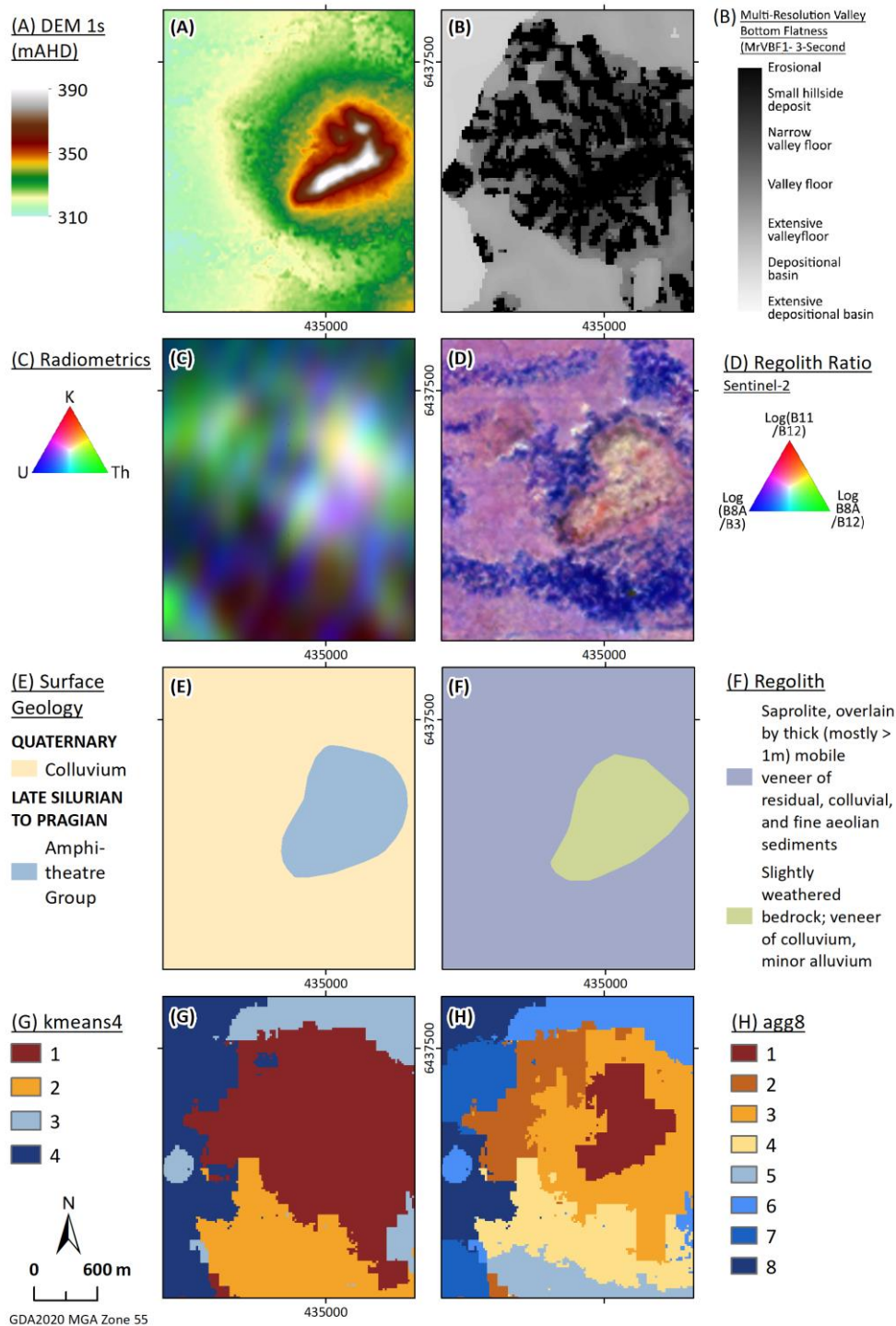


Figure 6 (previous page): Proxy regolith clustering input layers (A-D) and comparison of traditional geological maps (E, F) to machine learning derived outputs (G, H) over the Federation project area. (A) 1-second DEM SRTM (Gallant et al. 2011). (B) Continuous MrVBF (Gallant et al. 2012). (C) RGB image of radiometric grid of Australia (Poudjom Djomani and Minty 2019). (D) RGB image of sentinel-2 regolith ratios. (E) Surface Geology (Raymond et al. 2012) (F) Regolith Geology (Gibson 1998). (G) Proxy regolith types derived via k-means with four clusters plotted in spatial context. (H) Proxy regolith types derived via agglomerative clustering with eight clusters plotted in spatial context.

A comparison of the machine learning derived landscape clusters with input layers (Figure 6A-D) show that, uncharacteristically for such a small project area (approximately 11 km²), the complexity of the landscape requires a larger number of clusters than expected. This is especially apparent when the data is viewed in the jitter-box plot derived via UMAP which represents similar data points closely positioned together in a 3-dimensional space (Figure 7A). The UMAP jitter-boxplot shows low density clusters separated in space from each other, which may warrant further separation that may not be readily discernible for the human eye from input layers (Figure 6A-D). Due to this complexity, the standard amount of clusters (4 in Figure 7B, and 8 in Figure 7C) do not capture all of the distinct landscape types, and an even larger number of clusters (12; Figure 7D) results in a more detailed approximation of these regolith proxies (Figure 8A-D).

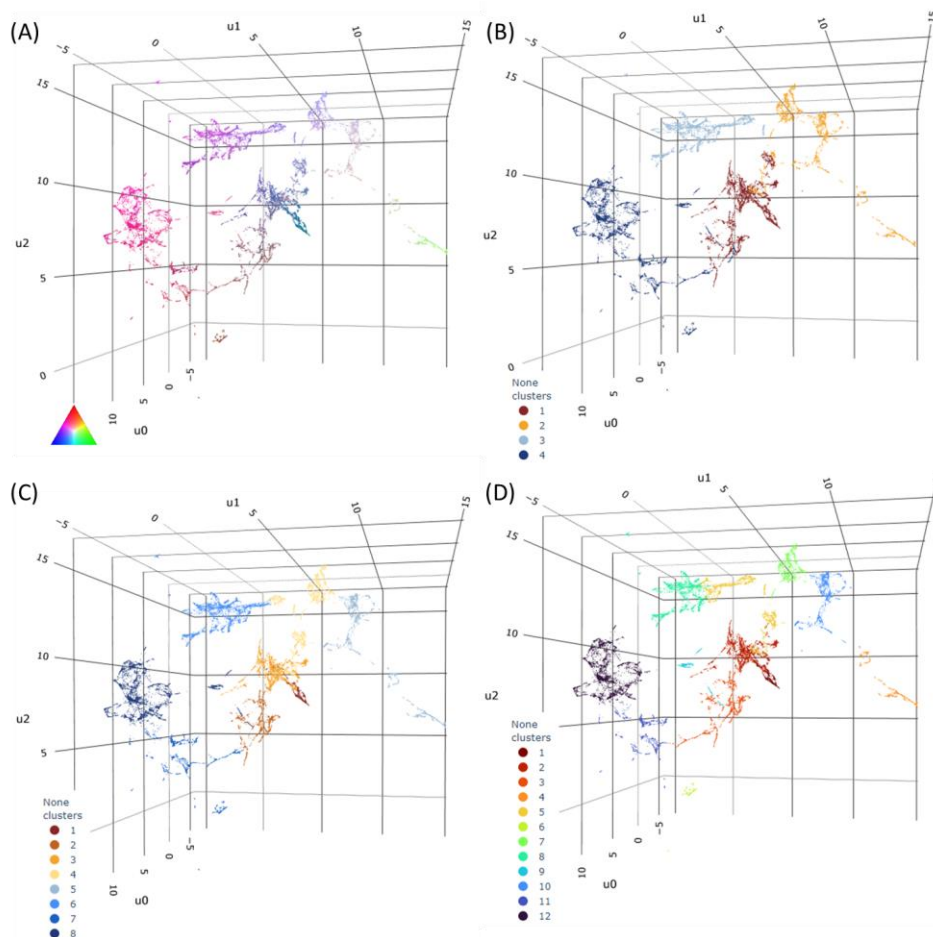


Figure 7: Comparison of 3-dimensional projection plots of data points for the Federation project area derived via UMAP and how these data points are clustered when different cluster numbers are applied. Colours are applied to each landscape cluster to visualise data separation. (A) Pixel values coloured using an RGB of the axes (u0, u1, u2) derived via the dimensionality reduction algorithm UMAP. (A) Data points clustered into 4 clusters using the k-means algorithm (kmeans4). (B) Data points clustered into 8 clusters using the agglomerative algorithm (agg8). (D) Data points clustered into 12 clusters using the agglomerative algorithm (agg12).

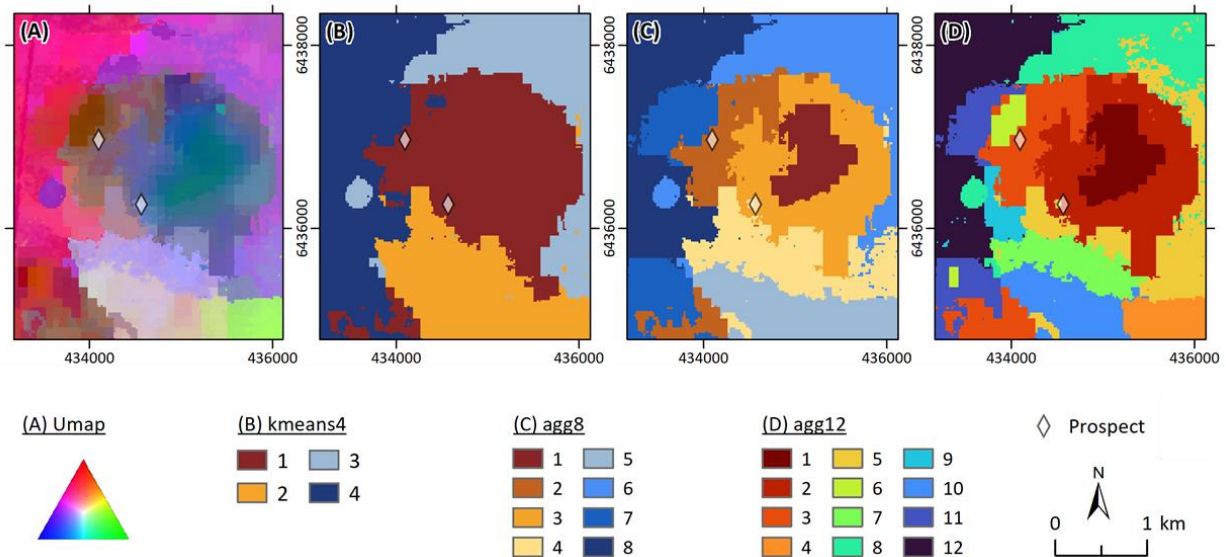


Figure 8: Comparison of dimensionality reduction and clustering algorithm outputs plotted in spatial context over the Federation project area. (A) Spatial representation of cluster similarities in RGB colours derived via the dimensionality reduction algorithm UMAP; the more similar the colour, the more similar the spatial characteristics of the data points. Subsequent landscape cluster outputs are derived from this output and in general, the closer they match the UMAP distribution the more representative these clusters are. (B) Landscape clusters derived via k-means clustering with four clusters. (C) Landscape clusters derived via agglomerative clustering with eight clusters. (D) Landscape clusters derived via agglomerative clustering with 12 clusters.

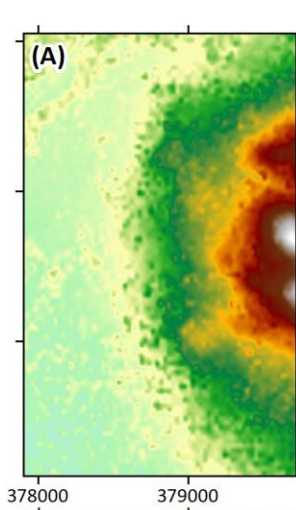
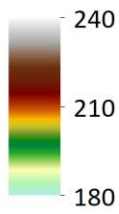
Despite the complexity of the landscape, the purpose of the landscape clustering is to generate landscape context for geochemical samples. Hence, the number of samples across a given area must be considered to avoid small clusters with few or no samples. The resulting number of landscape clusters are, therefore, a balanced approach to represent the major landscape types while also enabling meaningful interpretation of geochemical data. Due to these constraints, while the regolith over the Federation project area is more adequately represented by the agg8 or even agg12 outputs, we recommend the review of geochemistry in the context of the kmeans4 outputs.

Wagga Tank project area

For the Wagga Tank project area, both clustering algorithms, k-means (with 4 clusters) and agglomerative (with 8 clusters), captured the main features (maximum variation) of the input layers (Figure 9G, H) and provide a more detailed landscape context than publicly available regolith and surface geology products (Figure 9E, F). As is the case for the Federation project area, the Wagga Tank project area too, shows a highly complex landscape setting for such a small project area (approximately 8 km²) and requires a larger number of clusters than expected. The regolith over the Wagga Tank project area is more adequately represented by the agg8 outputs and, unlike the Federation project area, sample numbers per cluster are generally appropriate to review geochemical results in the context of the agg8 outputs.

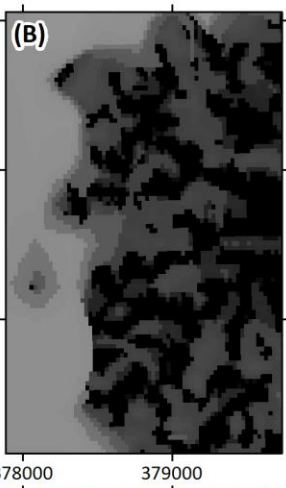
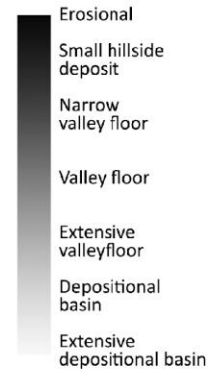
Figure 9 (next page): Proxy regolith clustering input layers (A-D) and comparison of traditional geological maps (E, F) to machine learning derived outputs (G, H) over the Wagga Tank project area. (A) 1-second DEM SRTM. (B) Continuous MrVBF. (C) RGB image of radiometric grid of Australia. (D) RGB image of sentinel-2 regolith ratios. (E) Surface Geology. (F) Regolith Geology. (G) Proxy regolith types derived via k-means with four clusters plotted in spatial context. (H) Proxy regolith types derived via agglomerative clustering with eight clusters plotted in spatial context.

(A) DEM 1s
(mAHD)

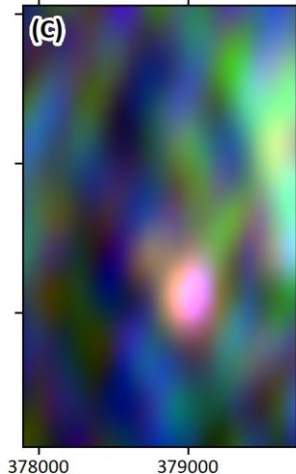
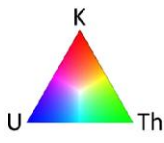


(B) MrVBF 1s

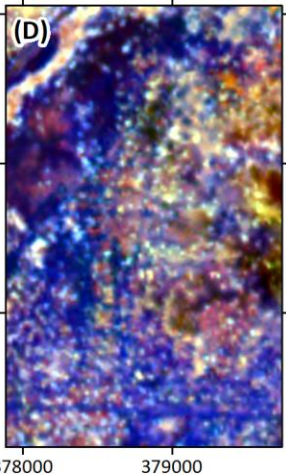
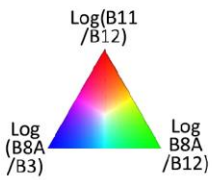
(B) MrVBF 1s



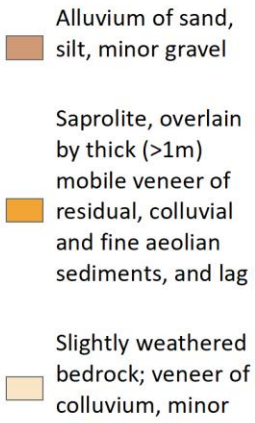
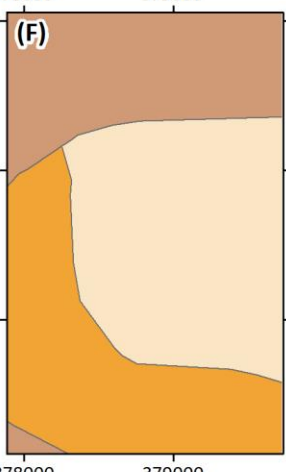
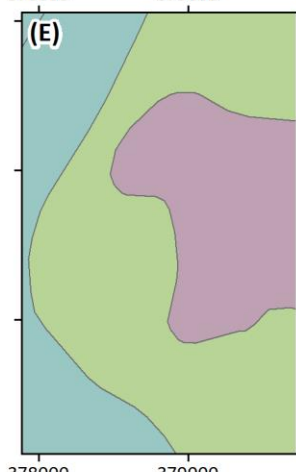
(C) Radiometrics



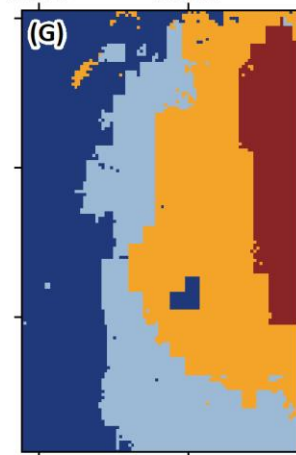
(D) Regolith Ratio
Sentinel-2



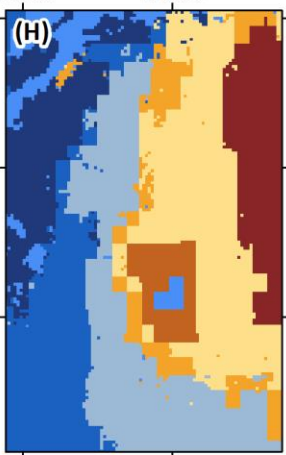
(E) Surface
Geology



(G) kmeans4



(H) agg8



3.1.2 Landscape types

While the unsupervised landscape clustering approach does not assign a particular class to a cluster (see three-dimensional projection in Figure 7A), the spatial representation of these clusters corresponds well with broad landscape patterns in both project areas (Figure 10 and Figure 12). Therefore, proxy regolith types for the project areas can be interpreted from the landscape clusters by comparing each cluster to the input layers (Figure 6A-D and Figure 9A-D). In addition, the clusters were also compared to publicly available surface geology (Figure 6E and Figure 9E) and regolith geology (Figure 6F and Figure 9F). It is important to note that these regolith proxies are generalised descriptors aligning with most of the landscape features within a cluster and no ground-truthing was undertaken for either project area. However, we highlight below several examples of the overall positive alignment of landscape clusters with the input layers and take note of some of the constraints.

Due to the complexity of the landscape, the eight-cluster agglomerative clustering output is recommended for both project areas. However, given the constraints around the number of samples per landscape clusters, in the following we assign regolith proxies to both the kmeans4 (recommended for Federation) and the agg8 (recommended for Wagga Tank) landscape clusters.

Federation project area

Overall, both kmeans4 and agg8 outputs are useful regolith proxies for the Federation project area and provide more landscape context than publicly available surface geology and regolith maps (Figure 6E, F). While kmeans4 readily provides an overview of the main elevated residual and subcropping landscapes (dark brown, landscape cluster 1, Figure 10A), differences in parent material related to the radiometric signature of shallow cover (landscape cluster 2, orange, versus landscape cluster 3, grey-blue) and areas of deeper cover (landscape cluster 4, dark blue), the agg8 output provides a more differentiated output, assigning three instead of one landscape clusters to residual and erosional settings (Figure 10B). The maximum variation of any input layer usually influences which landscape cluster a given data point is assigned to. This means that, where a model is set to only four landscape clusters and depth of cover is the parameter with the maximum variation, this feature will be defining. Additional landscape classes provide the possibility to include secondary features, such as parent material, as reflected in the radiometric data. This is most evident in the west of the Federation project area, where deeper cover materials have been separated into two distinct units based on their radiometric signature (landscape clusters 7, mid blue, and 8, dark blue). Shallow sheetwash materials in the south-east of the project area have also been separated into two landscape clusters (landscape clusters 4, yellow, and 5, grey-blue) in the agg8 output.

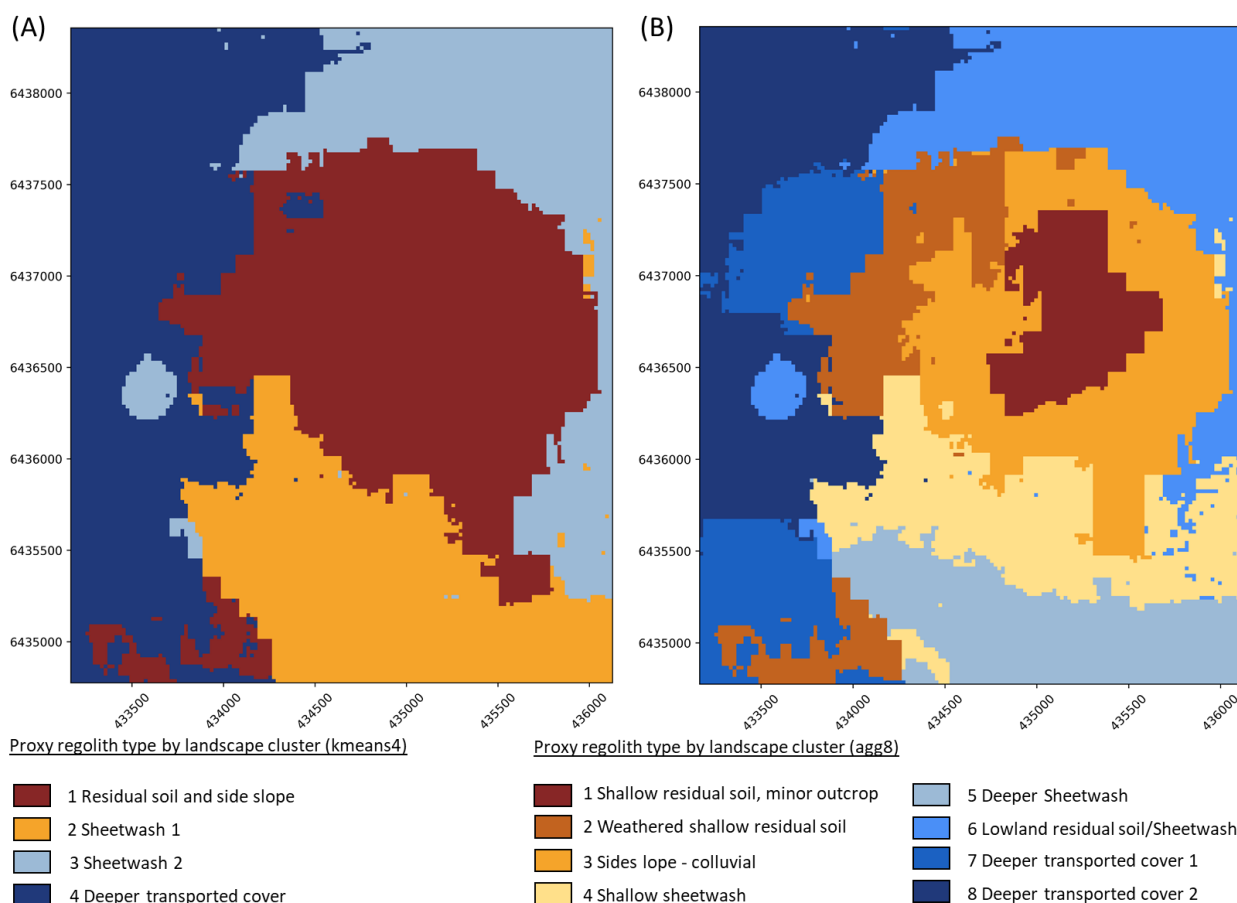


Figure 10: Correlation of proxy regolith types with landscape clusters for the Federation project area generated by (A) an agglomerative clustering algorithm with eight clusters and (B) a k-means clustering algorithm with four clusters. Please refer to the text for more detail on these proxy regolith types.

Outcrop, residual and erosional landscape settings

Agg8 landscape clusters 1 (dark brown), 2 (orange) and 3 (light brown) align well with residual and erosional landscape settings. As evident in DEM, MrVBF and satellite imagery (Figure 11D, F, G) landscape cluster 1 (dark brown) includes settings with the highest elevation and is characterised as residual soils and outcrop with a distinct radiometric signature (white corresponds with dark brown cluster, Figure 11E) and aligns well with the available regolith map, which indicates *in situ* regolith (Figure 6F). This cluster also displays the lowest weathering intensity within the project area (Wilford and Roberts 2019; Figure 11I). Landscape cluster 3 (orange) corresponds with slightly more weathered colluvial materials on side slopes with gradual changes in the radiometric signature (Figure 11E) and relatively sparse vegetation (see satellite imagery, Figure 11F). The light brown landscape cluster 2 is characterised by residual soils to shallow cover as indicated by MrVBF (Figure 11D) and differences to other landscape clusters are not readily evident when viewing input layers only. However, the spatial distribution of this landscape cluster correlates well with relatively strongly weathered materials as indicated by the weathering intensity (Figure 11I) which is derived from DEM and radiometric data and could be linked to the age of cover. A shift towards material richer in Th compared to the orange landscape cluster 3 can also be observed (Figure 11E). In the kmeans4 landscape cluster output, these three landscape settings (residual soils/outcrop, side slope and weathered residual soil) are combined into the dark brown landscape cluster 1 (Figure 11B).

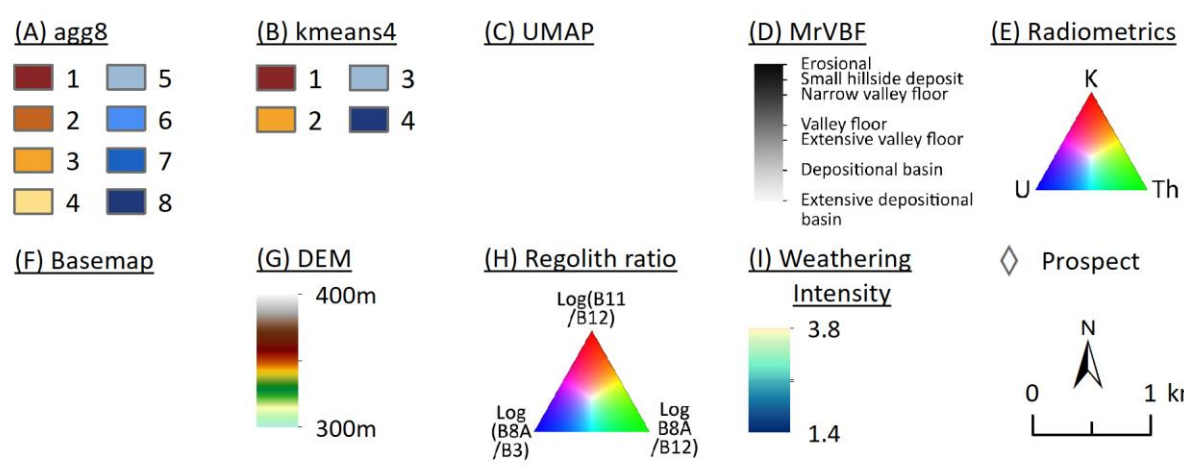
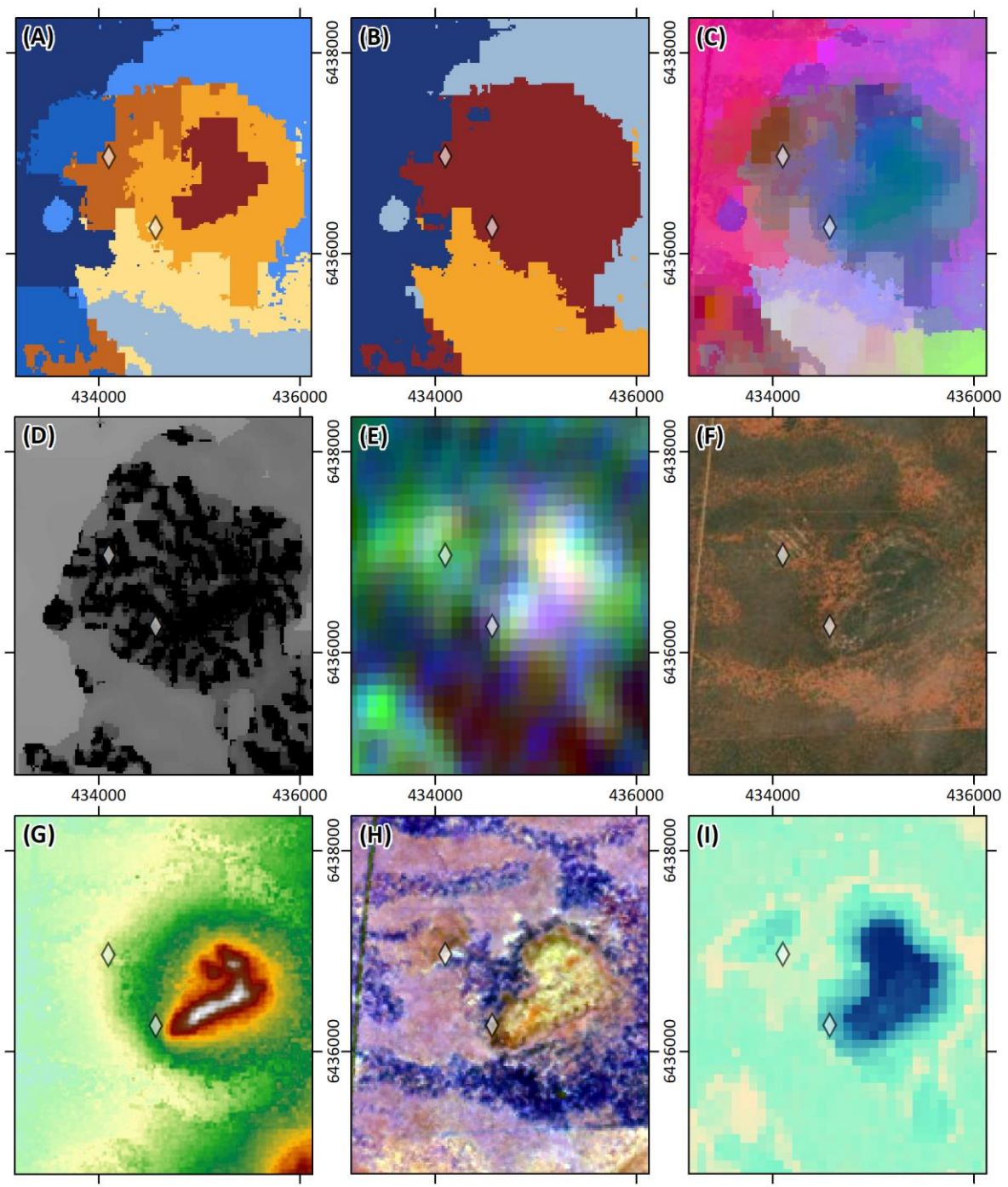
Cover materials in depositional landscape settings

The difference between agg8 landscape clusters 4 (yellow) and 5 (grey-blue) while similar in their radiometric signature (Figure 11E) is readily discernible in regolith ratios (Figure 11H) and corresponds well with changes in vegetation as indicated by satellite imagery (Figure 11F). These clusters also vary slightly in relative depth of cover as evident in MrVBF and variations in DEM (Figure 11D, G) with the yellow landscape cluster indicating relatively shallower sheetwash and grey-blue indicating relatively deeper sheetwash materials. In the kmeans4 output, these two landscape clusters are combined as landscape cluster 2 (orange) and are strongly influenced by their radiometric signature (increase in K, Figure 11E) compared to all other landscape clusters.

Landscape clusters 7 (mid blue) and 8 (dark blue) correspond well with deeper transported cover in lower lying landscape settings readily evident in DEM and MrVBF input layers (Figure 11D, G) and we term them here Deeper Transported Cover 1 and Deeper Transported Cover 2 with distinct differences in their radiometric signature, with landscape cluster 7 (mid blue) shifting towards Th-rich materials, while landscape cluster 8 has a stronger U component. The mid-blue landscape cluster in the north-western part of the Federation project area correlates strongly with an area cleared for drilling (Figure 11F) which may have influenced the regolith ratio (see brown area close to the Federation prospect in Figure 11H). This specific area also displays a prominent radiometric signature (Figure 11F) and has been separated out into a distinct and spatially closely defined landscape cluster in the trial agg12 output (Figure 8D). In the kmeans4 output the two deeper cover proxy landscapes are combined as landscape cluster 4 (dark blue; Figure 11B) with a strong correlation to areas of deeper cover (see MrVBF; Figure 11D).

Due to the limitations of the 8 clusters in a complex landscape setting, landscape cluster 6 (light blue) combines two regolith proxies. Lowland residual soils (e.g., “round blob” in the far west middle of the Federation project area, Figure 11A) are indicated by a slight increase in elevation with distinctly shallower cover and are evident in the MrVBF input layer in otherwise low-lying deeper cover (Figure 11D, G). Several of these landscape features stand out in the 2-dimensional representation of data point similarities as dark purple (Figure 11C). The agglomerative algorithm has combined these with other purple/pink shades in the northeast and easternmost parts of the Federation project area that is dominated by sheetwash material with similar depth of cover to landscape cluster 5 (grey-blue), however, with a distinctly different radiometric signature (less K; Figure 11E). The kmeans4 output (landscape cluster 3, grey-blue) differs little in these areas (Figure 11B).

Figure 11 (next page): Spatial layers used for the assessment of landscape clusters produced by machine learning over the Federation project area. (A) Landscape clusters derived via agg8. (B) Landscape clusters derived via kmeans4. (C) 2-dimensional representation of cluster similarities derived via UMAP. (D) MrVBF as proxy for depth of cover. (E) Radiometric data as indication for differences in parent materials. (F) Satellite imagery. (G) DEM. (H) Regolith ratio. (I) Weathering intensity. Grey diamonds in the figure indicate the approximate location of the Federation and Dominion prospects.



Wagga Tank project area

Overall, both kmeans4 and agg8 outputs are useful regolith proxies for the Wagga Tank project area, and both exhibit similar patterns mapping units in a transition from upland residuum into fluvial channels. In the agg8 output, the model included a major road in the north-eastern corner of the project area in landscape cluster 8 (dark blue), which exemplifies the influence of infrastructure on regolith landscape models. Where possible, in subsequent models of the UltraFine+® Next Gen Analytics project such features will be masked. Similarly to the Federation project area, the regolith within the Wagga Tank project is complex for such a small project area and additional landscape clusters would produce more representative proxy regolith types. This is especially apparent for landscape clusters 4 (kmeans4 output) and 6 (output) where a prominent radiometric potassium “anomaly” is not separated into its own cluster (Figure 13A-C, E, I). However, due to the constraints around representative numbers of samples in each landscape cluster, we recommend the review of geochemistry in the context of the kmeans4 outputs for the Wagga Tank project area.

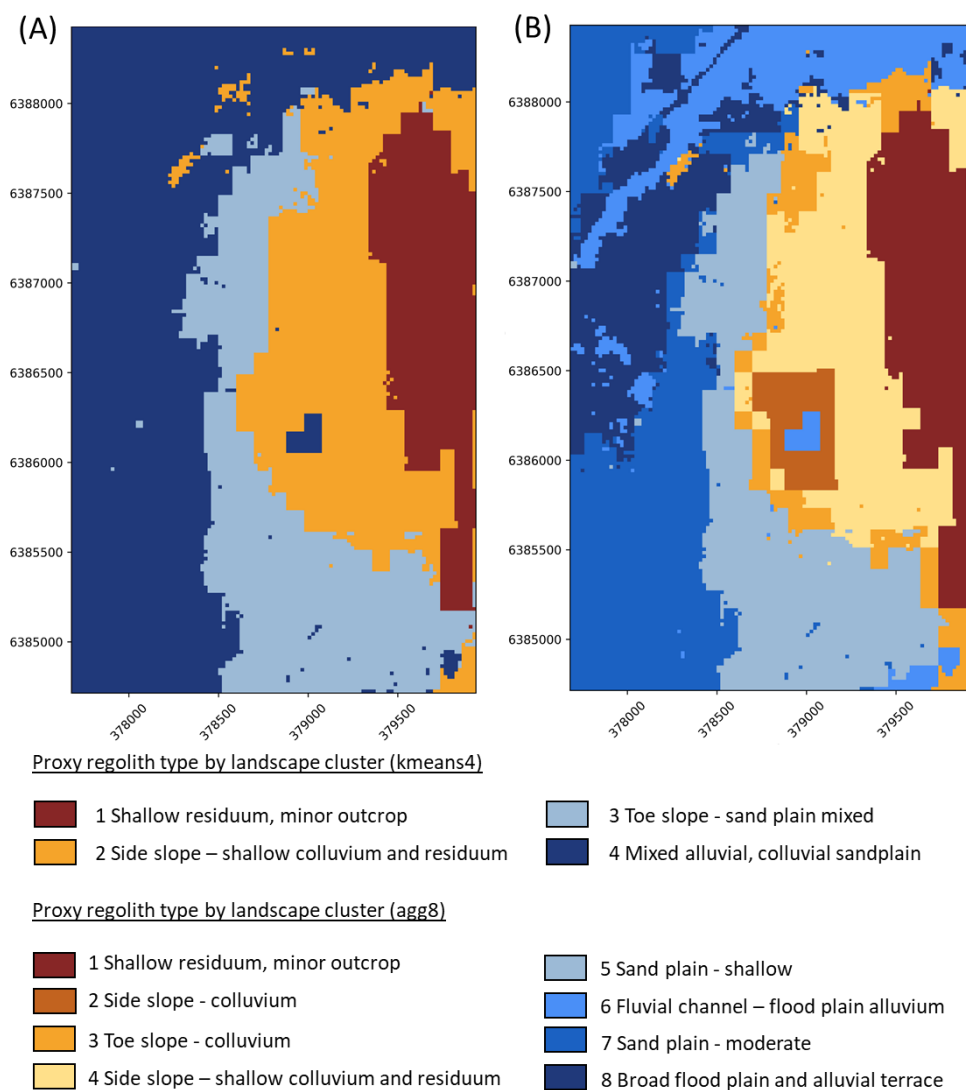


Figure 12: Correlation of proxy regolith types with landscape clusters for the Wagga Tank project area generated by (A) an agglomerative clustering algorithm with eight clusters and (B) a k-means clustering algorithm with four clusters. Please refer to the text for more detail on these proxy regolith types.

Outcrop, residual and erosional landscape settings

The agg8 landscape cluster 1 (dark red-brown) represents upland residual areas, with potentially some outcropping rocks. It is interesting to note that the pattern of the residual upland area in the agg8 output is almost identical to the same-coloured unit in kmeans4 showing that this unit is very distinctive regardless of the increase from 4 to 8 potential landscape types (Figure 12A, B). This unit is unlikely to have transported cover, although many of these environments may have some wind-blown contribution to the soil composition. Landscape clusters 2 (orange), 3 (light brown) and 4 (pale yellow) in the agg8 output relate to erosional landscape settings mainly in low slope positions. This is reflected in the DEM and satellite imagery (Figure 13F, G). These locations are also areas with potentially mixed cover, mainly colluvium with some aeolian materials, and are shallow in nature. The cover thickness commonly increases from dark red (landscape cluster 1) to dark blue (landscape cluster 8). However, at Wagga Tank the orange (landscape cluster 3 in agg8) is likely to have thicker cover and sit in lower slope positions than the pale yellow (landscape cluster 4) materials. This also explains why there are some small areas of the orange landscape observed adjacent to the depositional blue (landscape clusters 6 and 7) and blue-grey (landscape cluster 5) landscape clusters (Figure 13A, B, D, G).

The kmeans4 approach clusters landscape clusters 2 to 4 in the agg8 output into one class (landscape cluster 2) in orange (Figure 12A, B). The key defining feature for these erosional sites is dictated by the MrVBF showing several black and darker grey features that are representative of upland and erosional settings (Figure 13D).

The influence of radiometric data on the residual and erosional classes is not as significant in separating parent materials as in other regions where the same workflow has been used (e.g., MacDonnell Ranges in the Northern Territory) using the same input layers and dimensionality reduction and clustering algorithms. However, there is one key exception at Wagga Tank in both kmeans4 and agg8 outputs where the radiometric data shows a potassium-rich area (pink area, southeast of the Southern Nights prospect in Figure 13E). This zone is an outcropping zone or residual landscape and should ideally be plotted as a separate landscape cluster rather than the blue colours in the agg8 or kmeans4 outputs. This zone is distinctly different, but the radiometric response is more like the depositional settings. Hence, with limited landscape clusters available, it is clustered incorrectly. Looking at the 3D representation of the pixels (not shown; refer to Appendix D), the hot pink colour (Figure 13C) should be considered its own unit for interpretation. A useful tool for assessing landscape clusters is the weathering intensity index (derived from DEM and radiometric data) which often shows the separation of landscape types. The residual outcrops tend to plot as blue colours on the weathering intensity, with the more weathered regions plotting as pale colours and are generally representative of depositional environments (Figure 13I). The weathering intensity index clearly depicts the unusual, outcropping radiometric potassium “anomaly” as least weathered, supporting the proposed misclassification of this area in the kmeans4 and agg8 outputs. Agglomerative clustering with 12 clusters does indeed identify this area as a separate cluster. However, it was not yet part of the workflow at the time of output generation. A preliminary agg12 output for both Wagga Tank and Federation is attached in Appendix C and D, and future workflows will include these outputs as standard in response to the data shown herein.

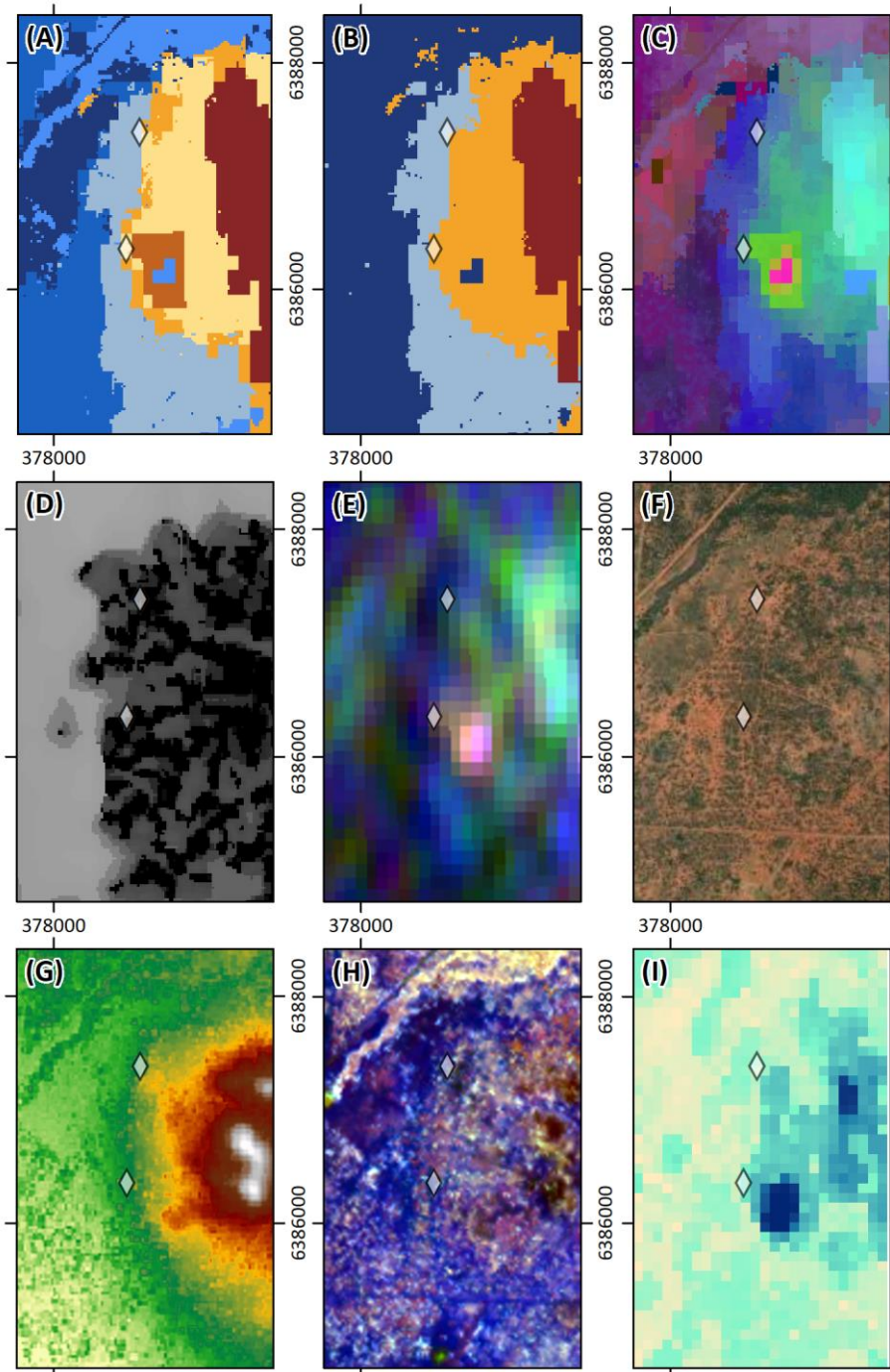
Cover materials in depositional landscape settings

The depositional landscape types are effectively demonstrated in the kmeans4 output as the blue-grey (landscape cluster 3) and dark blue (landscape cluster 4) colours (Figure 12A) whereas in the agg8 outputs depositional landscape types are represented by the grey-blue and blue shades (landscape clusters 5, 6, 7 and 8; Figure 12B). The separation of the two depositional units in kmeans4 is influenced by the DEM and MrVBF, with the blue-grey (landscape cluster 3) representing shallower transported cover compared to the dark blue (landscape cluster 4) that consists of deeper transported cover and active fluvial channels (Figure 13A, D, G).

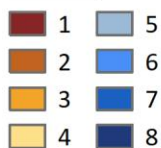
As was the case with the kmeans4 and agg8 dominant upland-residual unit (dark red landscape cluster 1), the blue-grey landscape cluster is also similar for both clustering approaches (landscape cluster 3 in the kmeans4, landscape cluster 5 in the agg8 output; Figure 13A, B). This appears to be shallow sandplain for the region and is a common landscape setting for vast areas of Australia.

The agg8 landscape clusters 6 (light blue), 7 (mid blue) and 8 (dark blue) correspond well with deeper transported cover in lower lying landscape settings and are represented by landscape cluster 4 (dark blue) in the kmeans4 output (Figure 12A, B). The depositional landscapes separated in agg8 are subtle in their differences. The light blue (landscape cluster 6) is distinct in that it hosts an active fluvial channel that passes through the northwest of the region. This landscape type is also very distinctive in the satellite imagery (Figure 13F) and the regolith ratio (yellowish colour in Figure 13H). Landscape clusters adjacent to this area are considered floodplain or perhaps ancient alluvial terrace soils, but it is challenging to qualify these without inspecting the terrain in person. The floodplain/alluvial areas adjacent to the channel are the darkest blue landscape cluster (8). The mid blue (landscape cluster 7) is also designated as sandplain and is differentiated from landscape cluster 5 (blue-grey) as likely having a thicker transported cover depth. The influence of the MrVBF and DEM (Figure 13D, G) are the main contributors to separating the sandplain materials, although there may also be a subtle radiometric data influence (Figure 13E) that may be due to changes in parent materials and the influence or dominance of aeolian soils.

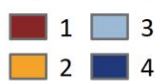
Figure 13 (next page): Spatial layers used for the assessment of landscape clusters produced by machine learning over the Wagga Tank project area. (A) Landscape clusters derived via agg8. (B) Landscape clusters derived via kmeans4. (C) 2-dimensional representation of cluster similarities derived via UMAP. (D) MrVBF as proxy for depth of cover. (E) Radiometric data as indication for differences in parent materials (F) Satellite imagery. (G) DEM. (H) Regolith ratio. (I) Weathering intensity. Grey diamonds in the figure indicate the approximate location of the Wagga Tank and Southern Nights prospects.



(A) agg8

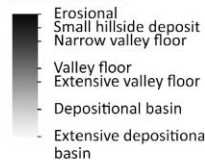


(B) kmeans4

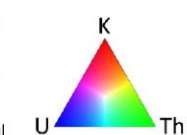


(C) UMAP

(D) MrVBF

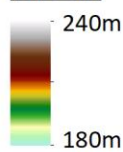


(E) Radiometrics

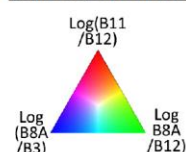


(F) Basemap

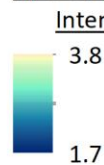
(G) DEM



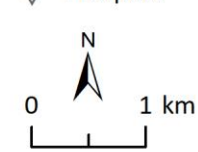
(H) Regolith ratio



(I) Weathering Intensity



◇ Prospect



3.2 UltraFine+® geochemistry results

The UltraFine+® soil analysis method is based on separating and analysing only the ultrafine fraction (< 2 µm) of a given sample, as most metals as well as some useful indicator elements in transported cover tend to adsorb preferentially to clay particles and other “scavenging” phases with large surface areas. By removing the bulk of the coarse-grained, “barren” portion of the sample, the signal to background ratio is increased and nugget effects are removed. In addition, the analysis requires smaller sample volumes due to the enhanced sensitivity with up to 100 – 250 % increased concentrations of Au, Cu and Zn observed (Noble et al. 2018).

Since the commencement of UltraFine+® Next Gen Analytics research project, the UltraFine+® soil analysis method has undergone continuous improvements. For geochemical data acquisition, the main objective was to improve detection limits. In the time between the data acquisition for Wagga Tank (November 2020) and Federation (December 2020), detection limits for 22 elements, including Ag, Ni and Pb, were improved. In addition, two elements, I and Br, were added to the multi-element suite. Since then, the detection limits for three further elements, Li, Sb and Y, were improved and Pd was added to the multi-element suite (Table 3).

Median concentrations for previous metals of interest, such as Ag and Au, are generally similar between both project areas (Table 3; Figure 14), and median concentrations for base metals, Cu, Pb and Zn, are only slightly higher within the Wagga Tank project area compared to the Federation project area (Table 3; Figure 14). However, maximum concentrations for Ag, Cu and Zn were measured within the Wagga Tank project area with 1020 ppb Ag, 146 ppm Cu and 598 ppm Zn, compared to 433 ppb Ag, 103 ppm Cu and 299 ppm Zn within the Federation project area. Maximum values for Au and Pb were measured within the Federation project area with 51 ppb compared to 22 ppb Au, and 585 ppm compared to 535 ppm Pb.

When reviewing the geochemical data without landscape context, higher relative concentrations of Cu were generally observed in elevated areas of subcropping/shallow soil cover in both the Federation and Wagga Tank project areas (Figure 15C, Figure 16C,). Lead and Zn in the Federation project area also show elevated concentrations in subcropping/shallow residual soil cover (Figure 15A, B). While there are some elevated concentrations near the Federation prospect, there are only diffuse signatures near the Dominion prospect. Gold is strongly elevated over the Federation project area (Figure 15D). However, the signal is diffuse with some higher concentrations also in subcropping/shallow soil cover. In the Wagga Tank project area, Au is only concentrated over the Wagga Tank prospect, with no elevated concentrations measured over the Southern Nights prospect (Figure 16D). Lead and Zn are elevated over the radiometric potassium “anomaly” (Figure 16A, B) and Pb is also elevated over the Wagga Tank prospect. No elevated concentrations were observed over the Southern Nights prospect under transported cover (Figure 16A, B).

Table 3 (next page): Comparison of detection limits, minimum, maximum, average and median values for available elements in the Wagga Tank (WT) and Federation (Fed) project areas. Values below the detection limit were replaced by half the detection limit prior to calculations, and values rounded to significant numbers according to the detection limit. Refer to the data packages in Appendix C and D for raw data. Differences in detection limits due to improvements in the methodology highlighted in bold. Detection limits in blue font are current as of July 2022.

*Analyses added after acquisition of Federation project data. **Analyses added after acquisition of both the Federation and Wagga Tank project data.

Element	Unit	DL WT	DL FED	DL July 2022	Min. WT	Min. FED	Max. WT	Max. FED	Aver. WT	Aver. FED	Median WT	Median FED
Ag	ppm	0.01	0.003	0.003	0.05	0.046	1.02	0.433	0.11	0.110	0.09	0.088
Al	ppm	10	10	10	53500	63300	122000	143000	95746	108225	96300	111000
As	ppm	0.5	0.5	0.5	3.6	6.1	47.6	44.9	8.8	12.6	8.1	11.5
Au	ppb	0.5	0.5	0.5	0.3	0.3	22.2	50.9	3.0	5.4	2.4	2.3
Ba	ppm	0.2	0.2	0.2	97.9	97.7	393.0	415.0	171.9	222.3	164.5	214.0
Be	ppm	0.2	0.01	0.01	1.2	0.92	3.9	3.77	2.6	2.69	2.5	2.76
Bi	ppm	0.1	0.002	0.002	0.4	0.356	9.9	2.790	1.1	0.592	0.8	0.514
Br*	ppm	1	N/A	1	1	N/A	32	N/A	13	N/A	12	N/A
Ca	ppm	10	10	10	112	123	12700	18700	1092	2439	986	2210
Cd	ppm	0.01	0.004	0.004	0.01	0.012	0.26	0.140	0.03	0.038	0.03	0.034
Ce	ppm	0.05	0.05	0.05	33.00	30.60	107.00	112.00	55.76	66.62	53.45	67.10
Co	ppm	0.2	0.01	0.01	4.4	4.36	51.3	34.10	15.5	16.71	14.9	16.00
Cr	ppm	2	2	2	37	48	221	95	59	70	58	69
Cs	ppm	0.1	0.03	0.03	3.9	4.73	13.2	9.08	6.9	6.85	6.9	6.72
Cu	ppm	0.2	0.1	0.1	16.9	17.1	146.0	103.0	34.7	31.2	31.3	27.7
Fe	ppm	100	50	50	38200	34100	71600	79300	56815	60696	57550	61700
Ga	ppm	0.05	0.05	0.05	17.10	17.30	41.30	31.50	23.87	24.49	23.60	24.40
Ge	ppm	0.05	0.05	0.05	0.08	0.03	0.26	0.24	0.17	0.14	0.17	0.15
Hf	ppm	0.02	0.002	0.002	0.06	0.026	0.86	1.240	0.20	0.535	0.16	0.485
Hg	ppm	0.01	0.001	0.001	0.01	0.014	0.15	0.063	0.03	0.036	0.03	0.036
I*	ppm	1	N/A	1	1	N/A	12	N/A	6	N/A	5	N/A
In	ppm	0.01	0.001	0.001	0.08	0.047	0.50	0.104	0.12	0.081	0.11	0.083
K	ppm	10	10	10	7280	7290	14500	16700	11628	11497	11700	11600
La	ppm	0.05	0.05	0.05	13.30	14.10	64.20	45.40	29.98	30.50	29.65	31.10
Li	ppm	0.5	0.5	0.05	15.0	13.0	82.3	64.9	38.6	45.7	39.0	48.0
Mg	ppm	10	10	10	2450	2400	5390	6710	3913	4238	3895	4250
Mn	ppm	2	0.5	0.5	103	89.9	4940	1520.0	533	475.5	473	412.0
Mo	ppm	0.1	0.03	0.03	0.7	0.57	9.0	4.47	1.5	1.01	1.4	0.91
Nb	ppm	0.01	0.01	0.01	0.61	0.38	1.79	2.28	1.06	0.87	1.04	0.81
Ni	ppm	2	0.2	0.2	18	18.2	85	65.9	35	43.6	35	43.6
Pb	ppm	0.2	0.05	0.05	14.2	20.40	535.0	585.00	56.1	62.97	33.0	30.10
Pd**	ppb	N/A	N/A	1	N/A	N/A	N/A	N/A	N/A	N/A	N/A	N/A
Pt	ppb	1	1	1	1	1	3	5	1	2	1	2
Rb	ppm	0.1	0.1	0.1	106.0	81.3	247.0	167.0	158.8	126.8	157.0	128.0
Re	ppm	0.0001	0.0001	0.0001	0.0001	0.0001	0.0123	0.0005	0.0002	0.0002	0.0001	0.0001
S	ppm	50	5	5	144	104	591	943	235	264	222	199
Sb	ppm	0.1	0.1	0.001	0.2	0.4	2.1	1.6	0.4	0.7	0.4	0.7
Sc	ppm	1	0.2	0.2	8	7.0	20	23.7	16	16.7	16	17.3
Se	ppm	0.05	0.05	0.05	0.53	0.62	3.24	2.16	0.80	0.94	0.76	0.89
Sn	ppm	0.2	0.02	0.02	2.0	2.25	5.1	4.11	3.2	3.14	3.2	3.17
Sr	ppm	0.1	0.1	0.1	26.6	27.9	135.0	153.0	68.3	71.4	68.0	71.3
Ta	ppm	0.005	0.001	0.001	0.003	0.001	0.040	0.053	0.017	0.012	0.017	0.012
Te	ppm	0.001	0.001	0.001	0.019	0.020	0.190	0.074	0.053	0.047	0.053	0.049
Th	ppm	0.02	0.02	0.02	5.63	3.43	16.40	16.30	10.54	12.05	10.60	12.50

Element	Unit	DL WT	DL FED	DL July 2022	Min. WT	Min. FED	Max. WT	Max. FED	Aver. WT	Aver. FED	Median WT	Median FED
Ti	ppm	10	2	2	427	542	1300	1310	996	919	1020	910
Tl	ppm	0.1	0.003	0.003	0.3	0.316	2.8	0.868	0.5	0.487	0.4	0.480
U	ppm	0.02	0.003	0.003	0.55	0.435	3.30	3.140	1.05	0.979	0.96	0.826
V	ppm	2	1	1	69	68	171	166	127	125	132	130
W	ppm	0.01	0.001	0.001	0.09	0.038	0.51	0.420	0.25	0.158	0.25	0.146
Y	ppm	0.05	0.05	0.005	6.55	5.42	48.90	33.70	15.45	19.76	13.05	20.00
Zn	ppm	0.2	0.2	0.2	34.9	45.0	598.0	299.0	82.9	82.7	75.1	73.5
Zr	ppm	1	0.1	0.1	2	0.6	43	44.3	10	21.8	8	24.1

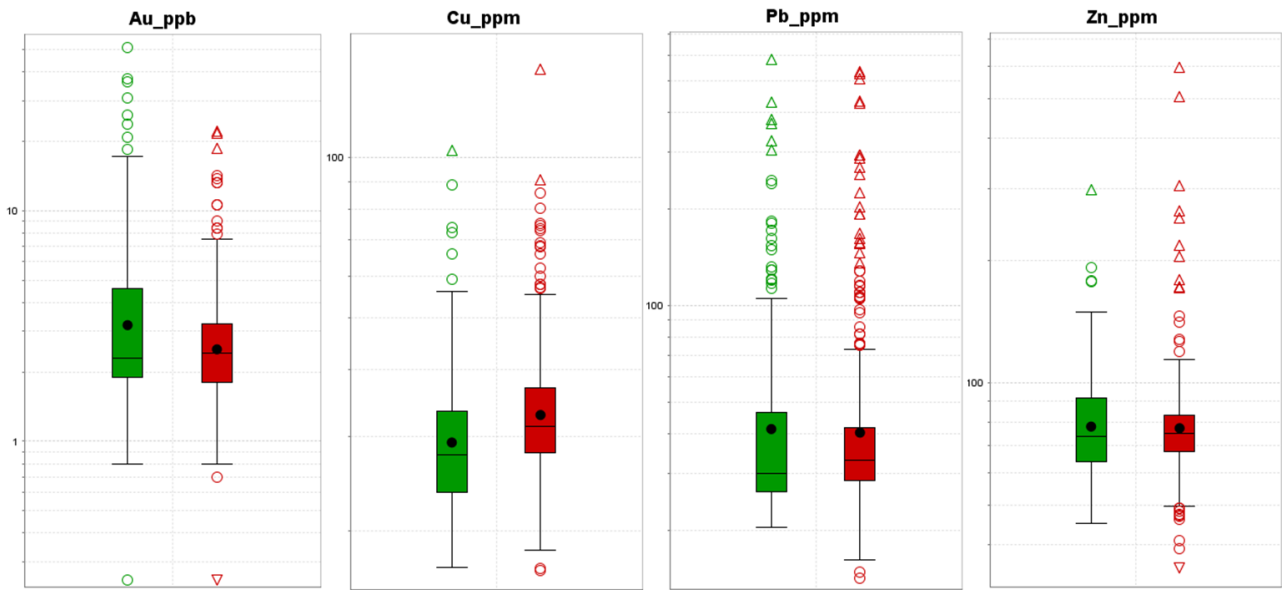


Figure 14: Boxplots of UltraFine+® analyses for Au, Cu, Zn and Pb on logarithmic scales. The Federation soil analyses results are displayed in green and the Wagga Tank results are displayed in red.

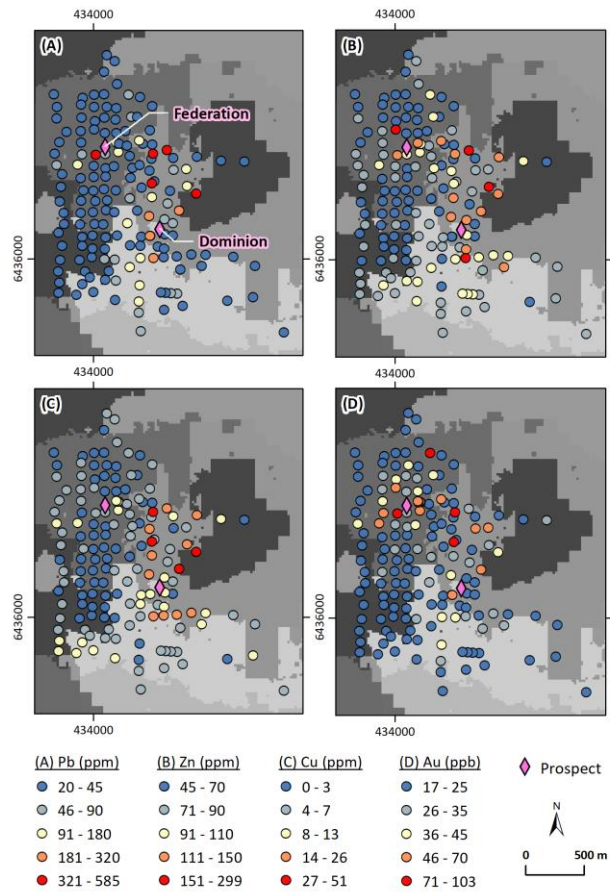


Figure 15: Spatial distribution of Pb (A), Zn (B), Cu (C), and Au (D) concentrations over the Federation project area.

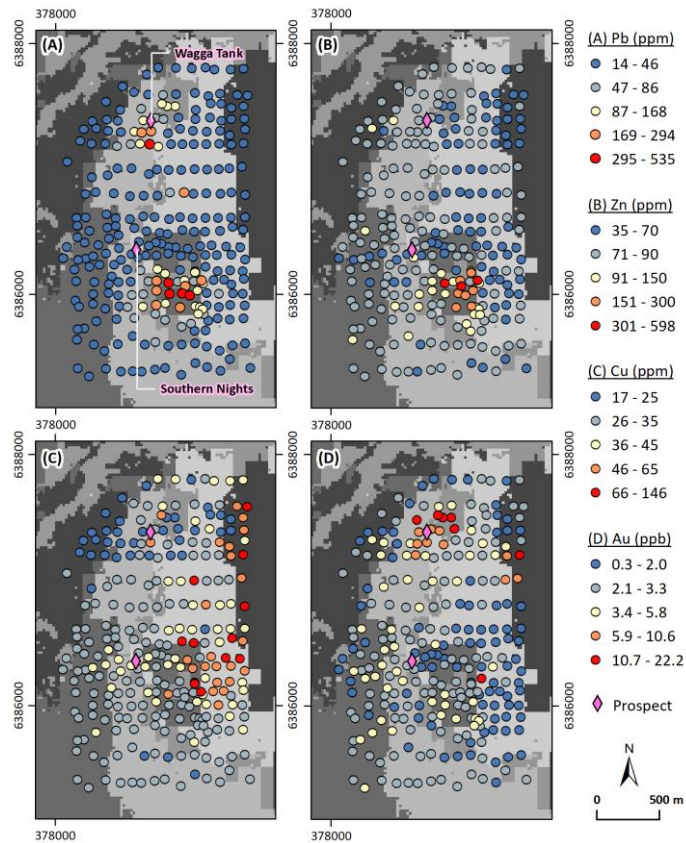


Figure 16: Spatial distribution of Pb (A), Zn (B), Cu (C), and Au (D) concentrations over the Wagga Tank project area.

3.3 Outliers by landscape type

Outliers in soil geochemical datasets are typically calculated based on all collected samples, regardless of their landscape context. However, this approach ignores the underlying processes that may affect metal dispersion. For example, high metal concentrations may be readily identifiable as outliers in a geochemical dataset where samples were collected over mineralisation beneath exposed outcrop or shallow residual materials, while the same mineralisation would have a much weaker elemental signal in samples collected over moderately thick depositional landscape types. With the ability to approximate landscape types from spatial data via machine learning, the UltraFine+® Next Gen Analytics workflow can identify outliers within each individual landscape cluster. This provides a basic, first-pass interpretation of geochemical samples by proxy regolith type and the identification of otherwise “overlooked” potential anomalies. The aim is to minimise overlooking mineral deposits in transported cover, which is common when targeting only the highest concentrations with little regard for changes in soil properties and landscape type.

To this end, the workflow generates plots of log transformed results of all analysed elements by percentiles and separates these by regolith type (Figure 17A). Traditional outliers calculated from all data as a single sample population are presented as comparison. However, by grouping the sample population by landscape clusters and calculating outliers for each of these populations, potential anomalies are highlighted within different landscape settings (triangles below the dashed line). For most of these landscape types, these outliers would have been considered unremarkable if evaluated as part of the whole data set, demonstrating the benefit of evaluating the geochemistry in a landscape/regolith context.

In the below example of Bi over the Wagga Tank project area (Figure 17), the dark brown and orange populations are from residual and/or erosional landscape settings and are therefore, as expected, well represented by outliers in the overall sample population (white box in Figure 17A). However, outliers in depositional settings (grey-blue and dark blue boxes in Figure 17A) would have been considered unremarkable if evaluated as part of the whole data set.

While the UltraFine+® Next Gen Analytics workflow was designed to identify outliers in transported cover, the workflow accommodates for identifying anomalies in other settings by also generating data, maps and shapefiles for the whole sample population and therefore original, elevated elemental signals will not be lost. This should be considered when interpreting data where prospects are located in outcrop, subcrop or shallow residual soils. The Federation prospect is an example, where anomalous values for Au are shifted northwest of the prospect into transported cover (compare Figure 18A and Figure 18B) even though the concentrations are lower than those to the southeast at the approximate location of the mineralisation. Hence, we recommend viewing outliers by landscape type in comparison with whole-population outliers and interpreting this with dispersion direction (see Section 3.6). The Wagga Tank and Federation project sites are valuable sites for testing the first-generation UltraFine+® Next Gen Analytics workflow outputs in areas with known mineralisation and will aid in the refinement of the final project outputs.

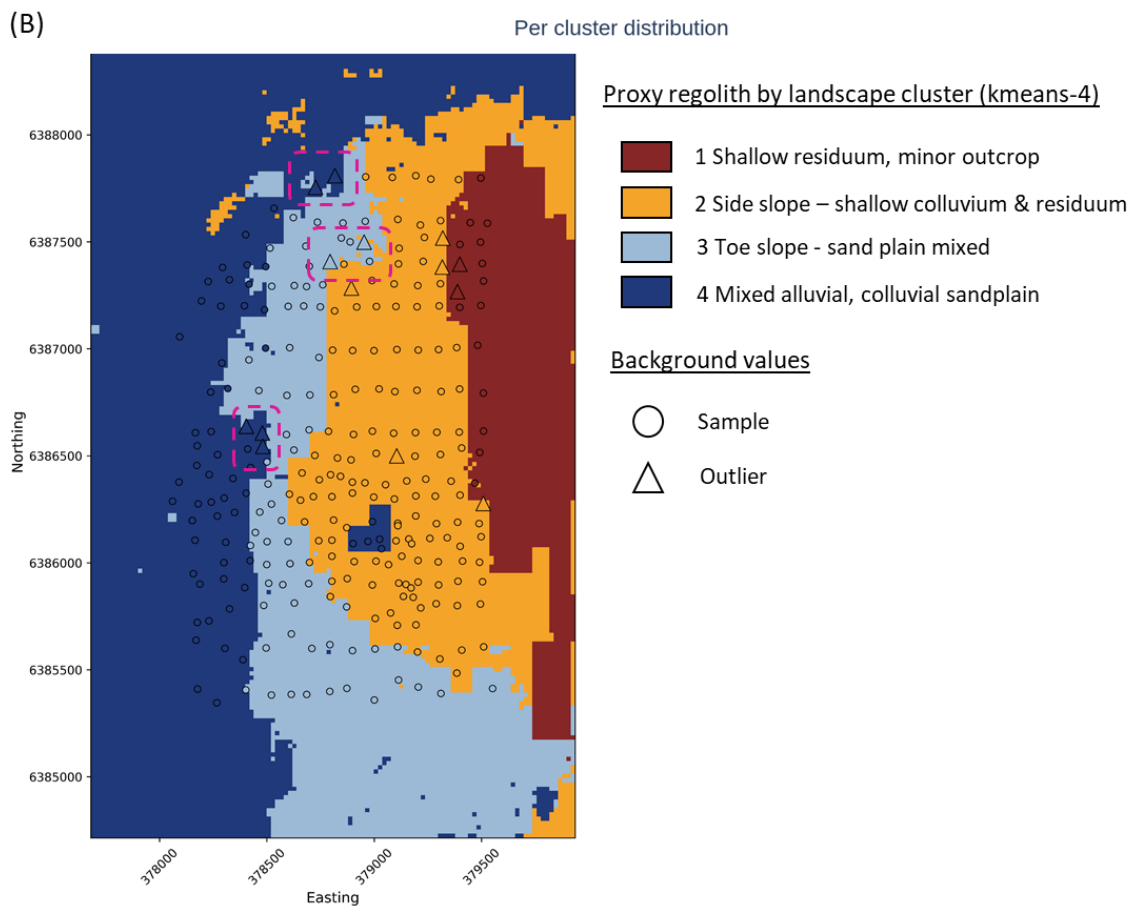
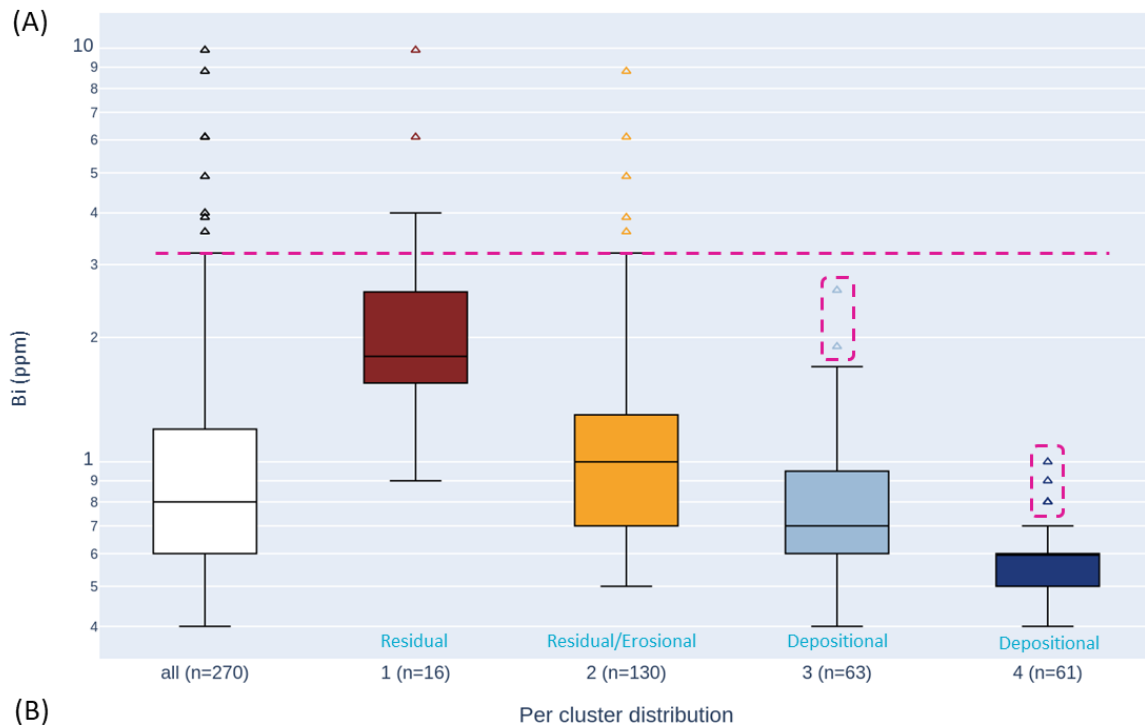


Figure 17: Example of machine learning derived outputs for outliers by landscape type over the Wagga Tank project area. (A) Boxplots for all Bi data (white box) and by landscape type (coloured boxes). Dashed line indicates the upper 25% boundary for the whole sample population. Easily observed soil anomalies are samples above the dashed horizontal line. Those shown below the dashed mauve line would not be easily observed without the landscape context. (B) Spatial distribution of Bi outliers (triangles) by proxy regolith type. Outliers in dashed boxes correlate to outliers below the dashed horizontal line in (A) in depositional landscape settings.

3.3.1 Examples of outliers by landscape type - Federation project area

The Federation project area covers two Pb-Zn-Cu (-Ag-Au) prospects, Federation and Dominion. The Federation prospect is currently being evaluated as a proposed underground mine development by Aurelia Metals who generously provided a draft surface projection of the mineralisation.

Although the agg8 landscape clusters generated for the Federation project area are more differentiated and thus represent more appropriate proxies for the regolith types within these areas (see section 3.1), the number of samples per landscape cluster limits the interpretation within the eight cluster outputs, and therefore, the four cluster outputs (k-means) are preferred. In general, we consider the ideal minimum number of samples for statistically relevant analyses to be 50 and recommend to disregard outliers generated by landscape clusters with less than 15 samples as these are not meaningful. As a precaution, outliers in clusters with less than 10 samples will not display on maps or in shapefiles generated with the UltraFine+® Next Gen Analytics workflow. However, some clusters within the agg8 output are still worth considering and in general may confirm parts of the kmeans4 outputs, and are hence included in the below discussion.

For the Federation outputs, sample populations in landscape clusters generated via agg8, including 1 (n=3), 5 (n=2) and 6 (n=4), are too small to be considered for meaningful interpretation and outliers are not displayed on maps. Landscape clusters 7 (n=19) and 8 (n=20) should also be regarded with caution. In the kmeans4 outputs, the sample population for landscape cluster 3 (n=4) is also too small to be considered for meaningful interpretation and outliers are not displayed on maps.

Gold and Ag outliers by landscape type

Within the Federation project area, Au concentrations range from below the detection limit (0.5 ppb) to 50.9 ppb with a mean of 5.4 ppb. The greatest concentrations were measured around the Federation and Dominion prospects in settings of residual soils (white triangles indicating outliers for the whole sample population in Figure 18A). Calculating outliers by populations within individual landscape types identifies outliers in areas of depositional settings. While these outliers would traditionally be considered unremarkable, they indicate a cluster of anomalous values within deeper transported cover (landscape cluster 4, dark blue, Figure 18B) north-west of the Federation prospect, and a second cluster of anomalous values within shallower sheetwash (landscape cluster 2, orange, Figure 18B) south of the Dominion prospect. Overall, this process results in more defined and denser clusters of outliers. Both outlier clusters occur downslope from the identified prospects in transported soils (please also refer to Section 3.6 Dispersion and Source Direction). Due to the low number of samples per landscape cluster, these trends are not well defined in the agg8 outputs, which resemble the signature of the overall outliers more closely than the kmeans4 output (Figure 18C).

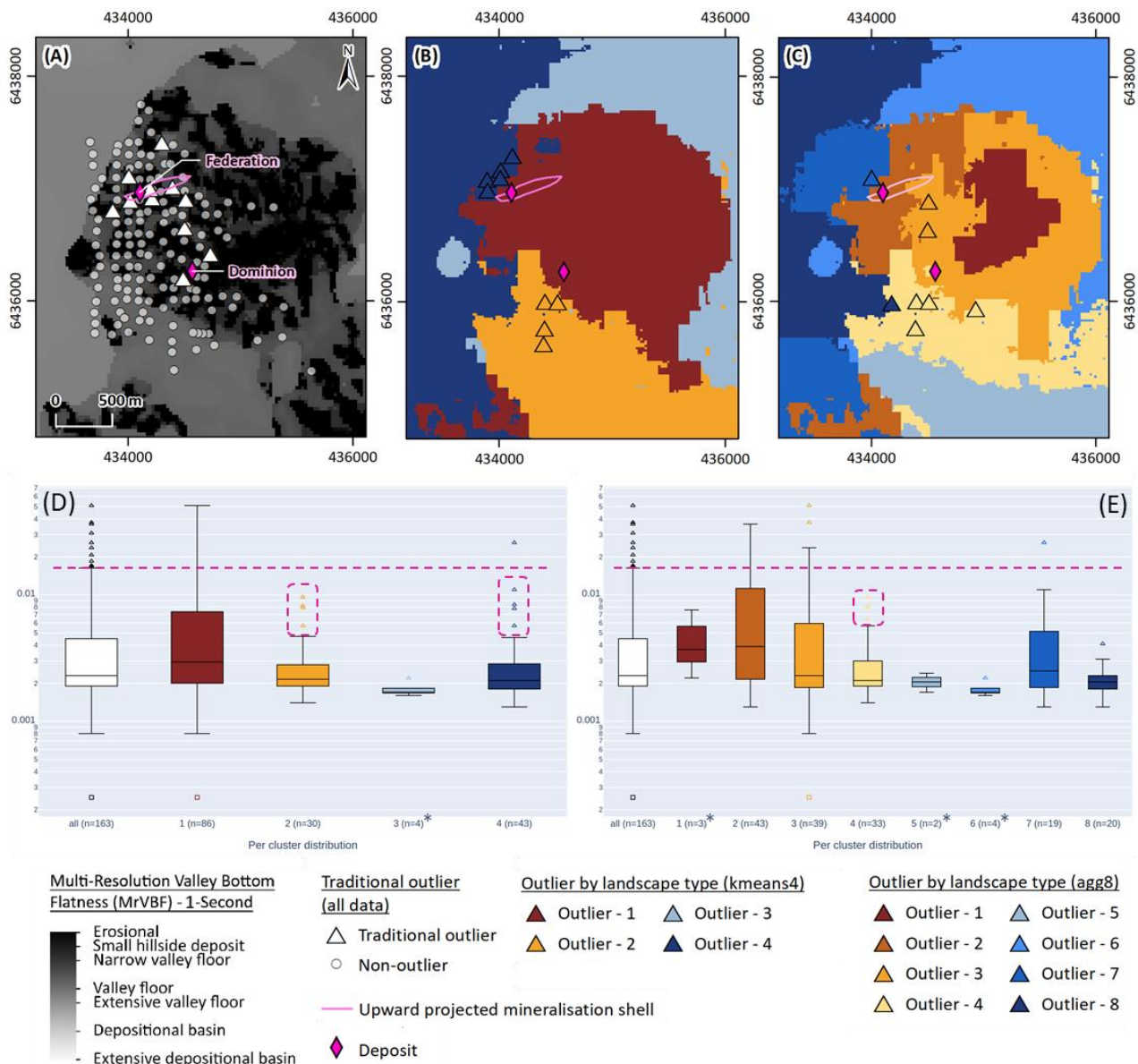


Figure 18: Comparison of Au outliers in the whole sample population to Au outliers by landscape clusters over the Federation project area. Outliers are plotted as triangles; background value samples are plotted in grey. (A) Spatial distribution of Au outliers for all data. (B) Spatial distribution of Au outliers by landscape population with four clusters. (C) Spatial distribution of Au outliers by landscape population with eight clusters. (D) Boxplots for all data (white box) and by landscape type (coloured boxes) when calculated based on four landscape clusters. (E) Boxplots for all data (white box) and by landscape type (coloured boxes) when calculated based on eight landscape clusters. Easily observed soil anomalies are samples above the dashed horizontal line (white triangles in (A)). Those shown below the dashed mauve line would not be easily observed without the landscape context (coloured triangles in (B) and (C)). *Note that outliers in clusters with <10 samples will not display on maps as these are statistically not meaningful.

Silver concentrations within the Federation project area range from 46 ppb to 443 ppb with a mean of 110 ppb. The greatest concentrations were measured in approximate vicinity to the Dominion prospect in settings of residual soils (white triangles indicating outliers for the whole sample population in Figure 19A). These outliers are not emphasised in the kmeans4 outputs, which instead draw out two outliers in depositional settings (landscape cluster 4, dark blue). While these outliers are spatially isolated, the northern outlier coincides with a cluster of Au outliers close to the Federation prospect (landscape cluster 4, dark blue, compare Figure 18B and Figure 19B). This outlier is still present in the agg8 output (landscape cluster 6, mid-blue, Figure 19C). The

southern outlier(s) in the dark blue landscape cluster in both the kmeans4 and agg8 outputs coincide with outliers for Zn (Figure 20) and Cu (Figure 22). However, it should be noted that these also coincide with anomalous values for Mn (see Appendix B). Both Zn and Cu are known to co-precipitate with secondary Mn-oxides. No outliers by landscape cluster were identified near the Dominion prospect.

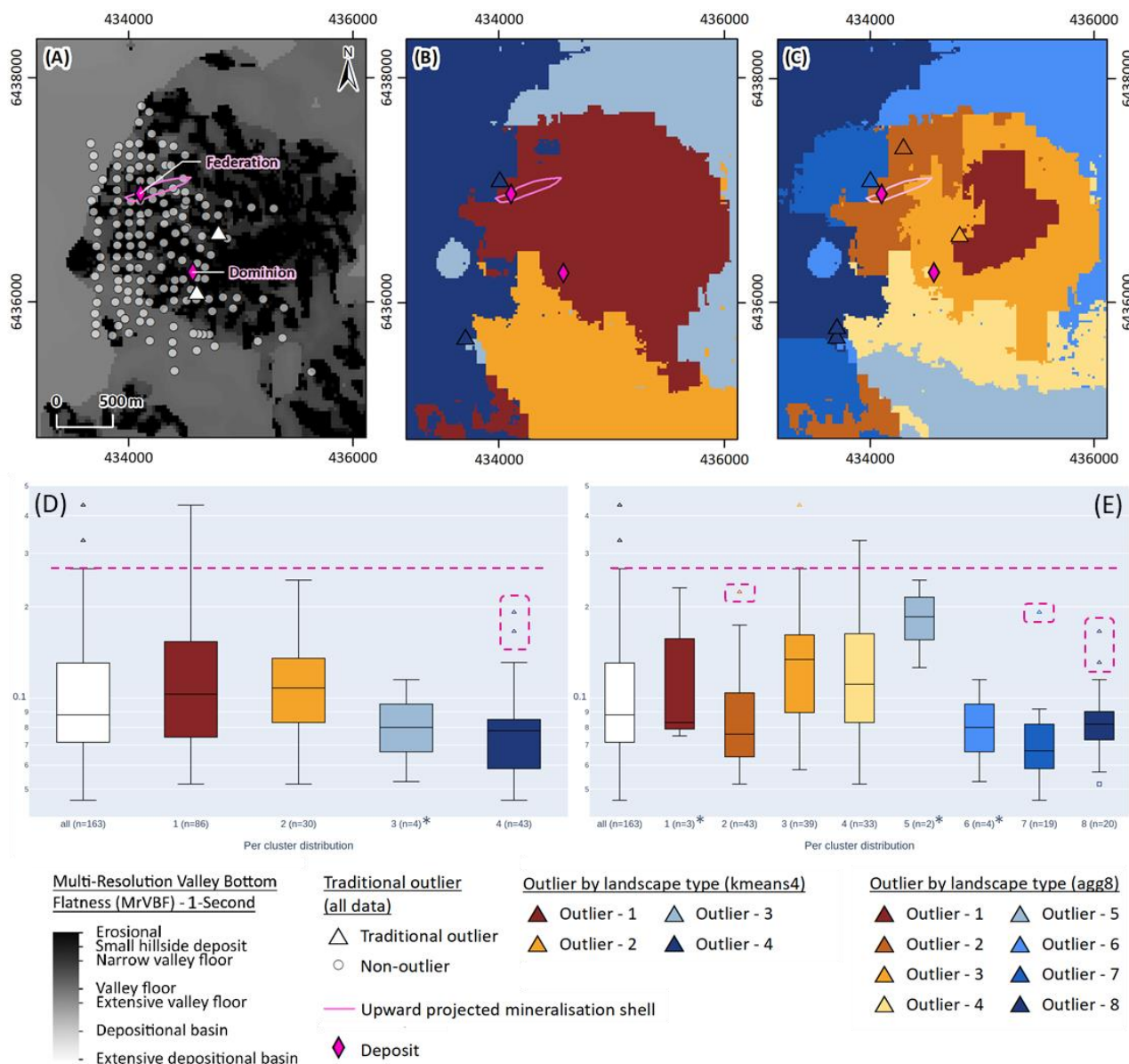


Figure 19: Comparison of Ag outliers in the whole sample population to Ag outliers by landscape clusters over the Federation project area. Outliers are plotted as triangles; background value samples are plotted in grey. (A) Spatial distribution of Ag outliers for all data. (B) Spatial distribution of Ag outliers by landscape population with four clusters. (C) Spatial distribution of Ag outliers by landscape population with eight clusters. (D) Boxplots for all data (white box) and by landscape type (coloured boxes) when calculated based on four landscape clusters. (E) Boxplots for all data (white box) and by landscape type (coloured boxes) when calculated based on eight landscape clusters. Easily observed soil anomalies are samples above the dashed horizontal line (white triangles in (A)). Those shown below the dashed mauve line would not be easily observed without the landscape context (coloured triangles in (B) and (C)). *Note that outliers in clusters with <10 samples will not display on maps as these are statistically not meaningful.

Base metal outliers by landscape type

The base metals Zn, Pb and Cu are the main elements of interest within the Federation project area. The spatial distribution of highest concentrations of these three elements varies (Figure 20A, Figure 21A and Figure 22A) with the least mobile element, Pb, displaying the strongest signal within the area in closest proximity to the Federation prospect (Figure 21A).

Zinc concentrations range from 45.0 ppm to 299.0 ppm with a mean of 82.7 ppm and the greatest concentrations were measured in the vicinity of the Federation and Dominion prospects (Figure 20A). Separating the sample populations by landscape type does not identify additional outliers in the kmeans4 output but rather removes an outlier in residual settings (Figure 20B). The agg8 output identifies outliers in deeper cover (landscape cluster 8, dark blue; Figure 20C) that coincide with high concentrations of Mn (Appendix B).

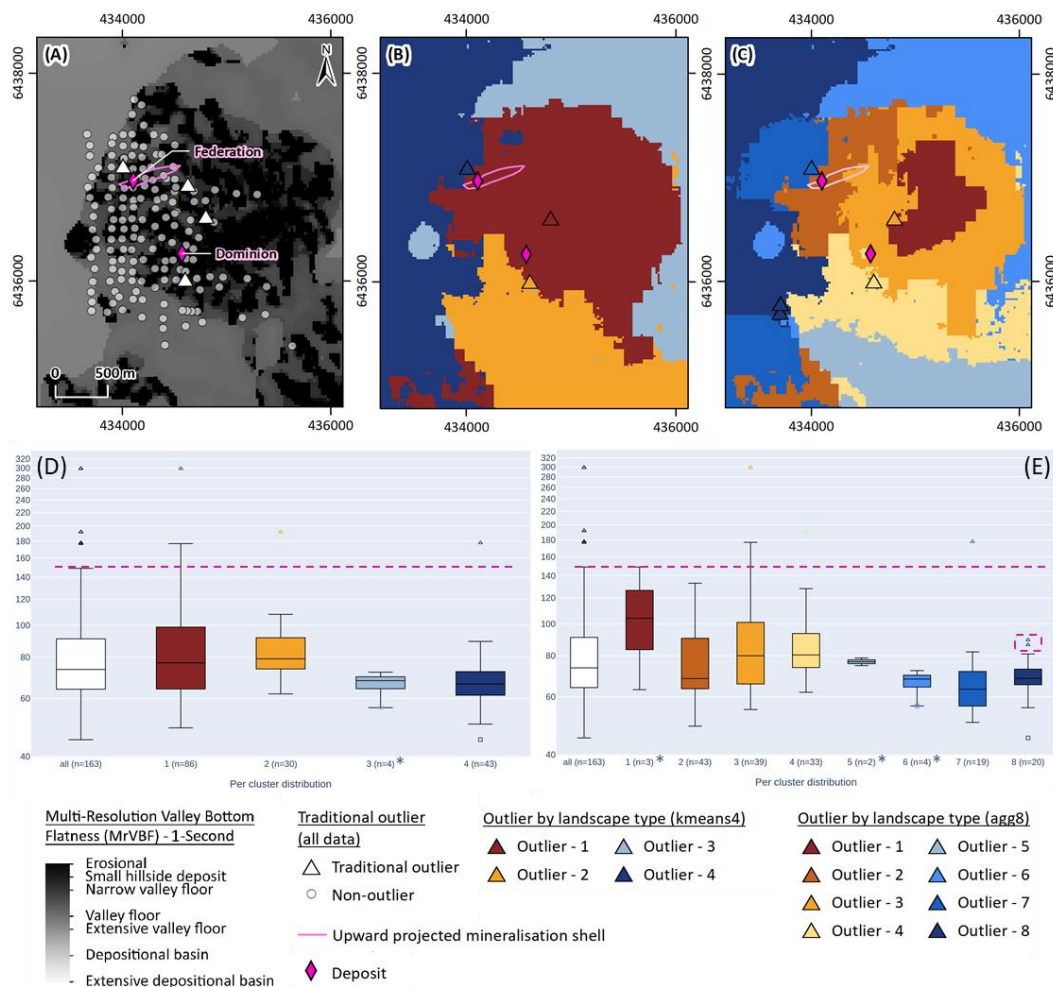


Figure 20: Comparison of Zn outliers in the whole sample population to Zn outliers by landscape clusters over the Federation project area. Outliers are plotted as triangles; background value samples are plotted in grey. (A) Spatial distribution of Zn outliers for all data. (B) Spatial distribution of Zn outliers by landscape population with four clusters. (C) Spatial distribution of Zn outliers by landscape population with eight clusters. (D) Boxplots for all data (white box) and by landscape type (coloured boxes) when calculated based on four landscape clusters. (E) Boxplots for all data (white box) and by landscape type (coloured boxes) when calculated based on eight landscape clusters. Easily observed soil anomalies are samples above the dashed horizontal line (white triangles in (A)). Those shown below the dashed mauve line would not be easily observed without the landscape context (coloured triangles in (B) and (C)).

*Note that outliers in clusters with <10 samples will not display on maps as these are statistically not meaningful.

Lead concentrations range from 20.4 ppm to 585.0 ppm with a mean of 63.0 ppm (Figure 21A). The greatest concentrations were measured trending southeast-northwest across the Federation prospect and a more diffuse, broad south-north trend across the Dominion prospect (Figure 21A). Both kmeans4 and agg8 outputs identified additional outliers in deeper transported cover WSW of the Dominion prospect (landscape cluster 4 and 8, respectively, dark blue in both outputs, Figure 21B, C). However, as expected, the process of defining outliers in populations by landscape type has removed many outliers in residual landscapes with only a few remaining near either prospect, since “normalising” concentrations by landscape proxies will favour subtle variations in landscape types with generally lower mean concentrations.

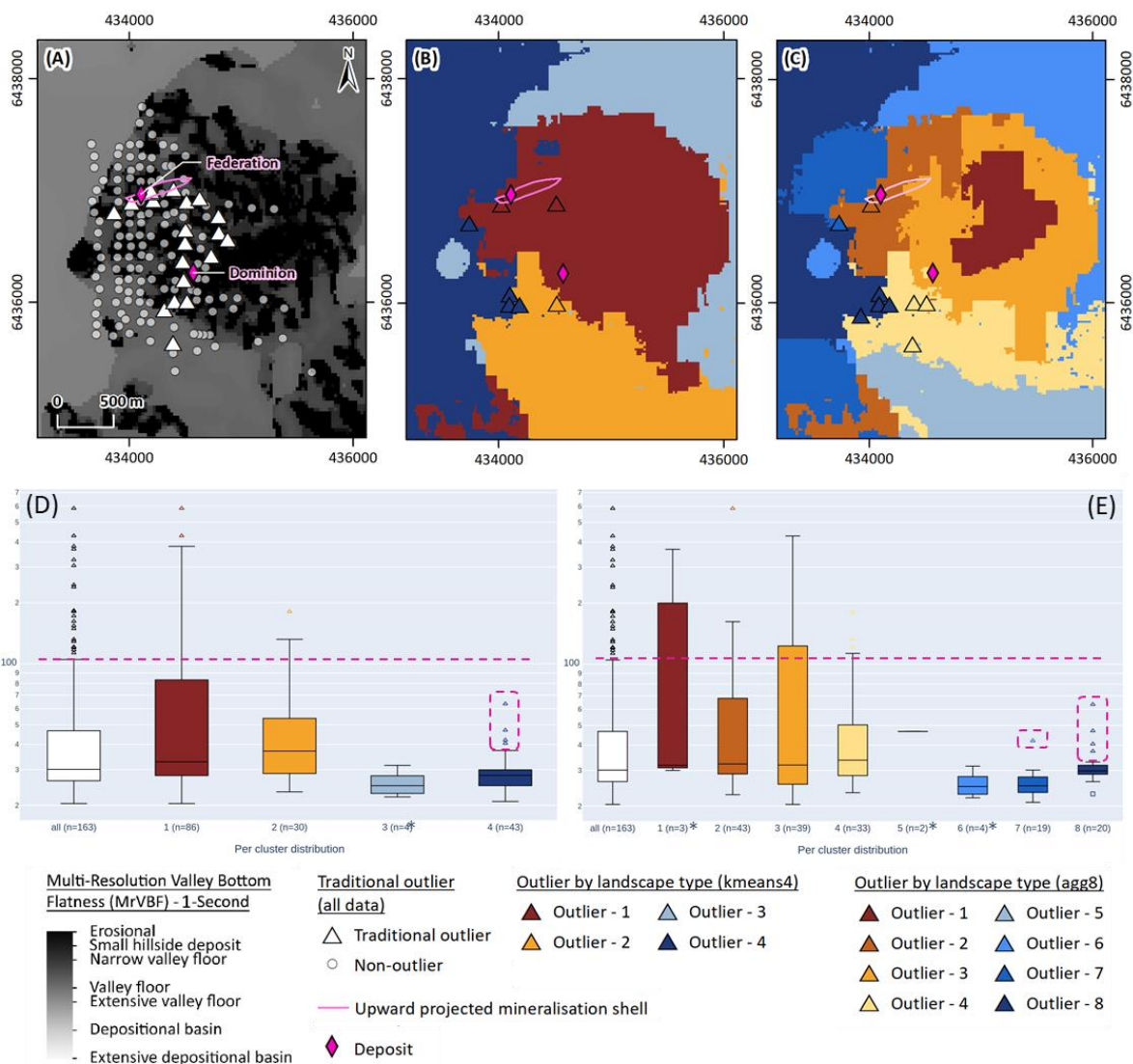


Figure 21: Comparison of Pb outliers in the whole sample population to Pb outliers by landscape clusters over the Federation project area. Outliers are plotted as triangles; background value samples are plotted in grey. (A) Spatial distribution of Pb outliers for all data. (B) Spatial distribution of Pb outliers by landscape population with four clusters. (C) Spatial distribution of Pb outliers by landscape population with eight clusters. (D) Boxplots for all data (white box) and by landscape type (coloured boxes) when calculated based on four landscape clusters. (E) Boxplots for all data (white box) and by landscape type (coloured boxes) when calculated based on eight landscape clusters. Easily observed soil anomalies are samples above the dashed horizontal line (white triangles in (A)). Those shown below the dashed mauve line would not be easily observed without the landscape context (coloured triangles in (B) and (C)). *Note that outliers in clusters with <10 samples will not display on maps as these are statistically not meaningful.

Copper concentrations range from of 17.1 ppm to 103.0 ppm with a mean of 31.2 ppm. The greatest concentrations were measured in residual-erosional landscape settings, but none in the vicinity of the Federation prospect (Figure 22A). While some additional outliers were identified in shallow transported cover south of the Dominion prospect in kmeans4 (landscape cluster 2, orange; Figure 22B) and agg8 (landscape cluster 4, yellow; Figure 22C) outputs, they too did not identify any Cu outliers near the Federation prospect. Both outputs by landscape cluster identify outliers in deeper cover (landscape cluster 4 and 8, respectively, both dark blue) that coincide with high concentrations of Mn (Figure 22B, C; Appendix B).

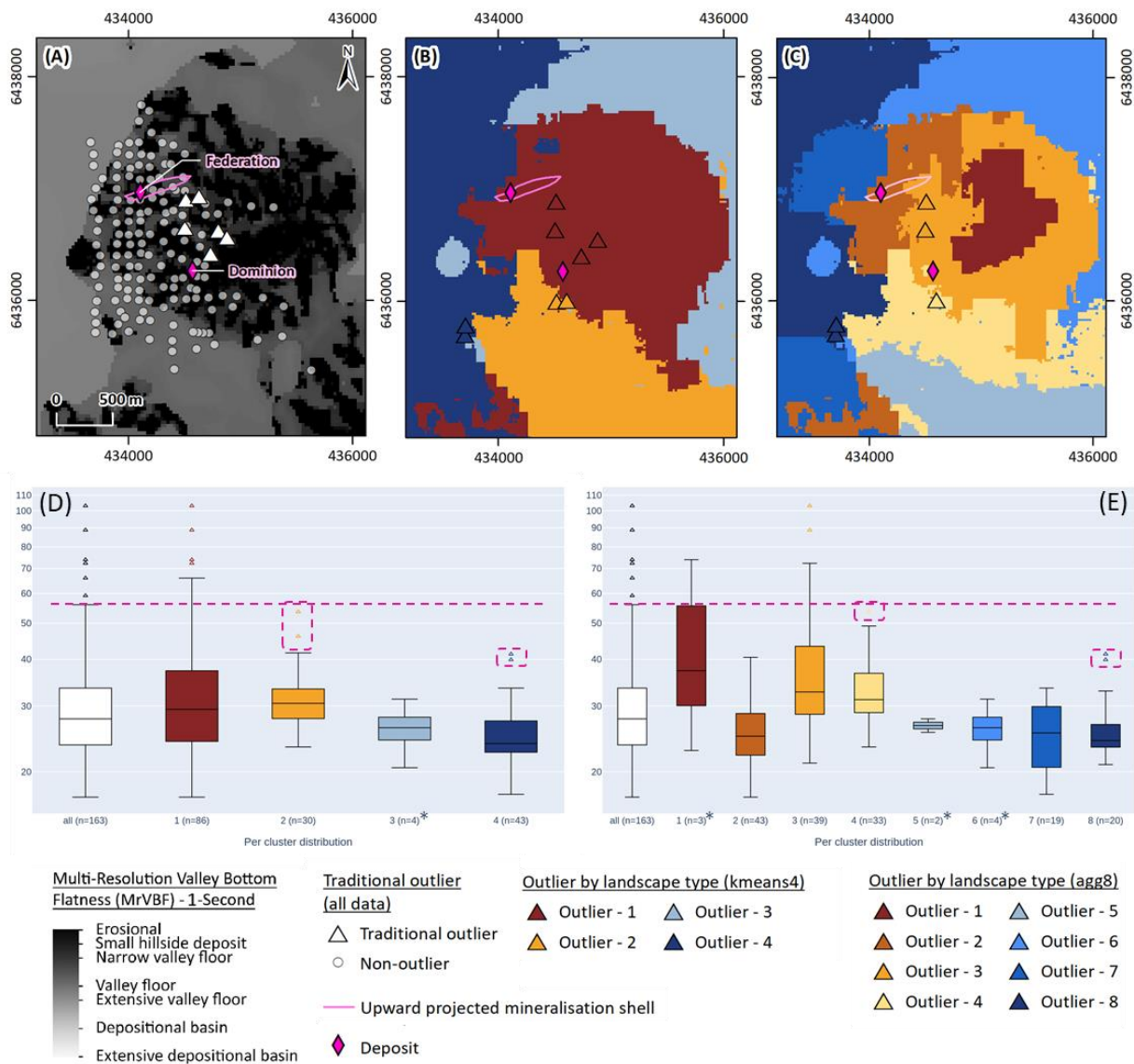


Figure 22: Comparison of Cu outliers in the whole sample population to Cu outliers by landscape clusters over the Federation project area. Outliers are plotted as triangles; background value samples are plotted in grey. (A) Spatial distribution of Cu outliers for all data. (B) Spatial distribution of Cu outliers by landscape population with four clusters. (C) Spatial distribution of Cu outliers by landscape population with eight clusters. (D) Boxplots for all data (white box) and by landscape type (coloured boxes) when calculated based on four landscape clusters. (E) Boxplots for all data (white box) and by landscape type (coloured boxes) when calculated based on eight landscape clusters. Easily observed soil anomalies are samples above the dashed horizontal line (white triangles in (A)). Those shown below the dashed mauve line would not be easily observed without the landscape context (coloured triangles in (B) and (C)). *Note that outliers in clusters with <10 samples will not display on maps as these are statistically not meaningful.

3.3.2 Examples of outliers by landscape type – Wagga Tank project area

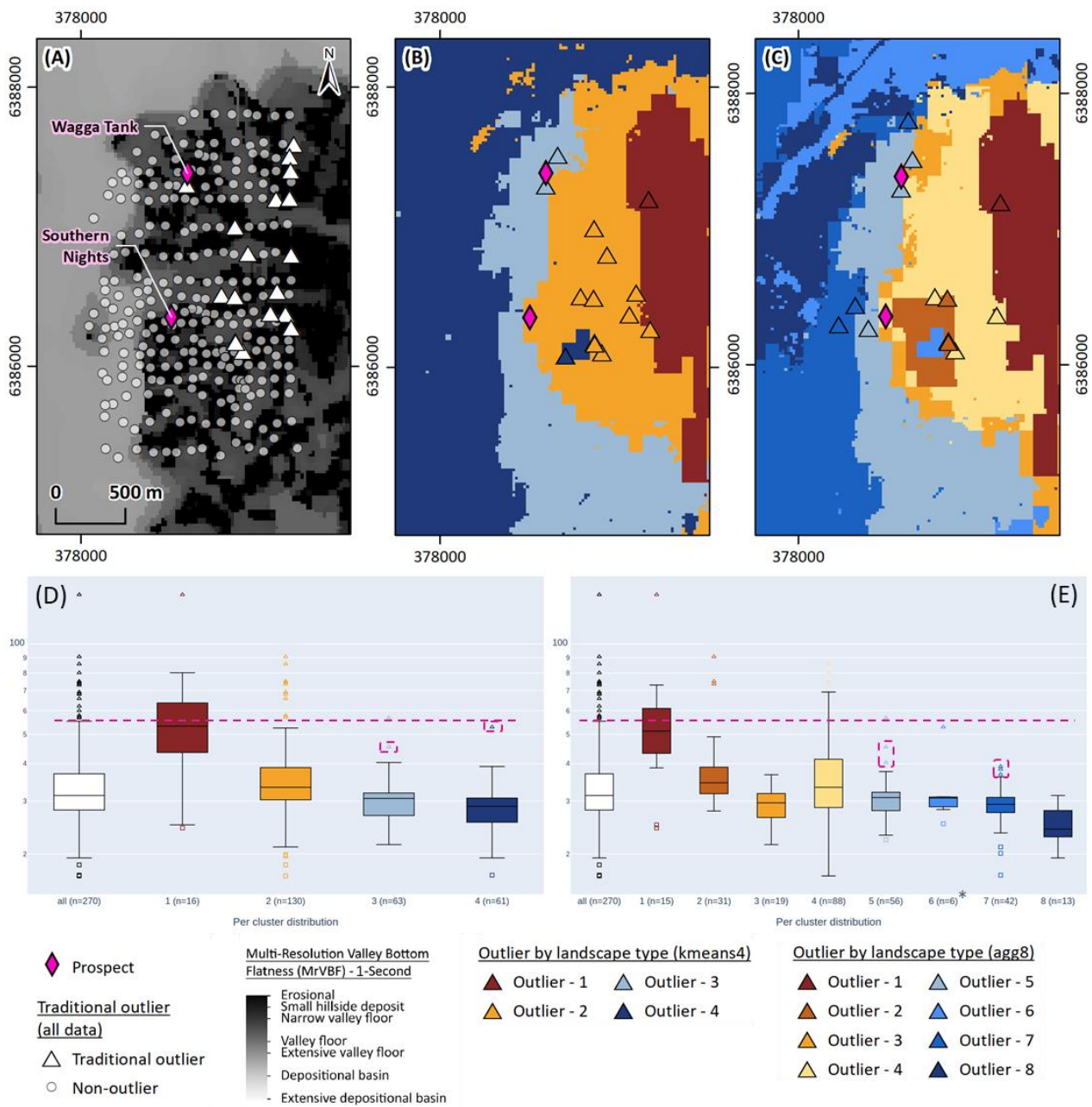
The Wagga Tank project area covers two laminated to massive stratiform sulphide prospects, the Wagga Tank and Southern Nights prospects. The Wagga Tank Pb-Zn-Cu (-Au-Ag) prospect is a shallow oxide target while the Southern Nights polymetallic zinc prospect is under thick transported cover. The agg8 landscape clusters generated for the Wagga Tank project area are more differentiated and thus represent more appropriate proxies for the regolith types within these areas (see section 3.1) and the number of samples per landscape cluster are generally appropriate for interpretation within the eight cluster outputs. However, for comparison with the Federation site and to highlight the differences of interpreting geochemical data within the appropriate landscape context, the kmeans4 outputs are included in the below discussion. For the Wagga Tank outputs sample populations in landscape cluster 6 (n=6) generated via agg8 is too small to be considered for meaningful interpretation and is not displayed on maps. Results for landscape clusters 1 (n=15) and 8 (n=13) should also be interpreted with caution. In the kmeans4 outputs, the sample population for landscape cluster 1 (n=16) should also be interpreted with caution.

Base metal outliers by landscape type

Copper concentrations within the Wagga Tank project area range from 16.9 ppm to 146.0 ppm with a mean of 34.7 ppm. The greatest concentrations over the Wagga Tank project area were measured in side slope settings with a wide, diffuse pattern in the east and one outlier near the Wagga Tank prospect (white triangles indicating outliers for the whole sample population in Figure 23A). The agg8 outputs extend the signal around Wagga Tank downslope (north), and reduce some of the background outliers in side slope settings and identifies a cluster in transported cover near the Southern Nights prospect (Figure 23C). These concentrations would be considered unremarkable if viewed in the context of the entire population. Similar outlier patterns can be observed for Bi and Sb (data not shown; refer to Appendix D).

Figure 23 (next page): Comparison of Cu outliers in the whole sample population to Cu outliers by landscape clusters over the Wagga Tank project area. Outliers are plotted as triangles; background value samples are plotted in grey. (A) Spatial distribution of Cu outliers for all data. (B) Spatial distribution of Cu outliers by landscape population with four clusters. (C) Spatial distribution of Cu outliers by landscape population with eight clusters. (D) Boxplots for all data (white box) and by landscape type (coloured boxes) when calculated based on four landscape clusters. (E) Boxplots for all data (white box) and by landscape type (coloured boxes) when calculated based on eight landscape clusters. Easily observed soil anomalies are samples above the dashed horizontal line (white triangles in (A)). Those shown below the dashed mauve line would not be easily observed without the landscape context (coloured triangles in (B) and (C)).

*Note that outliers in clusters with <10 samples will not display on maps as these are statistically not meaningful.



Lead concentrations within the Wagga Tank project area range from 14.2 ppm to 535.0 ppm with a mean of 56.1 ppm. The greatest concentrations of Pb are strongly concentrated over the Wagga Tank prospect and to the southeast of the Southern Nights prospect near the potassium-rich radiometric “anomaly” (white triangles indicating outliers for the whole sample population in Figure 24A). While kmeans4 outputs constrain this signal into a smaller area (Figure 24B), the agg8 outputs significantly reduce the signal around the radiometric potassium “anomaly” while confirming the signal over Wagga Tank (Figure 24C).

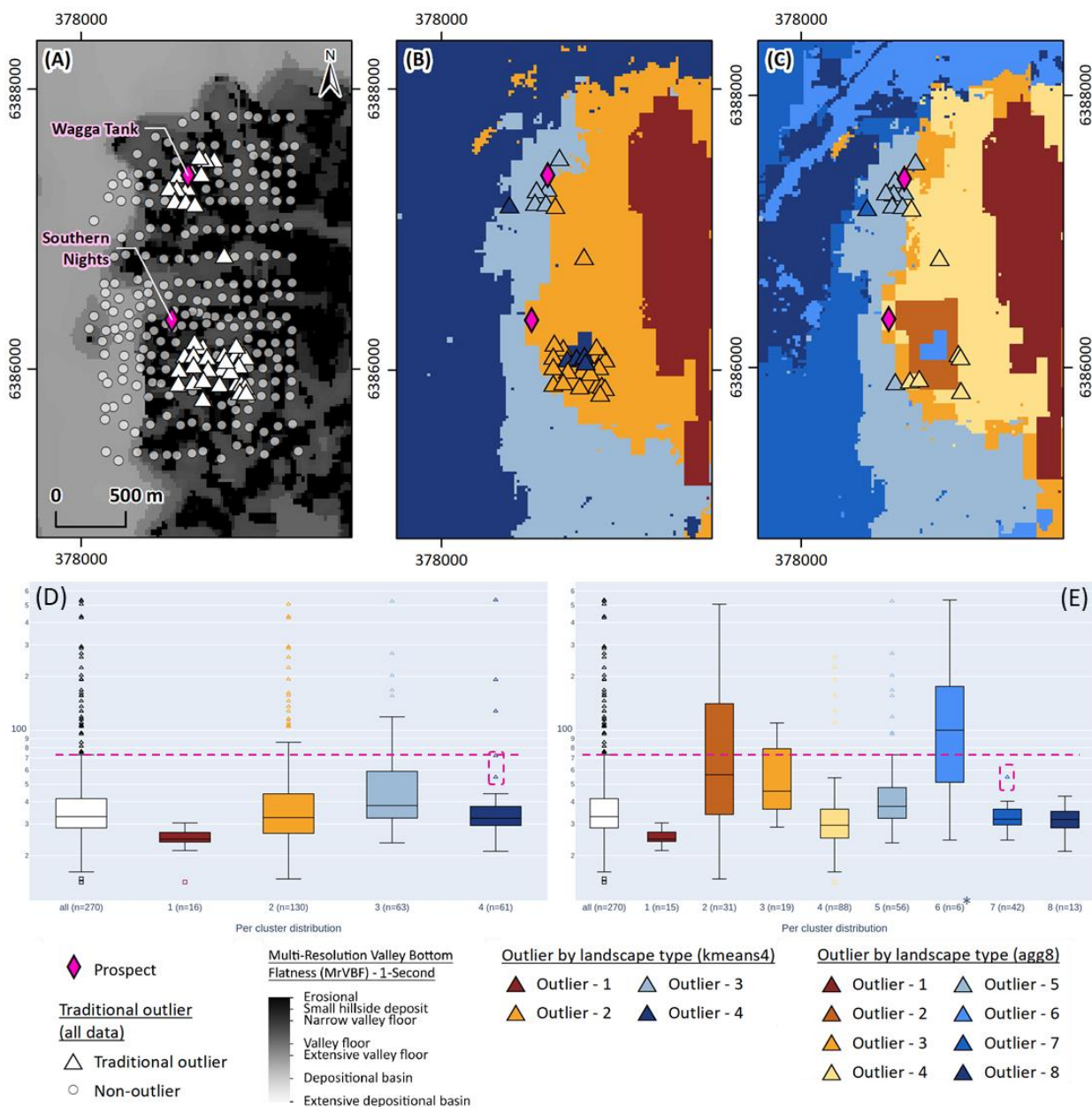


Figure 24: Comparison of Pb outliers in the whole sample population to Pb outliers by landscape clusters over the Wagga Tank project area. Outliers are plotted as triangles; background value samples are plotted in grey. (A) Spatial distribution of Pb outliers for all data. (B) Spatial distribution of Pb outliers by landscape population with four clusters. (C) Spatial distribution of Pb outliers by landscape population with eight clusters. (D) Boxplots for all data (white box) and by landscape type (coloured boxes) when calculated based on four landscape clusters. (E) Boxplots for all data (white box) and by landscape type (coloured boxes) when calculated based on eight landscape clusters. Easily observed soil anomalies are samples above the dashed horizontal line (white triangles in (A)). Those shown below the dashed mauve line would not be easily observed without the landscape context (coloured triangles in (B) and (C)). *Note that outliers in clusters with <10 samples will not display on maps as these are statistically not meaningful.

Zinc concentrations within the Wagga Tank project area range from 34.9 ppm to 598.0 ppm with a mean of 82.9 ppm. Greatest concentrations within the project area are clustered around the radiometric potassium “anomaly” in the south and no outliers were identified around the Wagga Tank or the Southern Nights prospects (white triangles indicating outliers for the whole sample population in Figure 25A). While the kmeans4 outliers only slightly constrain the signal around the radiometric potassium “anomaly” (Figure 25B), the agg8 output has effectively removed most outliers from this area (Figure 25C). Note that no outliers are identified in the outcropping and

side slope landscape clusters 6 and 2 (Figure 25E). While the number of samples within landscape cluster 6 (light blue) near the radiometric potassium “anomaly” is not representative, the agg8 boxplot visualises the higher median Zn concentrations within this landscape type compared to all other landscape types, closely followed by the surrounding light brown landscape cluster 2 (Figure 25E).

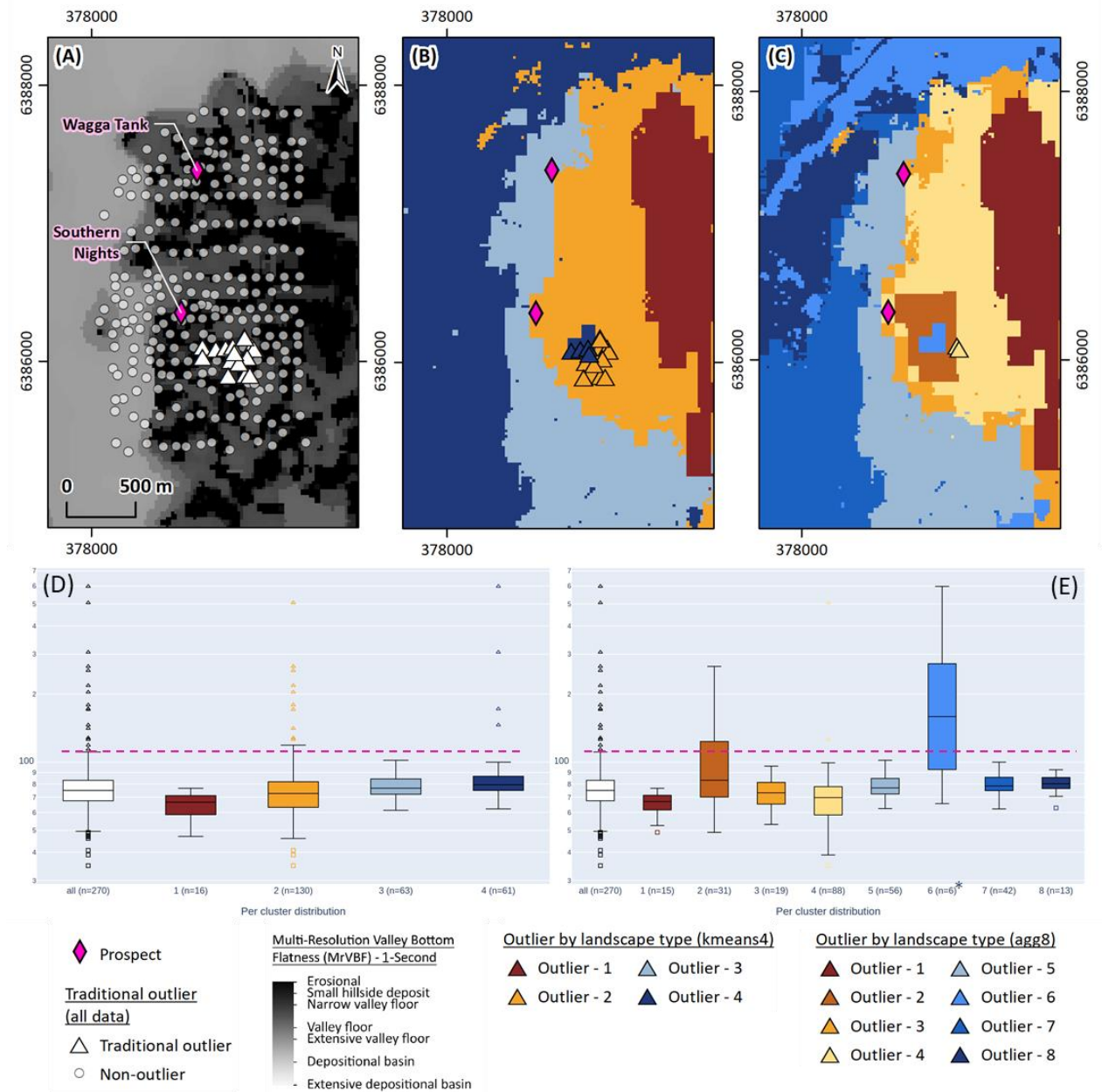


Figure 25: Comparison of Zn outliers in the whole sample population to Zn outliers by landscape clusters over the Wagga Tank project area. Outliers are plotted as triangles; background value samples are plotted in grey. (A) Spatial distribution of Zn outliers for all data. (B) Spatial distribution of Zn outliers by landscape population with four clusters. (C) Spatial distribution of Zn outliers by landscape population with eight clusters. (D) Boxplots for all data (white box) and by landscape type (coloured boxes) when calculated based on four landscape clusters. (E) Boxplots for all data (white box) and by landscape type (coloured boxes) when calculated based on eight landscape clusters. Easily observed soil anomalies are samples above the dashed horizontal line (white triangles in (A)). Those shown below the dashed mauve line would not be easily observed without the landscape context (coloured triangles in (B) and (C)). *Note that outliers in clusters with <10 samples will not display on maps as these are statistically not meaningful.

Gold and Ag outliers by landscape type

Within the Wagga Tank project area, Au concentrations range from below the detection limit (0.5 ppb) to 22 ppb with a mean of 3 ppb. The greatest concentrations were mainly detected around the Wagga Tank prospect a shallow oxide target in settings of colluvium, residual soils, and shallow sand plain materials (refer to white triangles indicating outliers for the whole sample population in Figure 26). Separating the sample populations by landscape type does not identify additional outliers in agg8 outputs, but rather removes outliers in side slope (colluvium and residual soil) settings while still highlighting those in toe slope settings (shallow sandplain materials; Figure 26C). No Au outliers were identified over the Southern Nights prospect under thicker transported cover.

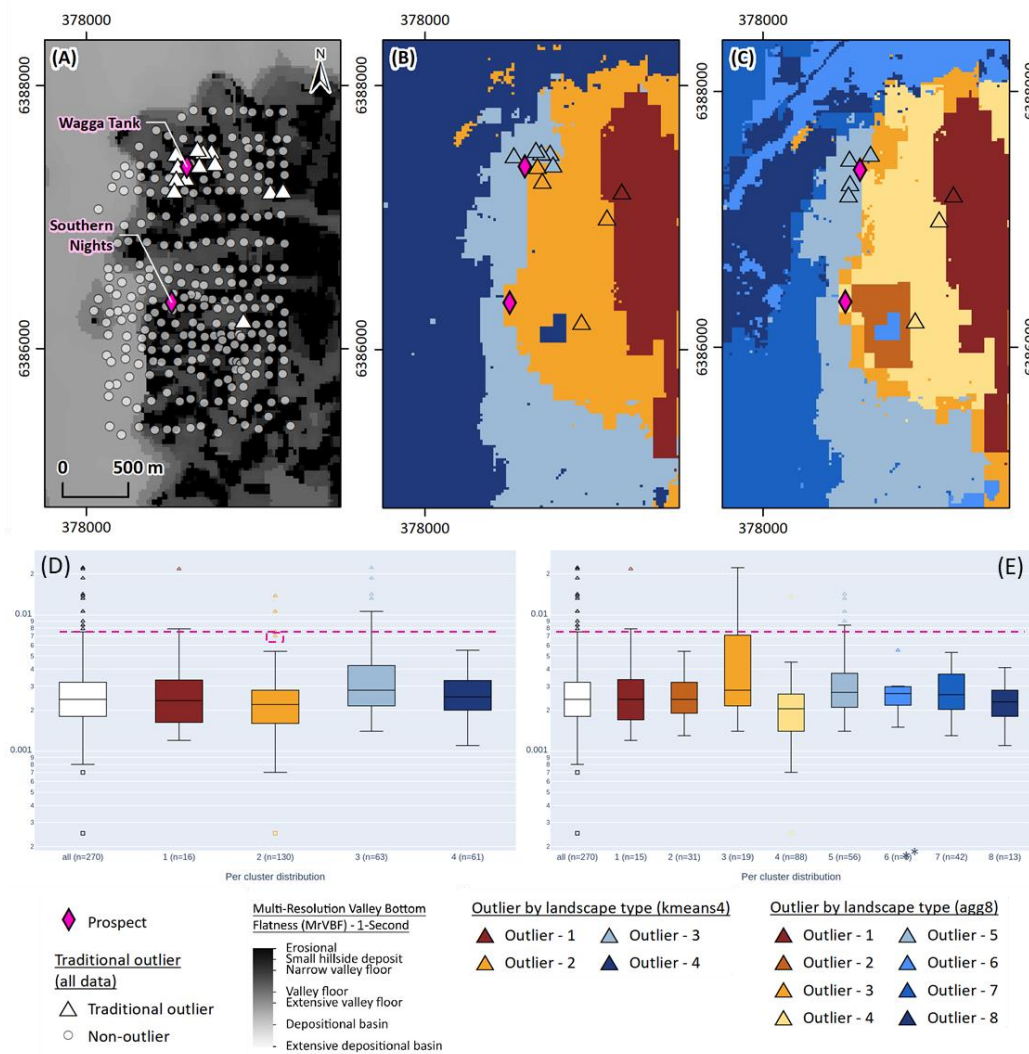


Figure 26: Comparison of Au outliers in the whole sample population to Au outliers by landscape clusters over the Wagga Tank project area. Outliers are plotted as triangles; background value samples are plotted in grey. (A) Spatial distribution of Au outliers for all data. (B) Spatial distribution of Au outliers by landscape population with four clusters. (C) Spatial distribution of Au outliers by landscape population with eight clusters. (D) Boxplots for all data (white box) and by landscape type (coloured boxes) when calculated based on four landscape clusters. (E) Boxplots for all data (white box) and by landscape type (coloured boxes) when calculated based on eight landscape clusters. Easily observed soil anomalies are samples above the dashed horizontal line (white triangles in (A)). Those shown below the dashed mauve line would not be easily observed without the landscape context (coloured triangles in (B) and (C)). *Note that outliers in clusters with <10 samples will not display on maps as these are statistically not meaningful.

Silver concentrations within the Wagga Tank project area range from 0.05 ppm to 1.02 ppm with a mean of 0.11 ppm. The greatest concentrations were primarily detected over and near the Wagga Tank prospect and clustering closely around the radiometric anomaly southeast of the Southern Nights prospect (see the white triangles indicating outliers for the whole sample population in Figure 27A). Separating the sample populations by landscape type confirms that these signatures are strong regardless of landscape type in both kmeans4 and agg8 outputs. Both kmean 4 and agg8 outputs identified additional outliers in residual settings. However, both populations are also small and likely not representative of the data spread and should be reviewed with caution (n=15 and n=16, respectively).

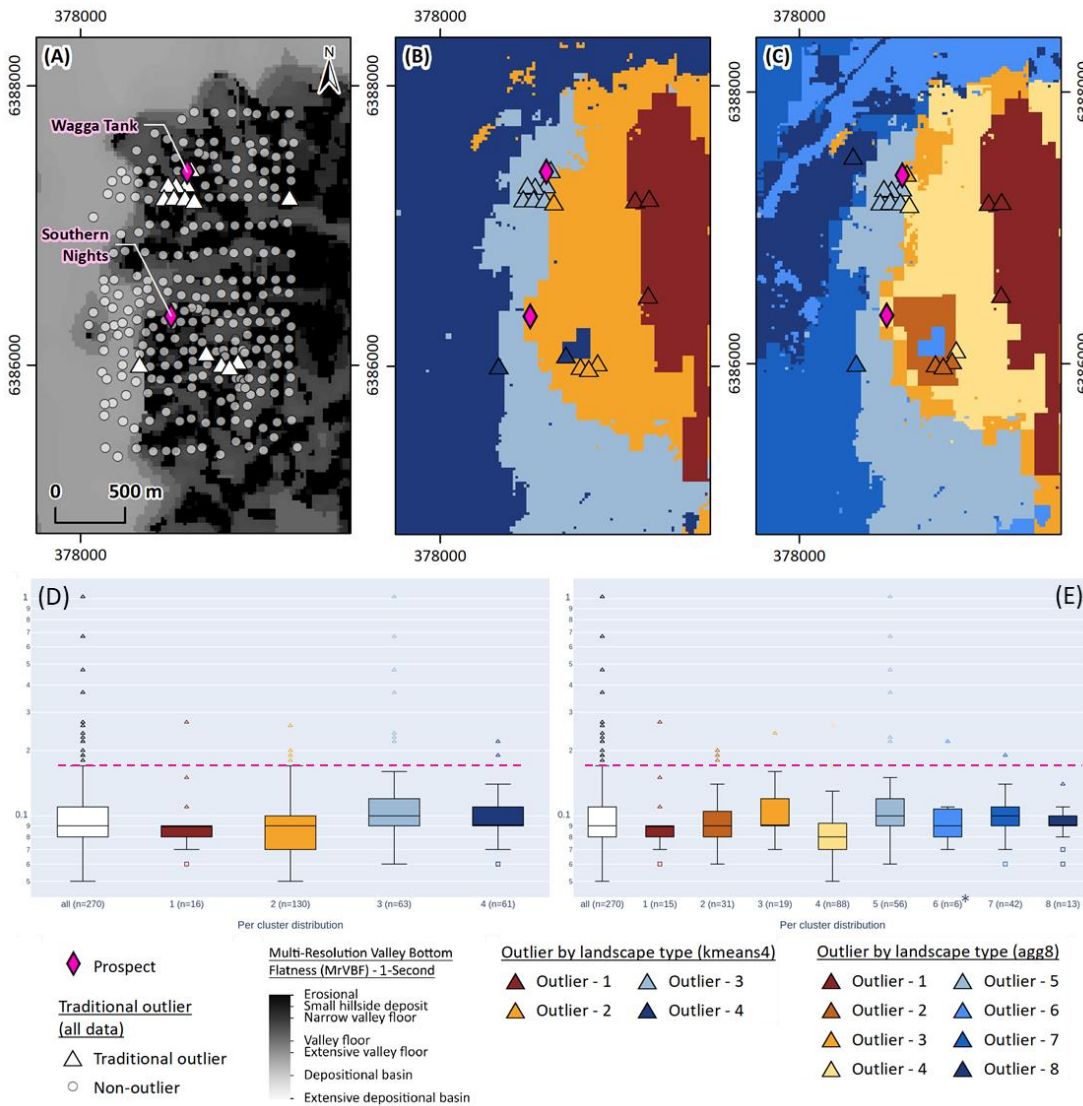


Figure 27: Comparison of Ag outliers in the whole sample population to Ag outliers by landscape clusters over the Wagga Tank project area. Outliers are plotted as triangles; background value samples are plotted in grey. (A) Spatial distribution of Ag outliers for all data. (B) Spatial distribution of Ag outliers by landscape population with four clusters. (C) Spatial distribution of Ag outliers by landscape population with eight clusters. (D) Boxplots for all data (white box) and by landscape type (coloured boxes) when calculated based on four landscape clusters. (E) Boxplots for all data (white box) and by landscape type (coloured boxes) when calculated based on eight landscape clusters. Easily observed soil anomalies are samples above the dashed horizontal line (white triangles in (A)). Those shown below the dashed mauve line would not be easily observed without the landscape context (coloured triangles in (B) and (C)). *Note that outliers in clusters with <10 samples will not display on maps as these are statistically not meaningful.

3.4 Exploration Indices

The UltraFine+® Next Gen Analytics workflow derives exploration indices to automate the identification of patterns in geochemical datasets. Exploration indices via principal component analysis (PCA) take all analysed elements into account. In addition, the future workflow will also derive regolith ratios and indices on a subset of elements that are likely representative of specific mineralisation types for first pass interpretation.

3.4.1 Principal Component Analysis

Principal component analysis is performed on quantile-normalised centre-log transformed data of all elements analysed for each soil sample. The automated output generates five principal components (PC0 to PC4). These principal components preserve the maximum variance between the samples while effectively reducing the number of dimensions. The loadings of each element for each of these five principal components are automatically output in a spider diagram (Figure 28A and Figure 30A). The further away an element plots from the zero line for a given principal component (coloured diamonds connected by coloured lines), the greater the loading for the specific principal component. The PCA allows for a rapid, first-pass identification of element association and potential exploration indices within the dataset. The spatial distribution of PCA-transformed sample data coloured by weight of the principal component is another automatic output (Figure 28B and Figure 30B). Principal component analysis for each sample is also available as shapefiles and CSV files, including eigenvalues, within the Federation and Wagga Tank project data packages (Appendix C and Appendix D, respectively).

While the importance (explained variance) of each of the principal components decreases from PC0 to PC4, principal components are influenced by their landscape setting. Lower principal components will therefore often pick out large-scale lithological variation as the major component(s). Principal components with exploration potential usually explain less variance in the data than the major elements related to geological influence. Hence, in many areas, PC2 and PC3 (3rd and 4th components) may represent the more relevant components in the context of mineral exploration. In some cases, signatures relating to mineralisation will constitute relatively low proportions of variance and thus not be represented by principal components.

Federation

In the Federation project area, the first principal component (PC0) explains 46.2 % of the variability within the dataset and highlights shallow geology and climatic influence (slope aspect or elevation; Figure 28B) and correlates reasonably well with the spatial distribution of pH (see Figure 32C in Section 3.5.1). PC1 explains 18.2 % of the variability within the dataset and picks out the area downslope from and immediately to the northwest of the Federation prospect (indicated by landscape cluster 6 in the agglomerative 12 output (Figure 8D) and is associated with As, Au, Ba, Ta, and Tl (Figure 28A and Figure 29A). PC2 only explains 14.7 % of the variability within the dataset, but shows some exploration potential with association of Ag, As, (Cd), Cu, Ni, S, W and Zn (Figure 28B). The spatial distribution of positive PC2 scores coincide broadly with the Dominion prospect but not with the Federation prospect (Figure 29B). This component has positive loadings with some target and pathfinder elements such as Ag, Cu and Zn, but no Au or Pb. It also is strongly influenced by Mn in the samples. PC3 is associated with lithophile type elements and

possibly reflects igneous rocks with strong positive loadings for Cs, Ga, Rb, Sn (Tl and As). PC4 is strongly positively loaded with Au, Li and Tl which may be a useful pathfinder suite, but this is hard to assess without more background geochemistry.

In retrospect, it appears that PC1 highlights the Federation mineralisation and PC2 highlights the Dominion prospect (Figure 29). This is unexpected as ideally both would be present with a similar elemental signature. Hence, this would assume a similar landscape setting (PCA is not separated by landscape type) and that the two mineralisation styles are also similar.

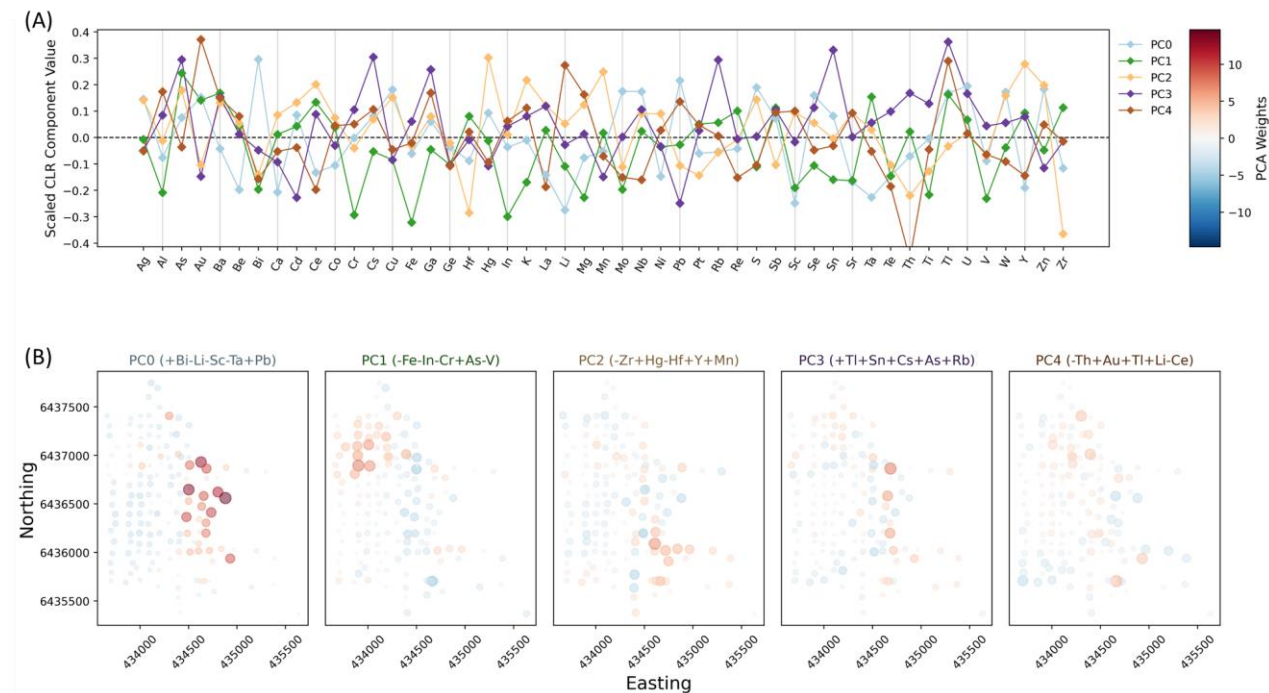


Figure 28: Automated PCA outputs from the UltraFine+® Next Gen Analytics workflow over the Federation project area. (A) Elemental loadings for each of the first five principal components. The further away an element plots from the 0 line, the greater the loading for (influence on) the specific principal component. (B) Automated output of the spatial distribution of principal components weighted by both colour and symbol size (absolute magnitude). The top five elemental loadings (greatest influence) for each principal component are indicated as headings. The colour red indicates a positive component weight (association); the colour blue indicates a negative component weight (association). The larger the symbols the stronger the association. From left to right boxes display spatial distribution of principal component 0, 1, 2, 3 and 4 weightings.

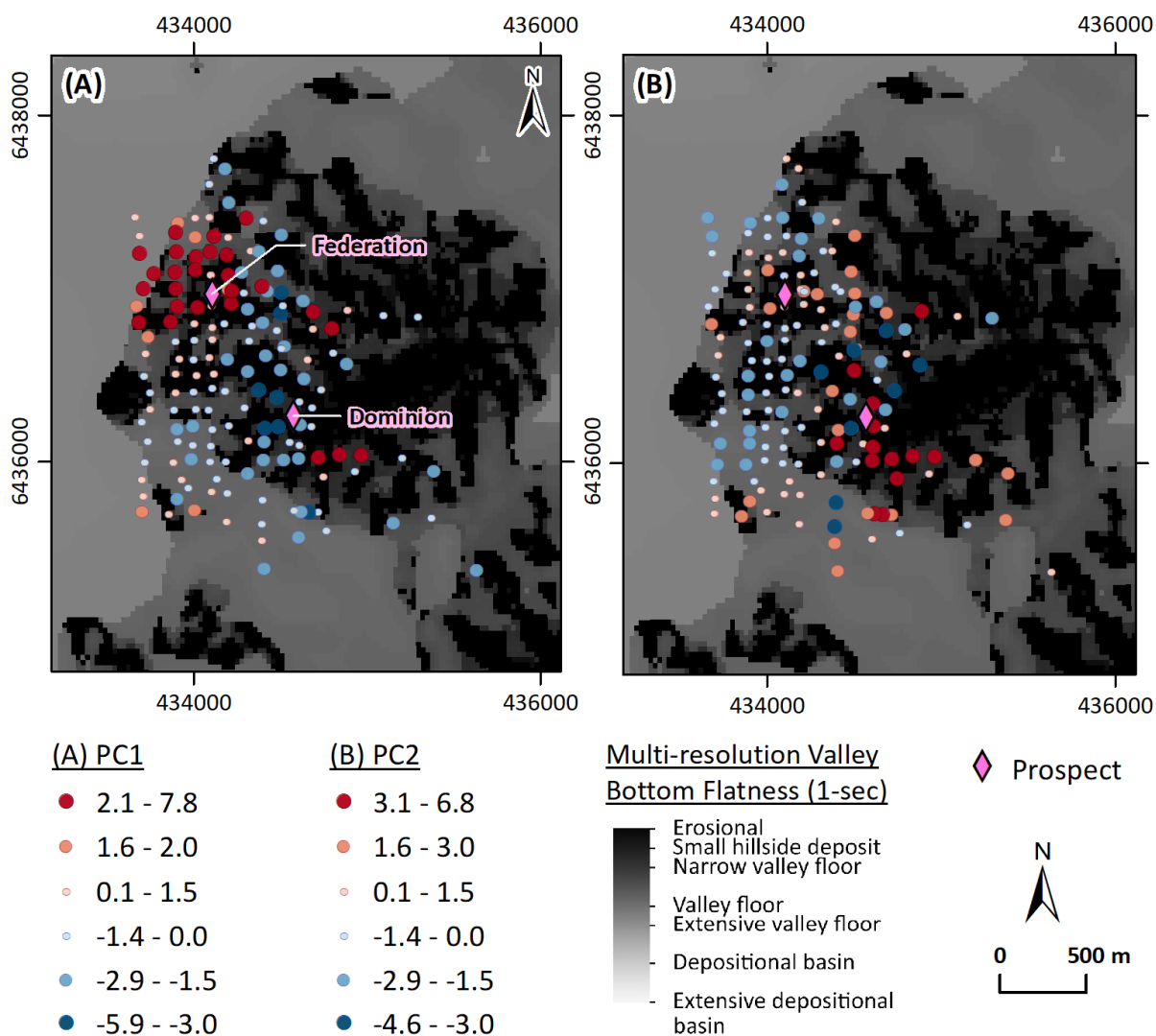


Figure 29: Spatial distribution of principal component 1 (A) and principal component 2 (B) over the Federation project area.

Wagga Tank

In the case of the Wagga Tank project the first principal component (PC0) explains 33.1 % of the variability within the dataset and PC1 22.7 %, PC2 17.1%, PC3 13.9 % and PC4 12.6 %. The generally low percentage of explained variability per principal component indicates that there are not a select few variables that could explain the results such as a dominant geological parent material or climatic influence (slope aspect or elevation) but rather indicate a more complex geochemical environment. Of these five principal components, PC3 and PC4 appear to map landscape types and/or slope position, while PC1 and PC2 show some exploration potential (Figure 30A). PC0 likely captures an analytical artefact related to quantisation (binning of data close to or below the detection limit) of Re data.

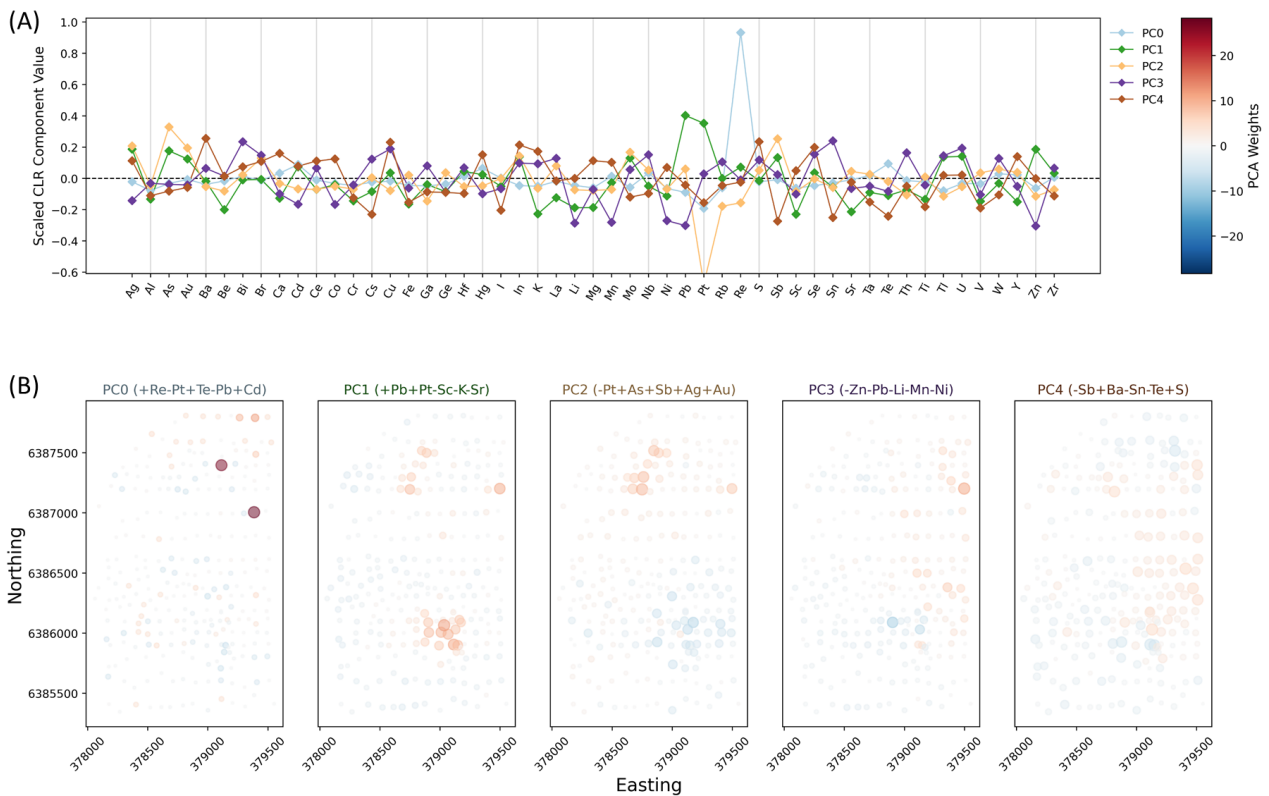


Figure 30: Automated PCA outputs from the UltraFine+® Next Gen Analytics workflow over the Wagga Tank project area. (A) Elemental loadings for each of the first five principal components. The further away an element plots from the 0 line, the greater the loading for (influence on) the specific principal component. (B) Automated output of the spatial distribution of principal components weighted by both colour and symbol size (absolute magnitude). The top five elemental loadings (highest influence) for each principal component are indicated as headings. The colour red indicates a positive component weight (association); the colour blue indicates a negative component weight (association). The larger the symbols the stronger the association. From left to right boxes display Spatial distribution of principal component 0, 1, 2, 3 and 4 weightings. The larger the symbols the stronger the association.

Both PC1 and PC2 show strong positive loadings for chalcophile target and pathfinder elements, such as As, Sb, Mo, Ag ± Se (Figure 30A). Principal component 1 also shows strong positive loading of target and pathfinder elements related to volcanic-associated massive sulphide (VAMS) deposits and sediment-hosted stratiform base metal deposits (Ag, Pb, Zn, Cd, Tl and a weak positive association with Cu) and various other pathfinder elements related to VAMS and sediment-hosted reef deposits, such as As, Au, In, Pb and Zn. While PC2 also shows positive loadings in most of the above elements, it shows only a weak positive loading for Pb and negative loadings for Cu and Zn.

The spatial distribution of PC1 coincides with the area around the Wagga Tank prospect and the area around the radiometric “anomaly” southeast of Southern Nights (landscape clusters 2 and 6; Figure 31A). The spatial distribution of positive loadings of PC2, while still strongest around the Wagga Tank prospect is much more diffuse in the northern part of the project area and only weak

positive loadings are present near the Southern Nights prospect, in deeper cover and rarely around the radiometric “anomaly” (Figure 31B).

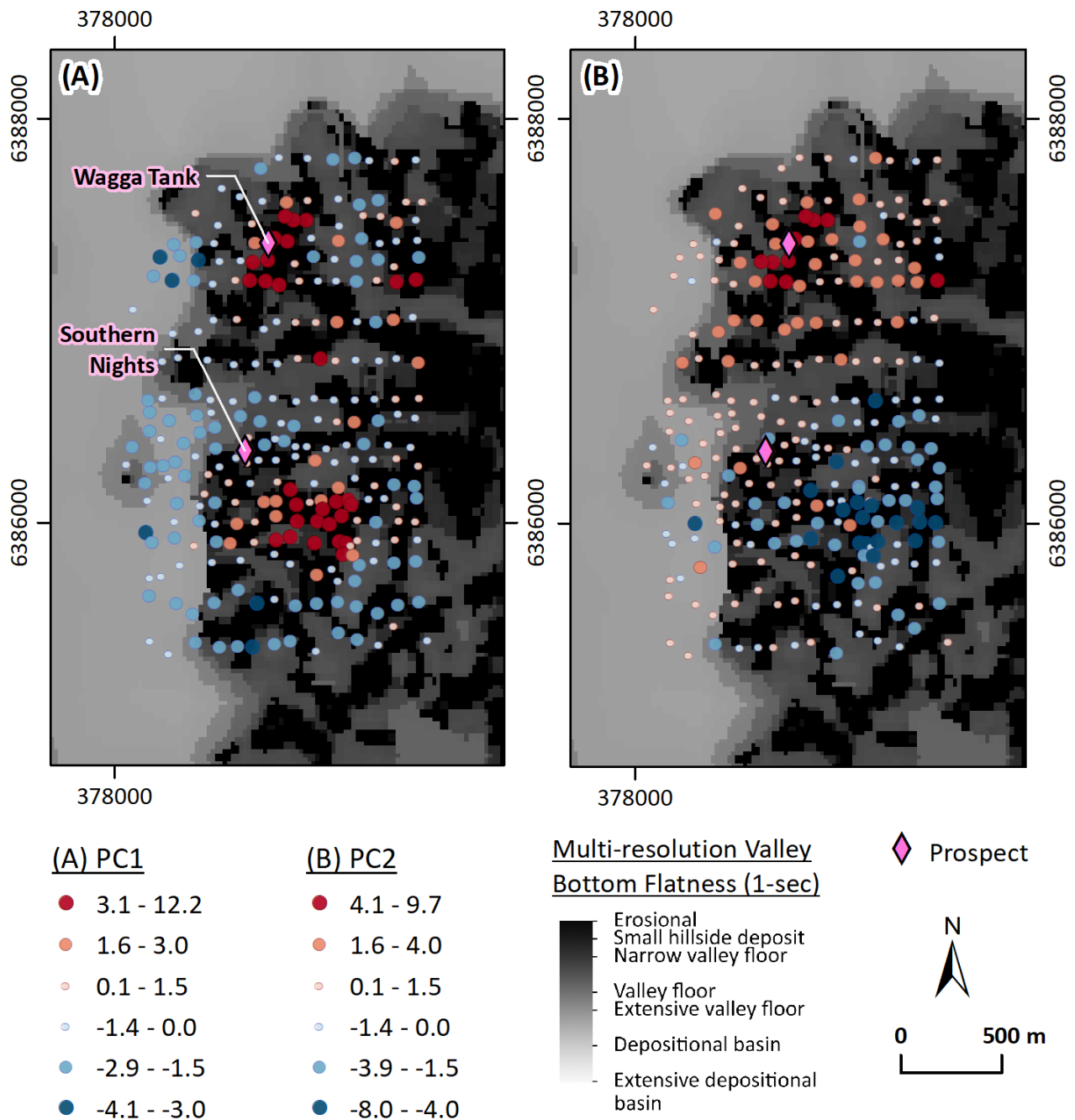


Figure 31: Spatial distribution of principal component 1 (A) and principal component 2 (B) over the Wagga Tank project area.

3.4.2 Regolith ratios and indices

Mineralisation style specific regolith ratios and indices for first-pass interpretation was still under development at the time of writing this report and will therefore not be reported for the GSNSW projects.

3.5 Other Soil Properties

In addition to the multi-element geochemistry suite, several other soil parameters that are related to understanding metal mobility have been added to the UltraFine+® Next Gen Analytics workflow. These include pH, conductivity, particle size distribution, and visible near-infrared (VNIR) mineral proxies and mid-infrared (FTIR) spectral properties. This data is intended to be used for the identification of soil property trends to enable the interpretation of geochemical results within landscape context, especially with respect to better explaining false positive results. At the time of analysing the Federation and Wagga Tank samples, much of the methods for testing for these additional soil properties were still under development and since then methods of data acquisition, processing and QA/QC have been refined. In addition, larger scale data comparison between different project sites to identify broader trends is ongoing. It is important to note that soil sample density near the Dominion prospect and in the area of the upward projection of the mineralisation at Federation is relatively sparse.

3.5.1 pH and EC

The mobility (solubility, transport and precipitation) of many metals, such as the elements of interest in the Federation and Wagga Tank project areas, are driven by pH and redox state. The pH of soils is mainly dependent on the mineralogy of the parent material and is, for example, expected to be more acidic around sulphide-rich deposits and more alkaline where parent material has higher buffering capacity, e.g., via silicate- or carbonate-mediated buffering during weathering and soil formation. Soil pH can therefore be a useful indicator for broad lithological changes, and potentially indicate certain types of mineral occurrences. Hence, it can be a useful tool to confirm landscape types for better context during geochemical sample interpretation. The EC indicates the salinity of soils, which in turn can affect the mobility of metals, such as Cu, Cd, Pb and Zn (Acosta et al. 2011).

Soil pH within the Wagga Tank project area is slightly acidic to alkaline, ranging from pH 4.4 to pH 8.5 with an average of pH 5.6 which is common for these soils (Figure 32A). Soil pH within the Federation project area is similar, ranging from pH 4.1 to pH 8.4, but with a more circumneutral average pH of 6.1 (Figure 32C). Soil EC over the Federation project area is very low (<175 $\mu\text{S}/\text{cm}$) indicating non-saline soils (Figure 32D). Soil EC over the Wagga Tank area is also generally low, but with some elevated values in deeper cover and isolated occurrences near the Wagga Tank prospect (Figure 32B). However, both the Federation and Wagga Tank sample analyses were part of the developmental phase of adding additional soil properties to the UltraFine+® method, and interpretations based on these analyses therefore need to be considered carefully.

More acidic pH (<5.0) occurs around the Wagga Tank prospect as well as the radiometric “anomaly” southwest of the Southern Nights prospect with some lower pH values in deeper cover to the west-northwest of the Southern Nights prospect close to where Cu outliers by landscape cluster (agg8) were identified (Figure 23C). The pH in the immediate vicinity of Southern Nights is slightly higher (pH 6 to 7). Within the Federation project area, pH appears to be more strongly associated with landscape clusters, with residual soils, outcrops and side slopes (landscape clusters 1 and 3) generally more acidic (< pH 6; weathered residual landscape cluster 2, ~pH 6), while pH increases in deeper cover/transported material (Figure 32C).

Interestingly, pH within the Federation project area displays a weak negative correlation with clay ($r = -0.57$) and silt ($r = -0.57$) contents indicating that the finer the grain-size, the more acidic the pH. This indicates that specific surface area (SSA) is related to metal uptake and pH. Unfortunately, this data is not available for this dataset as the method for SSA acquisition was not yet developed.

Despite the influence of pH on soil chemistry, especially adsorption and ion exchange capacity of trace metals on clay, no strong statistical correlation between pH and metal distributions were observed in either project area other than an increase in pH with increasing Ca ($r = 0.68$ in Federation and $r = 0.71$ in Wagga Tank) which is unsurprising given the buffering capacity of Ca.

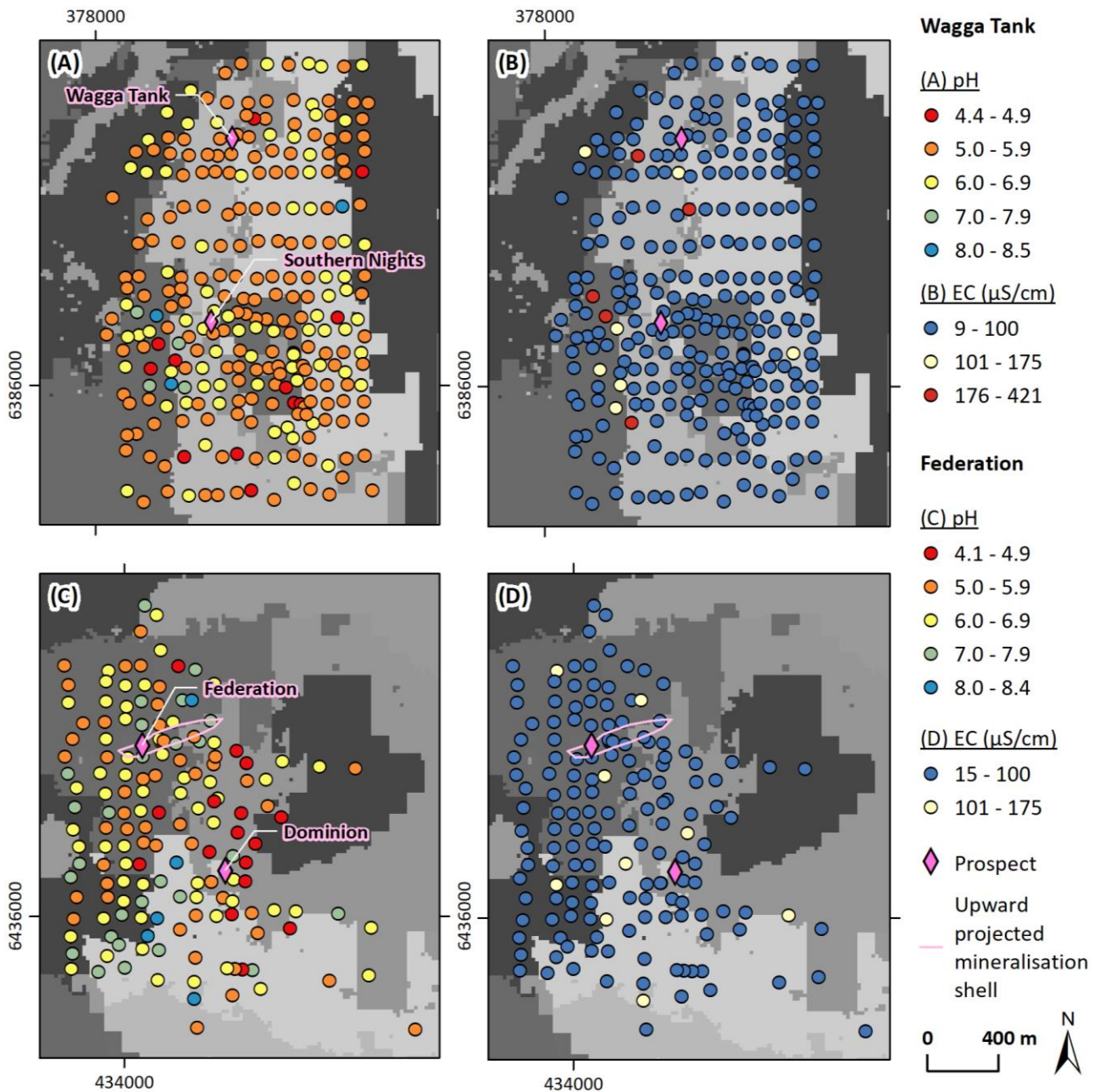


Figure 32: Spatial distribution of soil pH and EC over the Wagga Tank and Federation project areas. (A) pH over Wagga Tank. (B) EC over Wagga Tank. (C) pH over Federation. (D) EC over Federation.

3.5.2 Visible near-infrared spectroscopy (VNIR)

In addition to pH and EC, the concentration of many metals in soil samples is also related to the composition of a given sample, such as the abundance of iron oxides or clay phases. Visible to shortwave infrared reflectance measurements can indicate the presence of key spectrally active mineral groups and their chemistry, and provide relative abundance estimates for iron oxides and kaolinite. As part of the UltraFine+® analyses, 16 spectral soil parameters are reported, including main mineral groups detected in the visible to shortwave infrared region. The main mineral groups (Mineral Group 1 and 2) report only the dominant mineral-group that contributes >51 % to the spectral unmixing algorithm and does not report individual minerals but mineral groups (e.g., white mica rather than muscovite). The mineral groups reported with the UltraFine+® method are Kaolin, Smectite, White-Mica, Amphibole, Chlorite, Dark-Mica, Al-bearing minerals, Mg-bearing minerals, Carbonate and Sulphate.

While some trends can be observed within the Federation and Wagga Tank project areas, it is important to note that measurements were acquired in the early phases of the research project and methods of data acquisition, processing and QA/QC have since been refined. In addition, larger scale data comparison between different project sites to identify broader trends across multiple datasets from locations on the Australian continent was ongoing at the time of writing this report.

Federation

The ultrafine soil samples in the Federation project area are dominated by kaolinite and white mica with minor smectite in both the primary and secondary mineral groups, and broadly reflect different landscape types (Figure 33). Soils on side slopes (orange landscape cluster 2) in relatively sparsely vegetated areas are dominated by white mica which is commonly found associated with shallow soils near, or adjacent to, granitic material. Kaolinite, a common mineral in weathered terrains, is the dominant phase within the other, less residual landscape clusters. Smectite, which is common in alluvial settings, is the dominant phase in only a handful of samples in deeper cover (mid-blue landscape cluster 7; Figure 33A). Some additional samples show smectite as a major phase in mineral group 2, also in or adjacent to deeper cover (Figure 33B). There are no immediate samples over the Dominion prospect and large parts of the surface immediately above the mineralisation at Federation have also not been sampled, with the main mineral phase detected being kaolinite with some white mica detected in otherwise weathered shallow cover immediately adjacent to the Federation mineralisation surface projection.

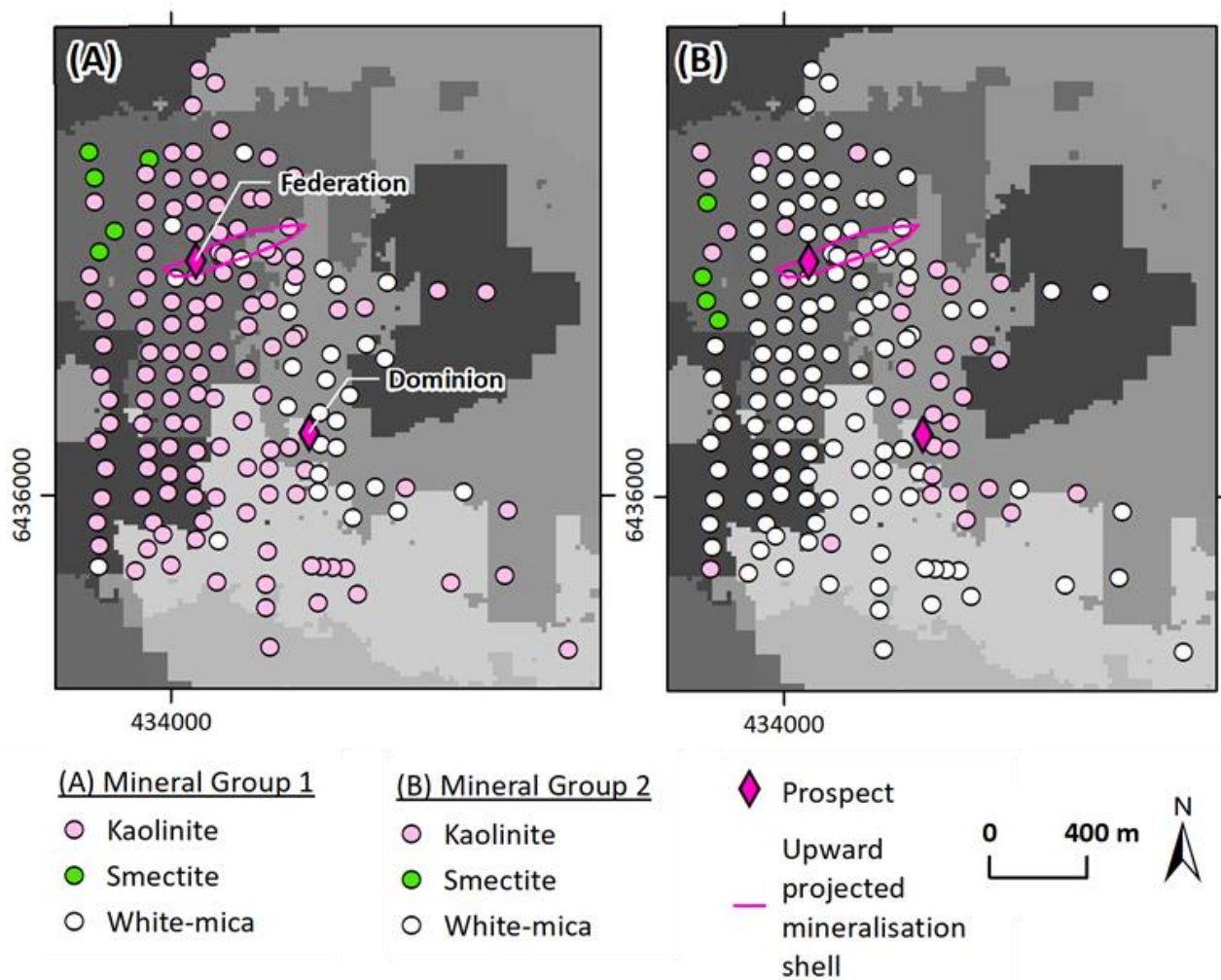


Figure 33: Spatial distribution of spectrally active mineral groups over the Federation project area. (A) Mineral group 1. (B) Mineral group 2.

Many trace metals are readily adsorbed to clays and iron (oxyhydr)oxides, especially those with a high surface area. Given the high adsorption capacity of iron oxides, it is worth considering whether an anomaly of a metal of interest is present in iron oxide-rich or -poor soils and normalise the geochemical data accordingly. Over the Federation project area, the relative abundance of Fe-oxides is very low in residual side slope soils and more abundant in the relatively strongly weathered landscape cluster 2 (Figure 34A). Soils are notably more goethitic within the surface projection of the planned mine shell at Federation and in adjacent transported cover downslope to the northwest (Figure 34B).

Unsurprisingly, relative kaolinite abundance follows a similar albeit less defined trend to the relative iron-oxide abundance, with more kaolinite present in landscape clusters with the strongest weathering (e.g., the landscape cluster hosting the Federation prospect; Figure 34D). Kaolinite crystallinity over the Federation project area is very low. Values below 1.015 are traditionally considered disordered, and the kaolinite crystallinity of all soil samples within the Federation project area are below this value and thus would indicate transported cover. However, these values were derived on different sample materials (rock chips) and the presence of smectite in soil samples can reduce the numerical value of the kaolinite crystallinity. Therefore, separating traditional levels of confidence for kaolinite crystallinity (>1.05 = high, 1.05 to 1.015 = moderate, <1.015 = disordered) might not be appropriate for this data. Hence, we focus here on subtle

variations in the data that correspond to landscape clusters and, in the case of the Federation project area, to areas of mineralisation (Figure 34F). Identifying similar trends in data across different project sites is part of the ongoing research project.

The soil colour is related to soil composition and it is therefore not surprising that the Munsell colour of samples also follows general landscape cluster boundaries (Figure 34C). One component of the soil colour, the saturation, within the Federation project area correlates spatially with side slope material as well as with the area around the Federation prospect. Interestingly, saturation (Figure 34F) increases with increasing pH in side slope settings ($r = 0.51$; see Figure 32C in Section 3.5.1) indicating that more acidic soils are more strongly leached and have paler colours.

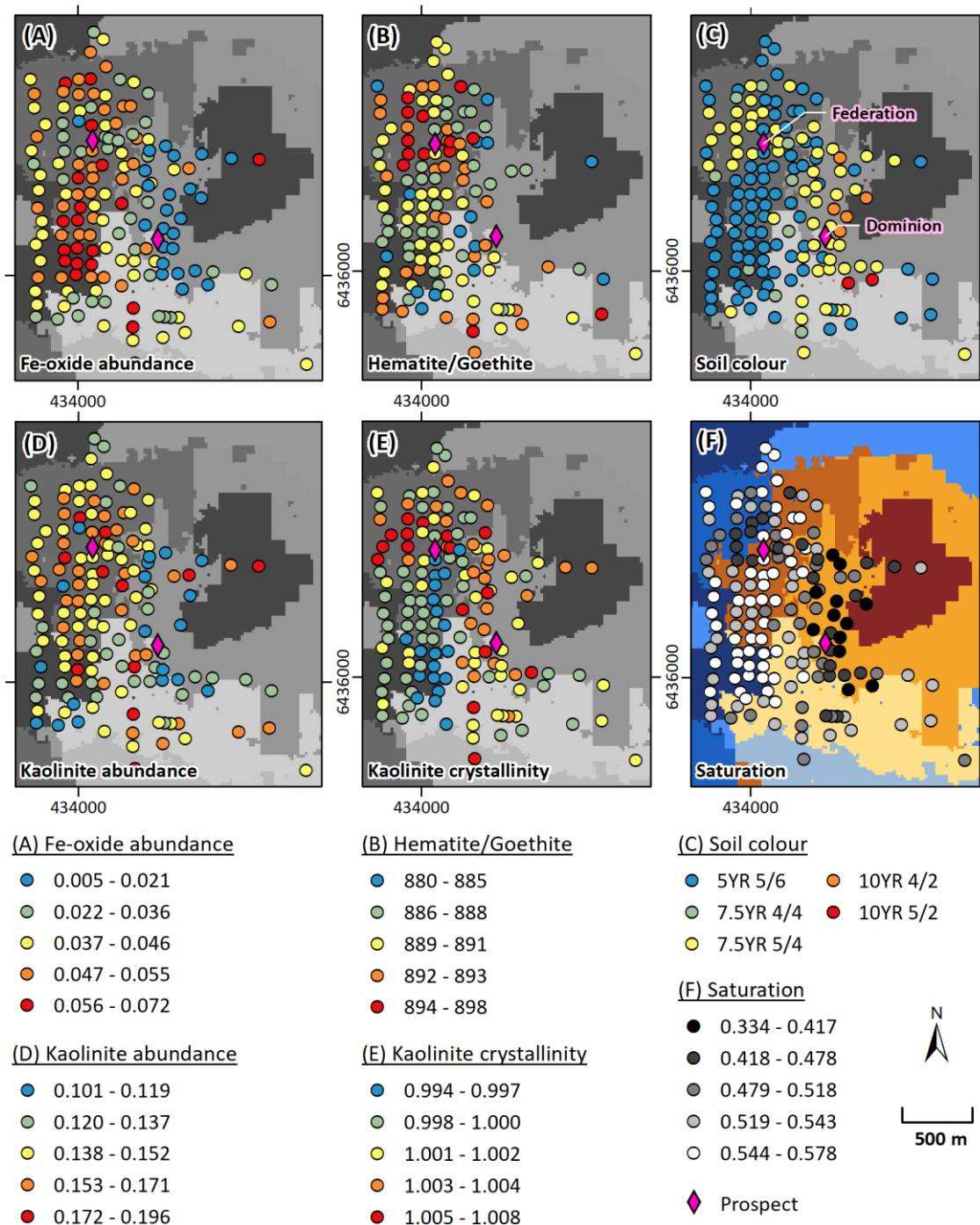


Figure 34: Example VNIR parameters in ultrafine soil samples over the Federation project area. (A) Relative iron oxide abundance. (B) Iron oxide species. Lower values (blue) indicate more hematitic materials, whereas higher values (red) mean the material is more goethitic. Note that where Fe-oxide abundance is very low, the iron oxide species is not defined and data is not plotted. (D) Relative kaolinite abundance. (E) Relative kaolinite crystallinity. (C) Munsell colour. (F) Saturation which indicates how washed out or pure the hue of a colour is.

Wagga Tank

The ultrafine soil samples in the Wagga Tank project area are dominated by kaolinite with minor white mica and smectite in the primary mineral group and mainly white mica with some kaolinite and smectite in the secondary mineral group. Smectite appears to be a dominant phase in the secondary mineral group near the Wagga Tank prospect and in adjacent deeper cover to the west,

and around the radiometric “anomaly” in the southern part of the project area where elevated metal concentrations have been observed (refer to Section 3.3.2).

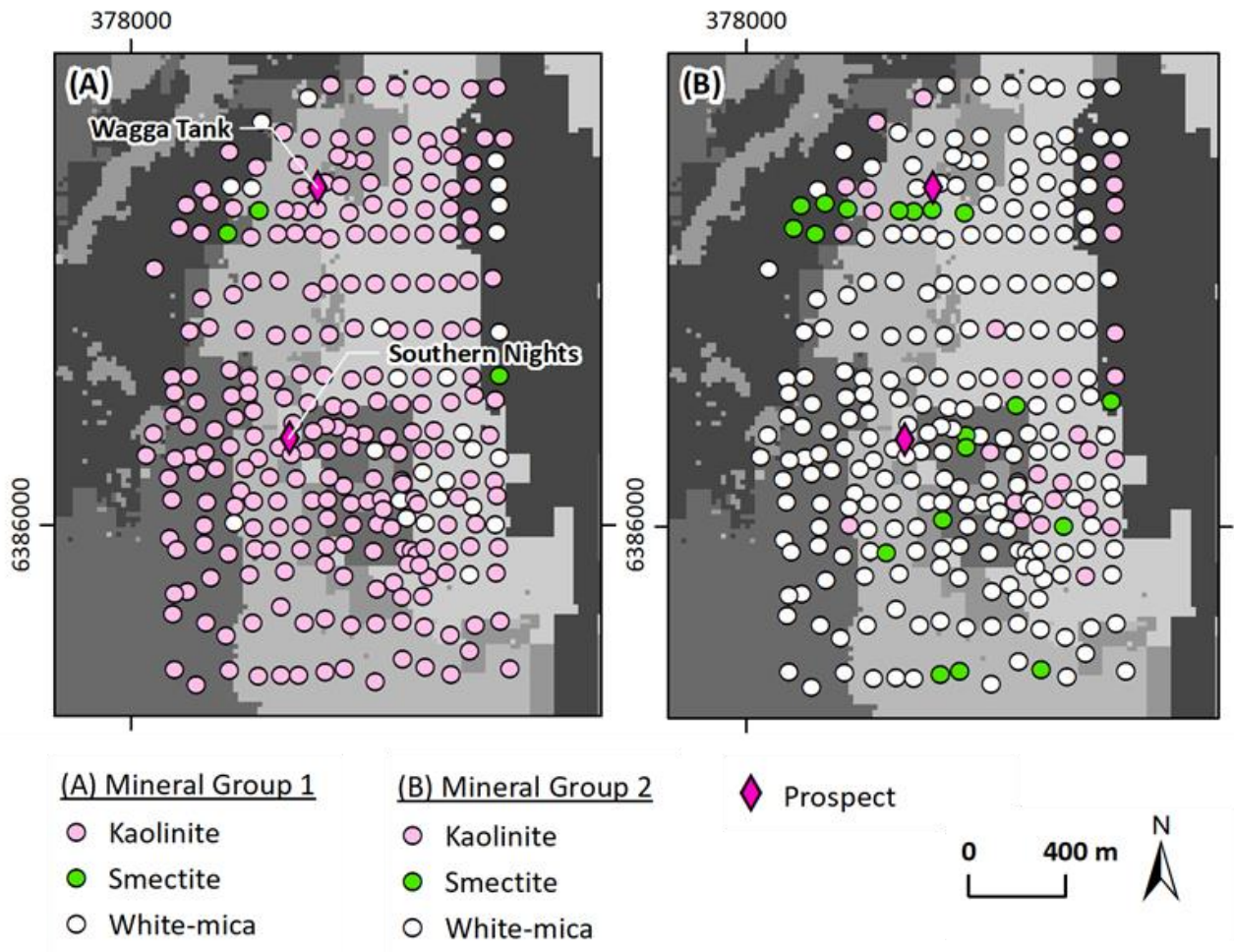


Figure 35: Spatial distribution of spectrally active mineral groups over the Wagga Tank project area. (A) Mineral group 1. (B) Mineral group 2.

Over the Wagga Tank project area, the relative abundance of Fe-oxides is generally higher than in the Federation project area (Figure 36A) and soils are notably more goethitic in side slope and outcropping landscape settings as well as near the Wagga Tank prospect (Figure 36B). As is the case for the Federation project area, kaolinite crystallinity over the Federation project area is very low but with general trends of more disordered kaolinite in landscape settings of deeper cover (Figure 36E). The soil colour and saturation follows general landscape cluster boundaries (Figure 36C, F).

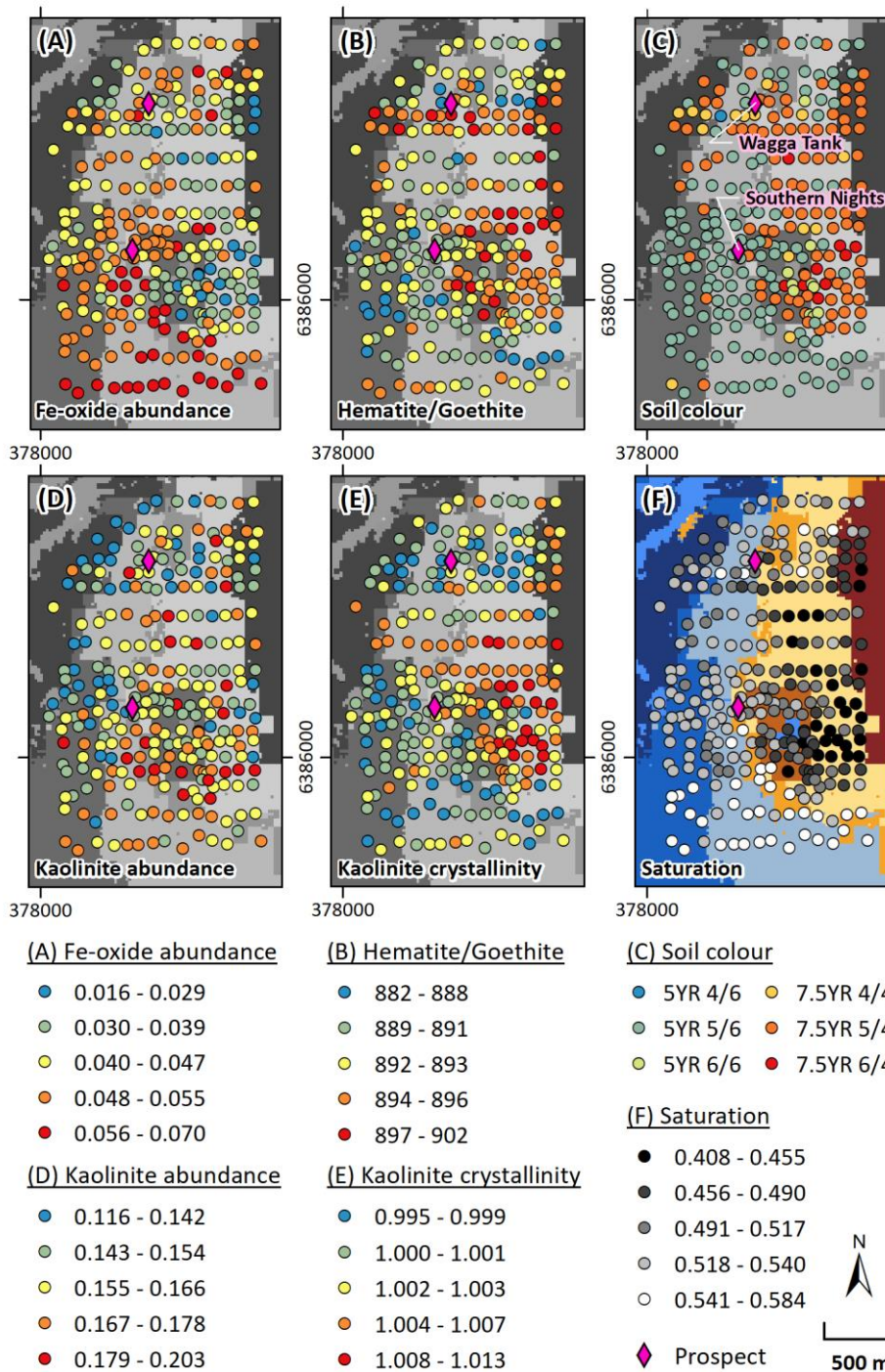


Figure 36: Example VNIR parameters in ultrafine soil samples over the Wagga Tank project area. (A) Relative iron oxide abundance. (B) Iron oxide species. Lower values (blue) indicate more hematitic materials, whereas higher values (red) mean the material is more goethitic. (C) Munsell colour. (D) Relative kaolinite abundance. (E) Relative kaolinite crystallinity. (F) Saturation which indicates how washed out or pure the hue of a colour is.

3.5.3 FTIR

Similar to VNIR, FTIR spectroscopy analyses contain information on the composition and chemical properties of the ultrafine soil samples. This information can help to better understand the influence of ultrafine soil composition on the mobile element uptake and adsorption. The analysis produces semi-quantitative information on the amount of clays, carbonates, quartz and organic

carbon in the soil samples and provides information about the presence of gibbsite along with an estimate of the gibbsite quantity.

Federation

Of the 163 samples over the Federation project area, 90 data points were excluded after data acquisition because they did not pass QA/QC. These samples were measured at the start of the research project when the methodology was still undergoing development and, unfortunately, not enough sample mass was retained to re-analyse samples. Little can therefore be inferred from these samples, as no analyses are available over the Dominion prospect and only few samples are located within the surface projection of the Federation mineralisation.

Wagga Tank

The FTIR data for Wagga Tank, while also part of the earlier methodology development, passed QA/QC for standards. As expected, clay is highest near Wagga Tank and in side slope material adjacent to the radiometric anomaly, while quartz abundance is highest in transported cover. Total organic carbon is low within the area, ranging from below the detection limit (0.5 %) in most samples to 1 %. Very little (< 1%) or no carbonate was detected in the Wagga Tank samples via FTIR analysis and gibbsite was only detected in a handful of samples at very low levels.

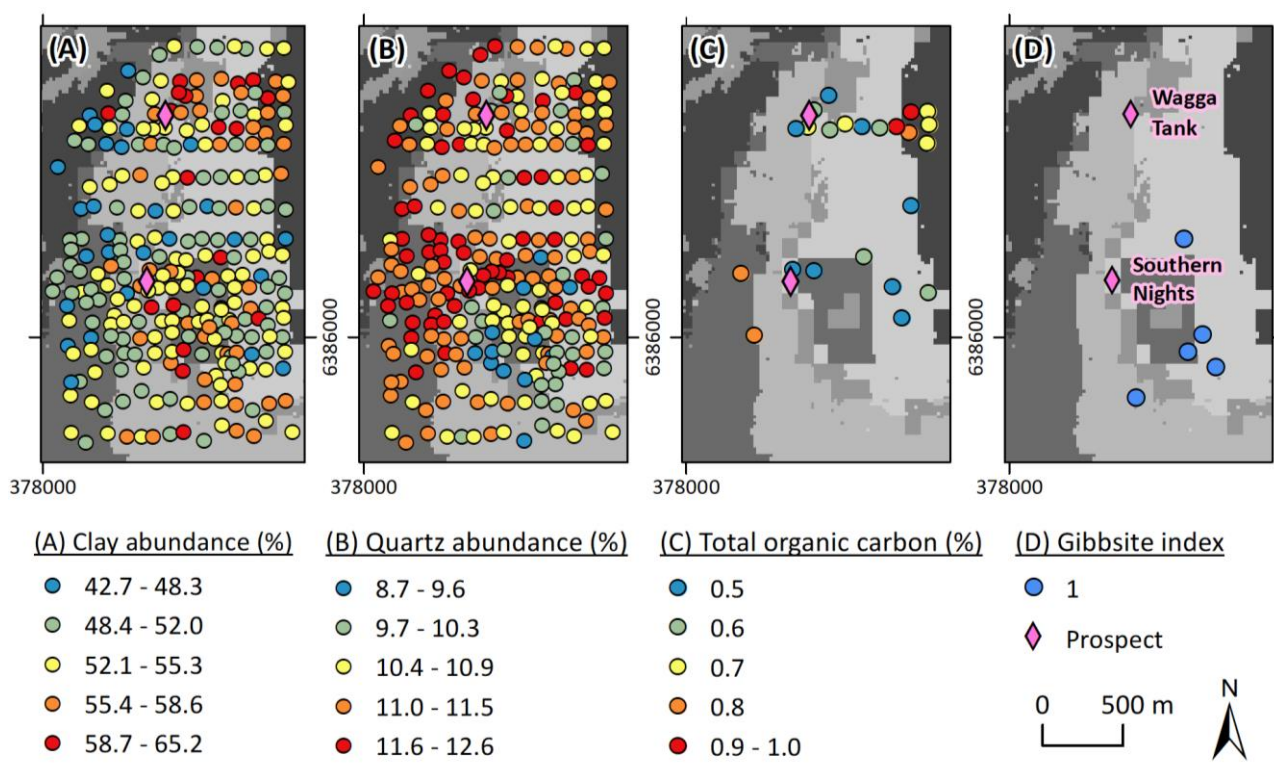


Figure 37: Spatial distribution of clay abundance (A), quartz abundance (B), total organic carbon (C), and gibbsite index (D), analysed via FTIR over the Wagga Tank project area.

Many trace metals are readily adsorbed to clays and it is worth considering whether an anomaly of a metal of interest is present in clay-rich or -poor soils and normalise the geochemical data accordingly. An example for the Wagga Tank project area is presented in Figure 38, where Au and Cu concentrations have been normalised by clay abundance. While there is a negligible effect on the Au concentrations supporting the elevated Au concentrations around Wagga Tank (Figure 38A,

B), many of the higher Cu concentrations have been levelled and in this context two samples in transported cover near the Southern Nights prospect are more visible.

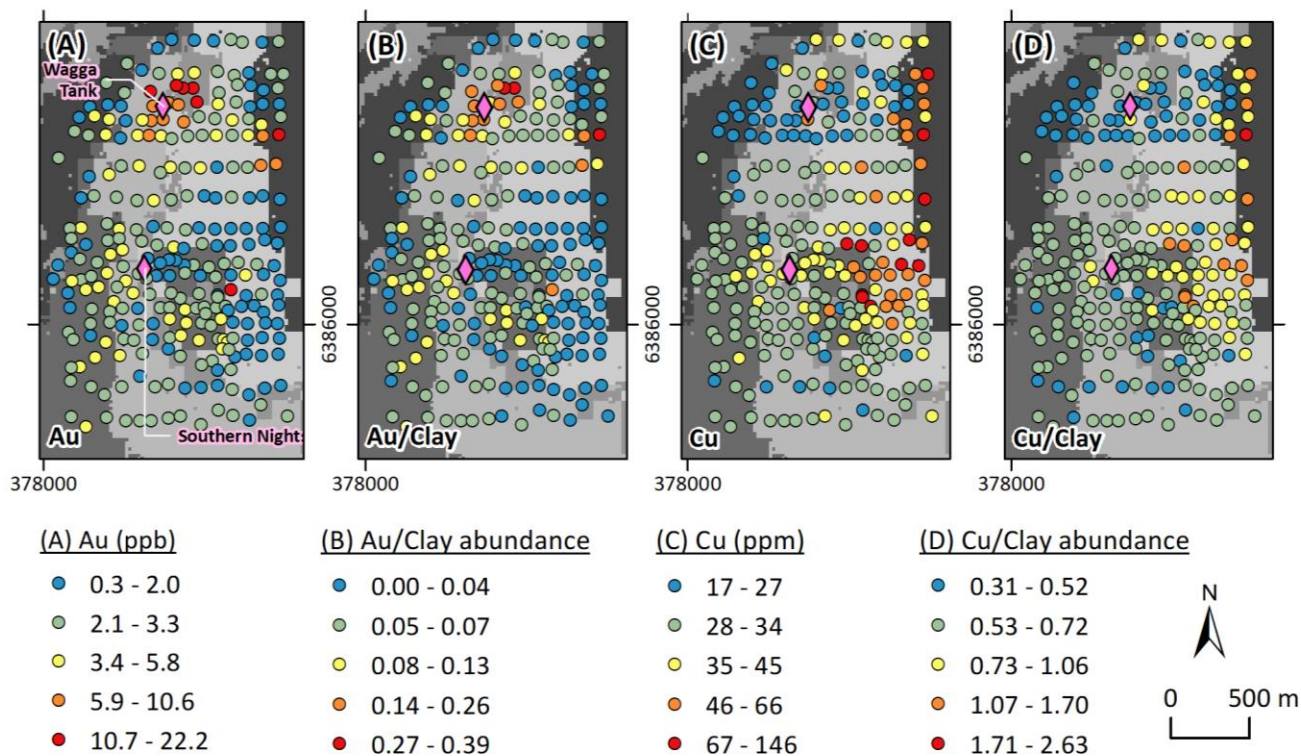


Figure 38: Spatial distribution of example metal concentrations normalised by clay abundance over the Wagga Tank project area. (A) Au concentrations in ppb. (B) Au concentrations normalised by clay abundance. (C) Cu concentrations in ppm (D) Cu concentrations normalised by clay abundance.

3.5.4 Sizing

The UltraFine+® particle size analysis reports the percentage of sand, silt and clay in bulk (<2 mm) soil samples. These values are then used to derive broad soil textural classes and can be used to identify key changes in landscape soil morphology. The mobility of many metals in soil is linked to soil texture due to their affinity to the clay fraction. The clay fraction effectively immobilises these metals, while a higher percentage of sand fractions with low binding strength leads to higher metal mobility (Rieuwerts et al. 1998). While the UltraFine+® soil sample analysis method takes this into account on an individual sample scale and especially within a specific landscape type, by extracting only the clay fraction of a given sample, the overall soil morphological environment will indicate larger scale soil development and composition. This in turn affects general trends of metal mobility in a given landscape environment and informs the context for the machine learning derived landscape clusters.

The soil texture in the Wagga Tank and Federation project areas is mainly sandy loam to loamy sand with little landscape variation in terms of coarse sand or channel deposits. Hence, soil texture in these particular project areas likely has little influence on the observed variations in metal concentrations.

In addition to the above, the UltraFine+® particle size analysis also measures the specific surface area of a given soil sample, which is an important control on cation exchange and adsorption

capacity in soils (Macht et al. 2011) with surface area inversely related to the particle size. Unfortunately, at the time of data acquisition the method for determining specific surface area was still under development and not enough sample was retained to re-analyse either the Federation or the Wagga Tank project soil samples. Spatially we observe patterns in the soil texture classes that align with some of the landscape cluster boundaries. For example, there is more loamy sand (coarse particles) in areas of sand plains and sheet wash (compare Figure 39 with Figure 10 and Figure 12).

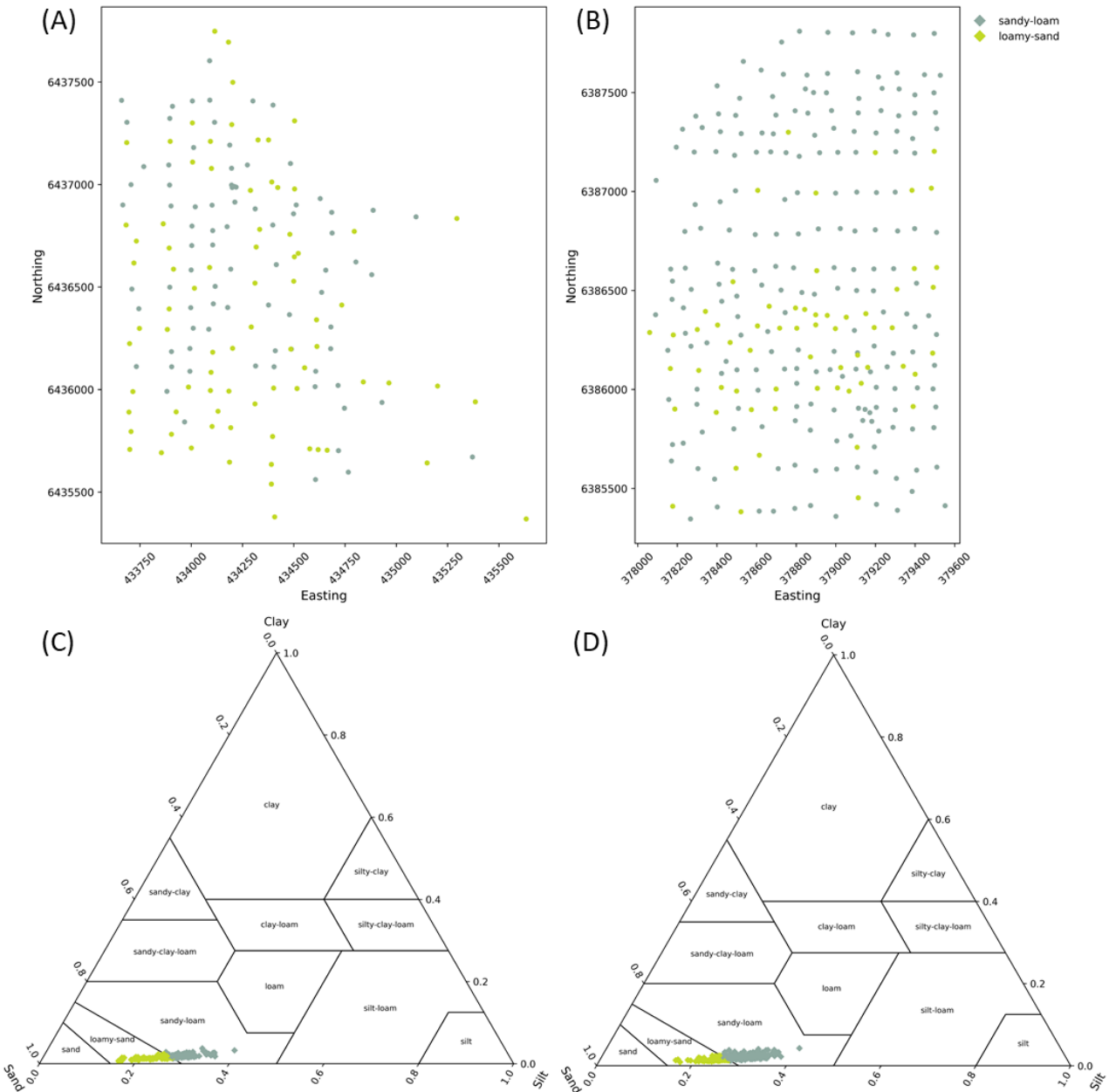


Figure 39: Soil texture triangle and spatial distribution over the Federation (A and C) and Wagga Tank (B and D) project areas.

3.6 Dispersion and Source Direction

At the time of writing this report, the dispersion direction was still under development. However, we show some preliminary outputs. Both source direction and dispersion direction are available as

shapefiles for the Federation and Wagga Tank project area. The source direction is derived for each sample with the arrow pointing up-slope and proportional to the steepness (likely greater dispersion distance). It is important to note that the accuracy of the source direction depends on the accuracy of the GPS reading of a given soil sample and multiple adjacent sample points should be considered when interpreting the likely source direction of a geochemical anomaly in transported cover. The dispersion direction is calculated on a grid over each project area rather than on each sample point and the arrows point down-slope and are intended to give a first-glance overview of broader dispersion trends within your area. This can be a useful tool for larger survey areas with transported cover and potential for infill sampling. The appropriate grid spacing for the dispersion direction as an automated output is under development.

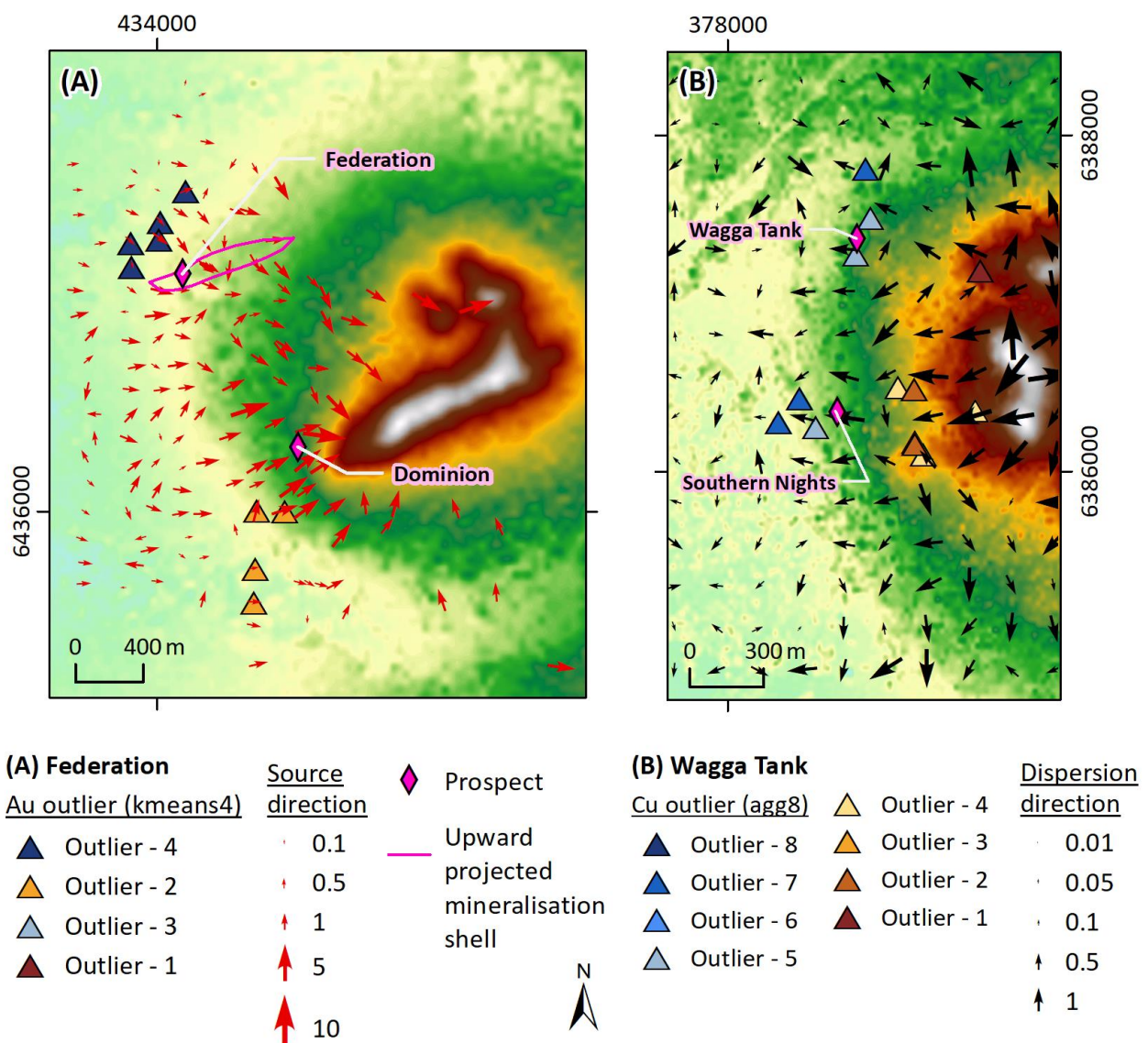


Figure 40: Source and dispersion direction over the Federation and Wagga Tank project areas. (A) Source direction of individual soil sample points and Au outliers by landscape type (kmeans4) within the Federation project area. Source direction is calculated from the DEM (background) but is dependent on accurate GPS readings. (B) Dispersion direction grid and Cu outliers by landscape type (agg8) within the Wagga Tank project area. Dispersion directions indicate broad scale trends. Arrows and numbers are proportional to the slope degree.

For both Federation and Wagga Tank most samples were collected in relatively flat landscape settings. The largest slope was 9.5 degrees within the Federation project area and 5.0 degrees

within the Wagga Tank project area. Within the Federation project area, source directions of individual sample locations identified as Au outliers by landscape cluster (kmeans4) to the northwest of the Federation prospect and immediately to the south-southwest of the Dominion prospect point up-slope towards these prospects (Figure 40A). Since these directions (and the slope angle) depend on accurate GPS readings, they indicate the immediate area context (several metres at most). As such, not all source directions for these samples point towards the prospects and the overall dispersion direction should be considered.

The dispersion direction for both project areas is available but is part of current developments and grid spacing is not yet uniform. For the Wagga Tank project area, dispersion directions were calculated on a 250 m grid. Copper outliers by landscape cluster (agg8) to the west of the Southern Nights prospect are broadly situated in the direction of the overall dispersion trend (down-slope) (Figure 40B). Outliers are also apparent in the direction of dispersion from the radiometric potassium “anomaly”, and dispersion directions around the Wagga Tank project area are influenced by the very small slope angle. It is important to note that the dispersion direction only takes current slope directions into account and palaeo-relief was not considered.

4 Summary

This report presented some example outputs of the UltraFine+® Next Gen Analytics workflow with the goal of using machine learning to integrate spatial data and soil properties to provide landscape context for geochemical data and basic, first-pass data interpretation. These outputs included proxy regolith landscape clusters, maps and boxplots of elemental outliers by landscape type, principal component analysis, soil texture diagrams and dispersion and source direction. Some components of the UltraFine+® method (e.g., mid-infrared spectral properties) and the Next Gen Analytics workflow (e.g., regolith indices and catchment analysis) were still underdevelopment during data acquisition and at the time of writing this report, and are therefore not available for these project sites.

The Geological Survey of New South Wales provided 433 soil samples from two sites in the Cobar Basin, NSW, to the UltraFine+® Next Gen Analytics research project in 2020. These samples were collected in tenements with four mainly Pb-Zn sulphide prospects owned by Peel Mining and Aurelia Resources, and both project sites were part of the first-generation developments of the research project with a focus on refining the UltraFine+® method, principal functionality of the machine learning workflow, and first-pass testing of the UltraFine+® Next Gen Analytics outputs over areas with tangible exploration targets.

The UltraFine+® Next Gen Analytics workflow was designed primarily for greenfield exploration over areas with 100s to 1000s of samples prior to significant ground disturbance. However, despite the small number of samples, especially in the immediate vicinity of the Federation and Dominion prospects, and some ground disturbance, both the Wagga Tank and Federation project areas provided valuable example sites to develop and test the workflow over known mineralisation.

The data herein provides useful information of background concentrations in soil samples as well as those over mineralisation in different landscape settings (shallow to deeper cover) for future exploration activities in the region and surrounding areas. Maximum concentrations of Ag, Cu and Zn were measured within the Wagga Tank project area with 1020 ppb Ag, 146 ppm Cu and 598 ppm Zn, and maximum concentrations for Au and Pb were measured within the Federation project area with 51 ppb Au and 585 ppm Pb.

A variety of clustering methods were trialled to generate landscape context for the geochemical data, and the recommended outputs for the Wagga Tank project area are those produced via an agglomerative algorithm with eight landscape clusters (agg8), and for the Federation project area, those with a k-means algorithm with four landscape clusters (kmeans4). Regardless of the number of clusters, all machine learning-derived outputs have produced more detailed regolith proxies than publicly available landscape maps for the Federation and Wagga Tank project areas. Due to the complexity of the landscapes, an even larger number of clusters would have resulted in a more detailed approximation of the complex regolith types. Testing additional clusters has been trialled for these sites. This has been crucial in developing the future workflow, which will include an additional output with 12 landscape clusters. However, the number of landscape clusters is the result of a balanced approach to represent the major landscape types of the area while also

enabling meaningful interpretation of geochemical data. Hence, the agglomerative 12 landscape clusters are not recommended for the interpretation of the soil data.

The Federation and Wagga Tank project areas were important to assess the workflow over areas of significant ground disturbance, which are usually masked out. However, given that the main areas of interest within the Federation and Wagga Tank project areas are those with the most apparent ground disturbance, masking was not applied to either project area. Despite this, the outputs still provide valuable information.

The GSNSW study sites were crucial to the development of the final data acquisition method and QA/QC procedure for the VNIR and FTIR analyses, and these have since been improved. Owing to being part of the development phase of the project, subsequently developed QA/QC failed many samples for FTIR over the Federation project area. Notwithstanding this, some subtle variations in the data correspond to landscape clusters and mineralisation, especially over the Federation project area, where soils are notably more goethitic within the surface projection of the planned mine shell and in adjacent transported cover downslope to the northwest.

While the UltraFine+® Next Gen Analytics workflow was designed to identify outliers in transported cover, the workflow accommodates for identifying anomalies in other settings (outcrop, subcrop or shallow residual soils) by also generating data, maps and shapefiles for the whole sample population. Therefore, original, elevated elemental signals will not be lost. The Federation prospect is an example, where strong signals are present over the mineralisation, but more subtle signals in adjacent transported cover to the northwest of the prospect are magnified by separating samples into populations by landscape clusters for Au. The dispersion and source direction outputs generated by the workflow enable rapid, first-pass interpretation of such relationships.

Principal component analysis indicates that principal components 1 and 2 show some exploration potential over the Federation project area with positive loadings of target pathfinders. Interestingly, it appears that PC1 shows the Federation mineralisation and PC2 shows the Dominion prospect. This is unexpected as, ideally, both would be present with a similar elemental signature, but this also assumes a similar landscape (PCA is not separated by landscape type) and that the two mineralisation styles are also similar. Over the Wagga Tank project area, both PC1 and PC2 show strong positive loadings for chalcophile target and pathfinder elements,

The Federation and Wagga Tank project areas are small sites by area and sample number compared to the larger-scale greenfield areas the workflow was intended for. Both sites have strong geochemical signals and subtle but complex regolith settings. Future work within the UltraFine+® Next Gen Analytics for Discovery research project aiming to incorporate these sites with broader background areas and combine landscape types from other landscape areas. These sites may, therefore, potentially serve as “training” data sets for future supervised machine learning to identify similar patterns in other areas of the Cobar Basin.

References

- Acosta, J.A., Jansen, B., Kalbitz, K., Faz, A., Martínez-Martínez, S., 2011. Salinity increases mobility of heavy metals in soils. *Chemosphere*. 85(8):1318-24. doi: 10.1016/j.chemosphere.2011.07.046
- Bureau of Meteorology, 2022. Online climate data for Alice Springs Airport station, http://www.bom.gov.au/climate/averages/tables/cw_015590.shtml [last accessed April 2022]
- Chan, R.A., Greene, R.S.B., de Souza Kovacs, N., Maly, B.E.R., McQueen, K.G., Scott, K.M., 2001. Regolith geomorphology, geochemistry and mineralisation of the Sussex-Coolabah area in the Cobar Girilambone region, north-western Lachlan foldbelt, NSW. CRC LEME Report 166, 56 pp.
- Chan, R.A., Greene, R.S.B., Hicks, M., Le Gleuher, M., McQueen, K.G., Scott, K.M., Tate, S.E., 2004. Regolith architecture and geochemistry of the Byrock area, Girilambone region north-western NSW. CRC LEME Open File Report 159, 71 pp.
- Chan, R.A., Greene, R.S.B., Hicks, M., Maly, B.E.R., McQueen, K.G., Scott, K.M., 2002. Regolith architecture and geochemistry of the Hermidale area of the Girilambone region, north-western Lachlan Fold Belt, NSW. CRC LEME Report 179, 48 pp.
- Edgecombe, D., Soininen, L., 2019. Wagga Tank/Southern Nights and Mallee Bull, evolving stories. AIG Mines & Wines, 26-27th September 2019, Wagga Wagga.
- Gallant, J., Austin, J., 2012a. Slope derived from 1" SRTM DEM-S. v4. CSIRO. Data Collection. <https://doi.org/10.4225/08/5689DA774564A>
- Gallant, J., Austin, J., 2012b. Aspect derived from 1" SRTM DEM-S. v6. CSIRO. Data Collection. <https://doi.org/10.4225/08/56D778315A62B>
- Gallant, J., Dowling, T., Austin, J., 2012. Multi-resolution Valley Bottom Flatness (MrVBF). v3. CSIRO. Data Collection. <https://doi.org/10.4225/08/5701C885AB4FE>
- Gallant, J., Wilson, N., Dowling, T., Read, A., Inskeep, C. 2011. SRTM-derived 1 Second Digital Elevation Models Version 1.0. Record 1. Geoscience Australia, Canberra. <http://pid.geoscience.gov.au/dataset/ga/72759>
- Gibson, D.L., 1998. Cobar 1:500,000 Regolith-Landform Map (Revised edition). CRC LEME, Canberra/Perth, Australia.
- Gibson, D.L., 1999. Cobar 1:500 000 regolith-landform map and explanatory notes. CRC LEME Map and Open File Report 76, 53 pp.
- Gray, D., Reid, N., Noble, R., Throne, R., Giblin, A., 2019. Hydrogeochemical Mapping of the Australian Continent. CSIRO, Australia. Report EP195905 110 p.
- Hall, G.E.M., 1998. Analytical perspective on trace element species of interest in exploration, *Journal of Geochemical Exploration*, 61 (1–3): 1-19. [https://doi.org/10.1016/S0375-6742\(97\)00046-0](https://doi.org/10.1016/S0375-6742(97)00046-0)
- Isbell R.F., 2021. National Committee on Soil and Terrain. The Australian Soil Classification. 3rd edn. CSIRO Publishing, Melbourne.

- Macht, F., Eusterhues, K., Pronk, G.J., Totsche, K.U., 2011. Specific surface area of clay minerals: Comparison between atomic force microscopy measurements and bulk-gas (N₂) and -liquid (EGME) adsorption methods, *Applied Clay Science*, 53 (1): 20-26.
<https://doi.org/10.1016/j.clay.2011.04.006>.
- McInnes, L, Healy, J., Melville, J., 2018. "Uniform manifold approximation and projection for dimension reduction". arXiv:1802.03426
- McKinnon, A., Munro, S., 2019. The Dominion and Federation discoveries at Numagee, NSW: An evolving exploration story. *AIG Bulletin 69, Discoveries in the Tasmanides*.
- McQueen, K.G., 2008. A guide for mineral exploration through the regolith in the Cobar Region, Lachlan Orogen, New South Wales. ISBN No. 1 921039 85 X CRC LEME, Canberra, A.C.T. p. 109.
- Noble, R., Lau, I., Anand, R., Pinchand, T., 2018. MRIWA Report No. 462: Multi-scaled near surface exploration using ultrafine soils: Geological Survey of Western Australia, Report 190, 99p.
- Noble, R.R.P., Lau, I.C., Anand, R.R. and Pinchand, G.T., 2020. Refining fine fraction soil extraction methods and analysis for mineral exploration. *Geochemistry; Exploration, Environment, Analysis* 20(1):113-128. <https://doi.org/10.1144/geochem2019-008>
- Poudjom Djomani, Y., Minty, B.R.S. 2019c. Radiometric Grid of Australia (Radmap) v4 2019 filtered ppm uranium. Geoscience Australia, Canberra. <http://dx.doi.org/10.26186/5dd48ee78c980>
- Poudjom Djomani, Y., Minty, B.R.S., 2019a. Radiometric Grid of Australia (Radmap) v4 2019 filtered pct potassium grid. Geoscience Australia, Canberra.
<http://dx.doi.org/10.26186/5dd48d628f4f6>
- Poudjom Djomani, Y., Minty, B.R.S., 2019b. Radiometric Grid of Australia (Radmap) v4 2019 filtered ppm thorium. Geoscience Australia, Canberra.
<http://dx.doi.org/10.26186/5dd48e3eb6367>
- Raymond, O.L., Liu, S., Gallagher, R., Highet, L.M., Zhang, W., 2012. Surface Geology of Australia, 1:1 000 000 scale, 2012 edition [Digital Dataset]. Geoscience Australia, Commonwealth of Australia, Canberra. <http://www.ga.gov.au>
- Rieuwerts, J.S., Thornton, I., Farago, M.E., Ashmore, M.R., 1998. Factors influencing metal bioavailability in soils: preliminary investigations for the development of a critical loads approach for metals, *Chemical Speciation & Bioavailability*, 10:2, 61-75. DOI:10.3184/095422998782775835
- Soil Science Division Staff, 2017. Soil Survey Manual. Eds. Ditzler, C., Scheffe, K., Monger, H.C. Government Printing Office.
https://www.nrcs.usda.gov/wps/portal/nrcs/detail/soils/ref/?cid=nrcs142p2_054262
- Wilford, J., Roberts, D. 2019. Weathering Intensity Model of Australia. Geoscience Australia, Canberra. DOI:10.26186/5c6387a429914.
- Wilford, J., Roberts, D., 2021. Sentinel-2 Barest Earth imagery for soil and lithological mapping. Geoscience Australia. <https://doi.org/10.11636/146125>
- Woolrych, T., Batty, S. D., 2007. A Semi Automated Technique to Regolith-Landform mapping in West Africa. *ASEG Extended Abstracts*, 2007(1), 1–4. <https://doi.org/10.1071/ASEG2007ab167>

Appendix A - UltraFine+[®] Sampling Workflow

Sampling conducted as part of the UltraFine+[®] Project should use the following as a minimum.

Main sample media

At each site collect a shallow soil sample from approximately 2-10cm in depth. Depth can vary and a lower soil horizon or similar morphological feature is a suitable target. Be consistent with other soil sampling protocols in general, although the benefits of UltraFine+[®] is that soil morphological changes tend to be compensated for and the mass of soil required is less than other methods and requires little preparation. The sample should be approximately 200 g.

Sample collection routine

- A clear space in the landscape should be selected, photographed and documented. Typical field notes are always beneficial. Date, time, conditions, regolith setting, vegetation and geology types etc.
- The top 1 cm scraped away using a plastic trowel. The area removed will be approximately 15 cm x 15.
- A further 5-10 cm is dug using a posthole shovel or a plastic scoop. The ultrafine soil fraction is collected from this material. In certain areas and soil types a geo-pick may make it easier to break up ground to depth and homogenise prior to sieving.
- Any coarse material from the soil >2 mm should be sieved out of the soil sample and discarded. The remaining (<2 mm size fraction) 200 g sample should be placed in a paper Geotech sample bag. Other bag types can be used but is important to have air dry samples, and breathable paper is better than plastic (for drying purposes).
- Following collection of materials the small hole will be back filled and returned to a near flat surface

Sample Locations

Samples should be collected on a pre-planned spacing and avoid sampling areas that have clear disturbance or contamination such as animal burrows, old drilling spoil, or mine/agriculture infrastructure. If working in Agricultural settings, sample below the plow depth (20 cm).

Sample Preparation

Samples should be collected when it is dry or dried soon after collection. This can be done in an oven at <80 degrees C and preferably 50 degrees. Once dry, sample bags should be closed and sent to Labwest for analysis.

Laboratory analysis

All soil samples sent to Labwest should request the UltraFine+[®] method, the UltraFine+[®] standard, and note that they are part of the CSIRO Next Gen Analytics project (if they are a sponsor to receive the additional new analyses and results). Other samples will receive the standard UltraFine+[®] analysis. This uses a separation technique to extract the <2 µm particle size fraction and provide geochemistry, spectral mineralogy, particle size distribution and a number of other parameters.

Appendix B - UltraFine+® Standard – UFF 320

Appendix C - UltraFine+[®] Next Gen Analytics data package – Federation

Appendix D - UltraFine+® Next Gen Analytics data package – Wagga Tank

As Australia's national science agency and innovation catalyst, CSIRO is solving the greatest challenges through innovative science and technology.

CSIRO. Unlocking a better future for everyone.

Contact us

1300 363 400
+61 3 9545 2176
csiroenquiries@csiro.au
csiro.au

For further information

Mineral Resources
Ryan Noble
+61 8 6436 8684
ryan.noble@csiro.au

Anicia Henne
+61 8 6438 8697
anicia.henne@csiro.au